Design and Analysis of Single-Sided Line-Start Axial-Flux Permanent Magnet Motor

Amandeep Singh Sasan

Master of Engineering (Electronics)

Flinders University

Supervisor**:** *Dr Amin Mahmoudi*

October 2017

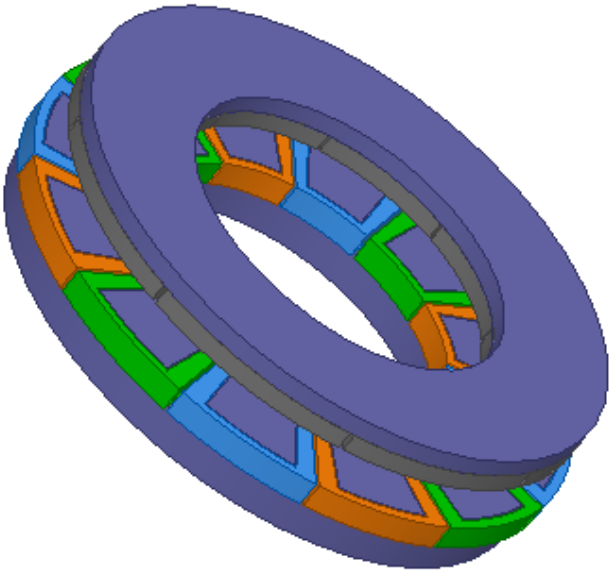

Submitted to the School of Computer Science, Engineering, and Mathematics to the Faculty of Science and Engineering for the degree of Master of Engineering (Electronics)

Abstract

This thesis examines the design and development of axial-flux permanent motor AFPM for the optimal performance. Two four-pole AFPM designs with same stator design, radial size and excitation is constructed and tested with different rotor geometries having distinction of induction rings and enclosing magnet within the rings. The two designs type-1 and type-2 are analyzed with and without magnets as synchronous and induction motors for comparative study. Both the designs are analyzed with rotor having separate ring and cage ring induction structure enclosing magnets. The starting of axial flux permanent magnet motors is based on induction principle like that of squirrel cage motor. The transient analysis includes the comparison using speed, torque, harmonics in current during startup. The designs are also tested and compared under no load and different load conditions. Steady state analysis includes comparative analysis of Input and Output power, losses and efficiency. Magnetic analysis is also performed for comparison which covers flux densities distribution in geometry and airgap of synchronous motor design types. The analysis and results could be used for further development in design of axial-flux motors.

Contents

List of Figures

List of Tables

Declaration of Academic Integrity

'I certify that this thesis does not incorporate without acknowledgment any material previously submitted for a degree or diploma in any university; and that to the best of my knowledge and belief, does not contain any material previously published or written by another person except where due reference is made in the text.'

Amandeep Singh Sasan
Date:

Acknowledgements

I would like to acknowledge my supervisor, Dr. Amin Mahmoudi for guiding me throughout the project and putting all the time and efforts during the time course.

Chapter 1
Introduction

1.1 Background

Induction Motors

Energy generation in future needs to finds an alternative for saving energy which is generated on the cost of environmental exploitation. One of the way to optimally use this energy is by optimizing the design of electric motors to achieve for more higher efficiency. Highly efficient induction motors are widely used in industrial applications in fact among all motor applications. Despite the fact more efficient motors are gradually grabbing focus of the developers.

The standard IEC 60034-30-1 published on March 2014 which replaces the standard IEC 60034-30:2008 by including fourth efficiency level for the classification. The standard has been appended with 8 pole motors and inclusion of extended power range. The updated efficiency classes for IEC 60034-30-1 is defined below where IE stands for International efficiency.

- IE1 (Standard Efficiency)
- IE2 (High Efficiency)
- IE3 (Premium Efficiency)
- IE4 (Super Premium Efficiency)

In the European Union, wide ranging legislation has been ratified with the objective to reduce energy usage and in turn CO_2 emissions. EU Regulation 640/2009 and the supplement 04/2014 involve energy usage and/or the energy efficiency of induction motors in the industrial environment. In the meantime, this regulation is valid in all countries belonging to the European Union.

Number of Poles	2, 4, 6, 8
Power range	0,12 – 1.000 kW
Level	IE1 - Standard Efficiency IE2 - High Efficiency IE3 - Premium Efficiency IE4 - Super Premium Efficiency
Voltage	35mm
Operating mode	S1 (permanent operation with constant load); motors, that are designed for different operating modes but can still be operated permanently with rated output.
Degree of temperature	-20°C to +60°C
Altitude	Up to 4 meters above sea level
Geared motors	Yes
Smoke Extraction Motors with a temperature class up to 400°C	Yes
Validity	Since March 2014

Table 1 Scope of Standard IEC 60034-30-1:2014[www.siemens.com/international-efficiency]

.

Line-Start Permanent Magnet Motors

Permanent magnet(PM) motors are gaining attention to replace the induction motors due to availability of cheaper rare earth permanent magnet in recent years. PM motors still alone is not economical for many single speed applications such as most fans, pumps and compressors as they need inverters for starting. Here comes line-start permanent magnet synchronous (LS-PMS) motors which have permanent magnet with induction rings for self-starting avoiding inverter fed mechanism have been developed since 1955. They became less preferable later due to high energy permanent magnet and improvement in induction motors but are now again gaining appeal due to introduction of high energy permanent magnet materials with reasonable prices.

Line Start permanent magnet synchronous are more efficient than standard induction motors efficiency levels in rated output power from 0.55kW to 7.5kW [34].

RATED OUTPUT POWER(kW)	0.55	0.75	1.1	1.5	2.2	3.0	4.0	5.5	7.5
WQuattro (LSPM)	84.2	85.6	87.4	88.1	90.2	90.4	91.7	92.5	93.0
IEC IE4		85.6	87.4	88.1	89.7	90.3	90.9	92.1	92.6
IEC IE3		82.5	84.1	85.3	86.7	87.7	88.6	89.6	90.4
IEC IE2		79.6	81.4	82.8	84.3	85.5	86.6	87.7	88.7

Table 2 Scope of Standard IEC 60034-30-1:2014[34]

Axial-Flux Permanent Magnet Motors

Machine can be classified based on direction of magnetic flux crossing the air gap of the machine. In axial-flux motor magnetic flux crosses the airgap axially in the machine. Figure shows the schematic representation of radial and axial flux machine.

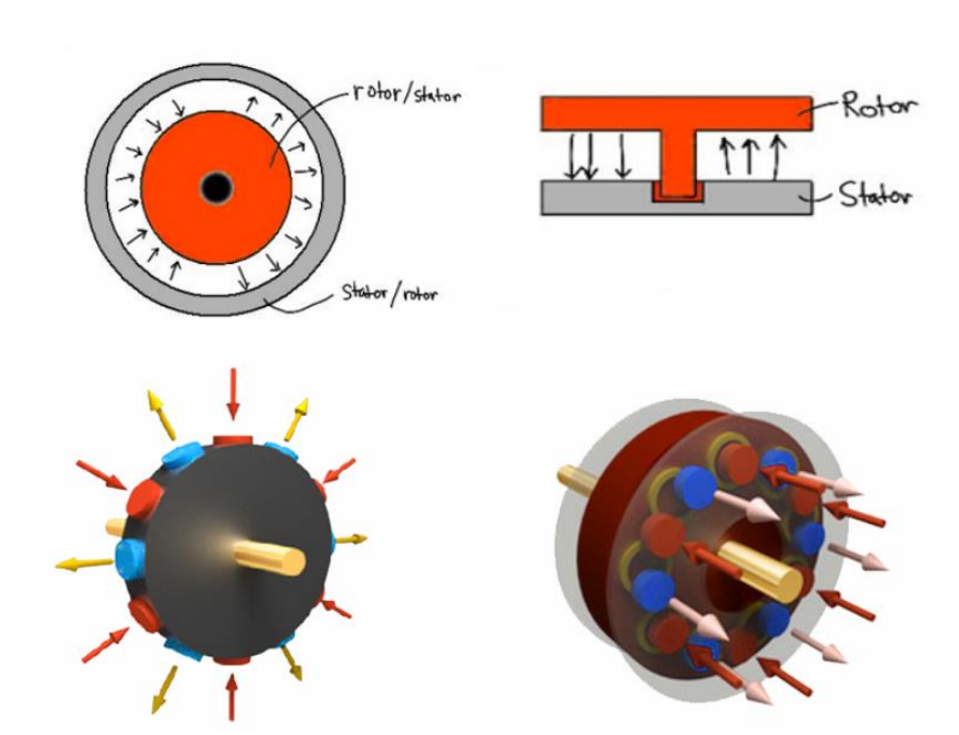

(a) Radial-flux machine (b) Axial-flux machine

Fig 1 Comparative geometries of radial and axial flux machine.

[www.magnax.com/magnax-blog/axial-flux-vs-radial-flux-for-direct-drive-generators]

In axial-flux permanent magnet motors rotor rotates with high-flux magnets and solid induction rings along disk shape windings on stator. These motors are gaining interest as major studies have been done in this motor configuration. The magnets are arranged in a circle enclosed with induction rings facing the stator with space in between to form an axial air gap.

Axial-flux permanent-magnet (AFPM) machines offers priority features to replace conventional field winding motor. As it employs permanent magnets losses in field excitation are completed avoided resulting in high efficiency and output power. Another advantage it offers is requirement of less core material in construction of such machines which in turn provides high torque to weight ratio reducing rotor losses significantly.

Recent innovations in axial flux technology low weight and highly efficient direct drive motors and generators are on the horizon. Table 3 shows the comparison of Axial drive produced by Magnax corporate of 100kW having rated speed of 60rpm and rated torque of 16kNm with radial flux direct drive and induction motor along with gearbox. The axial drive is more efficient than typical drives of same output power and rated torque. The axial drive is far better than commercially available radial and induction drive in terms of weight and size and are cheaper, reliable and have low maintenance cost.

100kW – 60rpm generator/motor - 16kNm Torque	Induction motor + Gearbox	Radial Flux Direct Drive	Magnax (Axial Flux) Direct Drive
Efficiency	80% – 88%	92% – 95%	95% - 97%
Axial Length	1500 mm	700 – 1200 mm	140 mm
Weight	2000-3000 kg	2400 - 5000 kg	850 kg
Investment cost	€	€€	€
Reliability	+	+++	+++
Ease of installation	-	+	++
Maintenance cost	Very high	Low	Low

Table 3 Technology comparison chart of Magnax Axial drives[www.magnax.com-product]

1.2 Problem statement

The axial flux permanent magnet motors today needed to be optimized for industrial application as it has higher efficiency, high power factor as they are synchronous motors and addition to that they have other advantages like airgap adjustment because of their air gap geometry. First of all, it employs permanent magnet which would save lot of power losses which occurs in winding. Secondly, it uses the axial flux geometry which have advantage of easily adjustable air gap. Optimized design of such motors would take the capability of motors to the next level in terms of efficiency and required operating power. Also, the permanent magnet motor can be useful in constant speed application in industries and it can replace the small and the medium size of the motor.

1.3 Objectives

1. Create two 3D designs of axial-flux line-start permanent magnet motor with same stator, same radial size and parameters but different rotor geometries.
2. Simulate and analyze the designs with their magnets removed as well and perform static and dynamic analysis on both the design types to compare their performances.
3. To compare the both motor design types with separate ring inductor and cage ring inductor and study the dynamic and steady state response.

1.4 Methodology

The project uses the software Ansys Maxwell 3D to design models of three-phase 4-pole axial-flux line-start permanent-magnet synchronous motor and simulate geometries for performance comparison. The project focuses on determining an approach to build single-sided axial flux line start motor having optimal performance.

Demo models of axial-flux permanent-magnet synchronous motor to give output power of about 10kW were build and simulated to have prejudgment of parameters to build the motor with specific requirement to be used in industrial applications. The ideal size, diameter and width of axial motor is finalized. The first thing was to build the stator which would be used in all the motors with identical 3-phase source of frequency 50 Hz. Following that rotor

with different geometries were tested and designs were developed for AFPM motors. Two designs were finalized for the comparison of AFPM motors geometries having distinction of number of induction rings per pole and then motors geometries were also analyzed without their magnets as induction motor.

Approach to design and development of induction motors prior to synchronous motor was considered first but adding magnets to induction motor did not give satisfactory results in analysis so synchronous motor designs were modeled, analyzed and finalized prior to their analysis with their magnets removed as induction motors. The two designs are analyzed with separate ring and caged ring rotor. Transient and steady state parameters of the machines were analyzed and compared and magnetic analysis including distribution of flux densities, flux lines in design geometry are performed to select the optimal design.

1.5 Limitations and scope

Since the software uses FEM Finite Element Method changing the time step for analysis affect the dynamic and steady state performances so both the synchronous motors are tested under same inertia and damping as the geometries are approximately identical in volume.

The results obtained were satisfactory but are limited to simulation analysis and no hardware model were constructed to validate the analysis.

The motor dynamic and steady state performances could be improved by using hybrid arrangement axial, radial and circumferential magnetic field of magnets by using corresponding magnets instead of only axial field magnets. Material used for magnets could be replaced with NdFeB and aluminum could be replaced with copper for solid rotor cage in small motors to improve the performance parameters.

1.6 Thesis outline

Chapter 1: Introduction

The chapter gives the background information of axial flux synchronous motor. The chapter describes the Problem Statement, Objective, Methodology, Scope and Limitations of the project with the Thesis Outline.

Chapter 2: Literature Review

The chapter gives the literature review on the past work being done on axial flux line start permanent magnet synchronous motor. Relevant information in previous researches are mentioned as it is considered significantly for the design of motor.

Chapter 3: Design of Motors

The chapter gives the description on types of motors designed, their geometries and material used in designing. It presents the parameters undertaken during the design and simulation of motor. The chapter concludes with design of two types of motor Type-1 and Type-2 with 4 induction ring structures (including separate ring and cage ring for both the types) so that design types can be simulated as induction and synchronous motors.

Chapter 4: Simulation Results and Analysis

This chapter presents dynamic and steady state analysis of all the motors. It compares all the motors under no load conditions, compare them under different load conditions. It also compares their performance when used with separate ring and caged ring structures. The chapter concludes with the outperforming behavior of synchronous motors over induction motors and better starting and synchronistic performance of type-1 motor over type-2 motor.

Chapter 5: Conclusion and Future Work

This chapter sums up the work done and analysis in a conclusion. It also proposes the alternate design variation to optimize steady state behavior and starting performance of an axial flux synchronous motor.

Chapter 2
Literature Review

2.1 Line Start Permanent Magnet Motor vs Induction Motor

Line Start Permanent Magnet Motor if compared to induction motor are more efficient, has higher power factor and torque density. Also, it has better thermal properties and are less sensitive to frequency variations [1]. Starting and Synchronization of such motors depends on the motor itself and applied load conditions [2].

The permanent magnets provide optimal magnetic flux to minimize the exchanged reactive power with power supply which in turn provide high power factor corresponding to minimum line current [4]. The LSPM synchronous motor has two operating modes: asynchronous mode at starting and transients and synchronous mode at steady state [2]. So, permanent magnets work under the effect of breaking torque during starting period and alignment torque during steady state which should be taken into consideration while signing permanent magnets.

The permanent magnets creating breaking torque during starting is responsible for low starting torque [5, 6]. The magnetic flux barriers present in the rotor back iron as permanent magnets are buried below the squirrel cage (for radial flux motor) introduces a breaking reluctance torque because of rotor saliency, which further lowers the total torque in starting period. So, the design of LSPM synchronous motor has problem of degrading line starting performance to be tackled.

2.2 Axial Flux Motor vs Radial Flux motor

Axial flux machines are also gaining appeal as a replacement to radial flux machines as several researches are carried out in the past few years. The disk shape geometry of this type of motor offers an advantage of maintaining small air gap in relatively large machines. Despite of the advantages offered by Axial flux permanent magnet over conventional motor it was not economically feasible until the rare earth permanent magnets came into use. There are vast range of papers on this type of machine including more than dozen related to airgap treatment. AFPM motors have application in electric vehicles which contribute to help in avoiding environmental pollution.

In [12] Parviainen, Niemela, Pyrhonen, and Mantere reported a detailed study comparing traditional radial flux geometry to the two-slotted stator one rotor axial flux machine, (AFPM-21). Mechanical constraints were discussed and included in the analysis. Their final comparison was on cost of the active materials only. Their conclusions were that at 8 poles the 2 designs were very similar cost, and that at greater than 8 poles the axial flux geometry was lower cost than the radial flux.

2.3 Single sided geometry of axial flux synchronous motor

Single sided axial flux machine offers some considerable advantages over the conventional radial flux machine and double sided axial flux machine. Fig 3 shows the slotted and slot less geometry of single sided axial flux permanent magnet motor [13]. There are certain developers who developed the axial flux permanent motor such as SAIETTA, MSF Technologies, EVANS ELECTRIC.

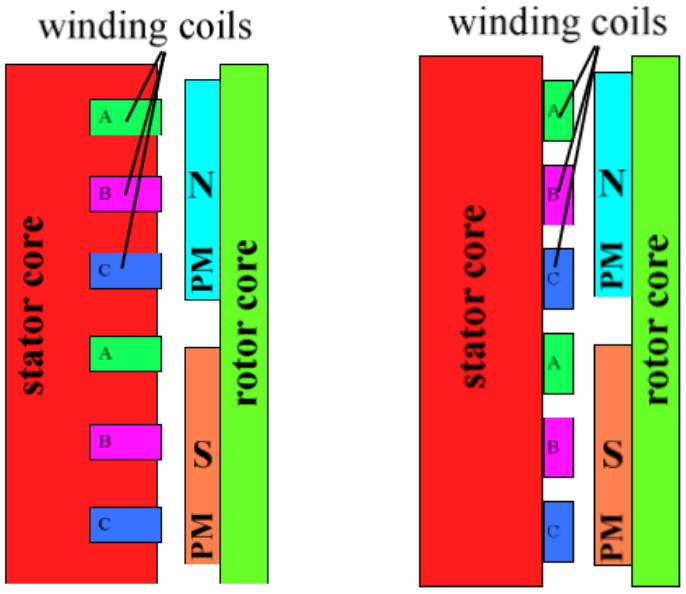

Fig 2 Slotted and Slot less geometry of axial flux permanent magnet machine [13].

Studies shows that the single sided axial flux machine has a considerable volumetric advantage over the traditional radial flux machine. The inside volume of a traditional radial flux rotor, or indeed the stator on an outside rotor radial flux machine, is not used electromagnetically. There is a very definite volumetric advantage to axial flux machines at reasonably high pole counts. The inside volume of a traditional radial flux rotor, or indeed the stator on an outside rotor radial flux machine, is not used electromagnetically. Ingenious solutions for "slinky" style wound stators for outside rotor machines, and spiders to support a rotor structure, will not save volume, but will save active material, and hence both active and passive mass [8]. Also in slot less stator magnetic force is exerted on iron rather than on copper winding resulting in twisting of the structure [9].

In [16] a preliminary design of double slotted axial flux permanent magnet AFPM motor was designed for electric vehicle direct drive. The design was tested with 6 rotor poles for high torque density and stable rotation. The designed motor is capable to produce 10kW power and the maximum amplitude of the sinusoidal back EMF was 105V at 1000rpm rated speed.

In [7] Sitapati and Krishnan focuses on comparison of radial and axial flux geometries. They employed 5 geometries a slotted single sided, an unslotted single sided, (both AFPM-11), two stators and one rotor (the AFPM-21), and a variant on the TORUS NS machine in which the single stator had no iron, using just an airgap winding. They tested their geometries with 5 different power levels and concluded that for the same torque rating axial flux machine would have less volume in comparison to radial flux and that it is advantageous to have slots in stator and rotor of axial flux machine as it reduces the copper and magnetic material for coils and magnets to work effectively.

On the downside in [10,11] single stator single rotor geometry of axial flux permanent magnet AFPM machine have unbalanced axial force between their stator and rotor which consequently requires thick rotor disk and complex bearing arrangement if compared to double sided geometry.

2.4 Startup of Line Start and Axial Flux Permanent Magnet Motor

In [17], axial flux permanent magnet motors having solid rotor and composite rotor designs were compared. Results showed that the composite rotor significantly improving both starting torque and synchronization capability over solid rotor. The thin layer of copper on the rotor-ring surface is employed to increase conductivity of the material for more current circulation on the rotor-ring surface during start-up to improve dynamic response, synchronization time and drive heavier loads.

In 2015, 1.1 kW three phase 4 poles hybrid LSPMSM for fans systems is analyzed using Rmxprt and Maxwell 2D simulation. The effect of the magnet size on breaking torque is examined in Line Start permanent magnet synchronous motor. It is concluded that breaking torque which is the sum of cage torque and breaking torque is proportional to the magnet size directly.

2.5 Gap Statement

The literature review includes the studies on line-start permanent magnet motors and axial motors and points out advantages of single sided geometry of axial-flux permanent magnet motors. Also, there is appreciable work done on improving the synchronization time of the rotor while considering the cost factor as well but the studies demand much more work as there is a lot of scope to test and improve other parameters to improve the dynamic and steady state response. This project compares the effect of number of rings under single pole on the performance of motor. Two four pole axial-flux permanent magnet synchronous motors are designed with similar stator geometry and analyzed with rotor having distinction of number of rings and magnets enclosed in them. The project also shows the comparison with their performance as induction motor when analyzed without magnets.

2.6 Contribution

The project aims to develop optimized design of highly efficient axial flux permanent magnet motor. Two designs constructed are chosen for the comparative analysis to understand role of parameters considered during the design for such kind of motor. The two designs are analyzed with and without the magnets to compare their performance in terms of efficiency, output power, maximum load bearable. The analysis is performed to compare how the dynamic and steady state behavior get effected with change in induction ring geometry and magnets and compare the performances on the similar grounds without magnets as induction motors.

Chapter 3
Design of Motors

3.1 Line Start Permanent Magnet Synchronous Motor

Line Start Permanent Magnet Motor if compared to induction motor are more efficient, has higher power factor and torque density. Also, it has better thermal properties and are less sensitive to frequency variations [1]. Starting and Synchronization of such motors depends on the motor itself and applied load conditions [2].

3.2 Axial Flux Motor

Axial-flux motor are the motors with different magnetic flux path compared to conventional radial motor. The magnetic flux flows parallel to axial of the motor. Axial-flux permanent-magnet (AFPM) motors over conventional radial-flux permanent-magnet (RFPM) motors are more efficient, better torque-to-weight ratio, more balanced rotor-stator attractive forces, and better heat-removal [3,4]. Also, axial-flux motor air-gaps are planar and adjustable [5].

3.3 Motor Design Types

Two axial flux line-start permanent magnet motors having same stator geometry are designed for this project. The synchronous motors are then analyzed without magnets as induction motors. So, there are 8 different types of motors under analysis in the project. All the four motors have same stator configuration. The motor differs in induction rings geometry and magnets embedded on rotor.

Two design types are designed and operated with separated and cage rings with and without magnet. The stator slot wounded with three phase supply (shown in color green, orange and blue in Figure 4 and Figure 5) of four poles produces rotating magnetic field. Magnets enclosed in induction rings are combined with rotor will start as induction motor under the effect of this rotating magnetic field. On achieving synchronous speed magnets of the rotor get locked with rotating magnetic field and hence move with synchronous speed.

3.3.1 AFPM Motor Type-1

The design type has eight rings and eight magnets embedded on rotor disk with two similar poles together so that rotor poles would have resultant four poles to interact as it is a four-pole motor. Figure show exploded view of the axial flux permanent magnet motor type-1.

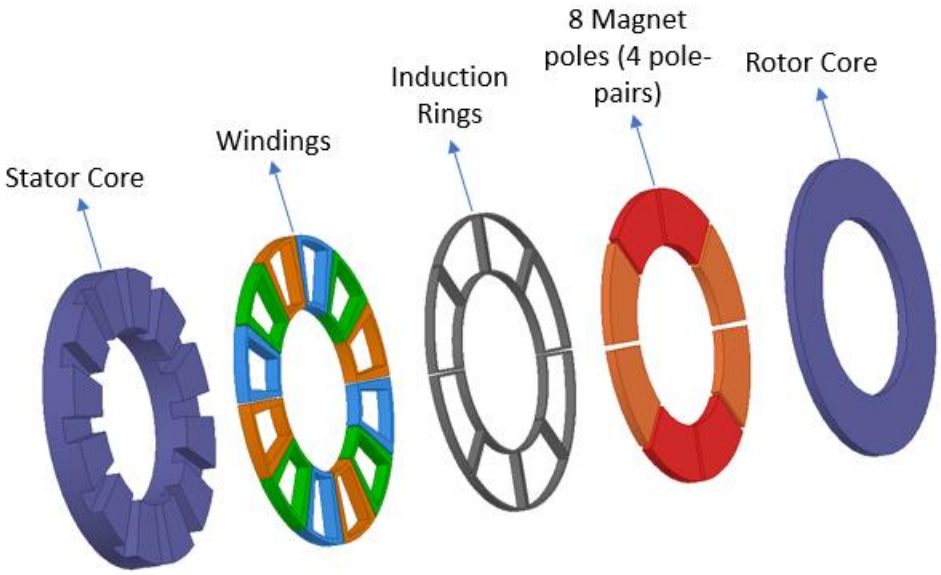

Fig 3 Exploded view of design Type-1 AFPM motor.

3.3.2 AFPM Type-2

The design type-2 of axial-flux permanent magnet motor is different from type-1 in a way that it has sixteen rings with magnets embedded on the rotor disk. For magnetic locking between stator and rotor poles of pole motor four similar magnets are placed consecutively.

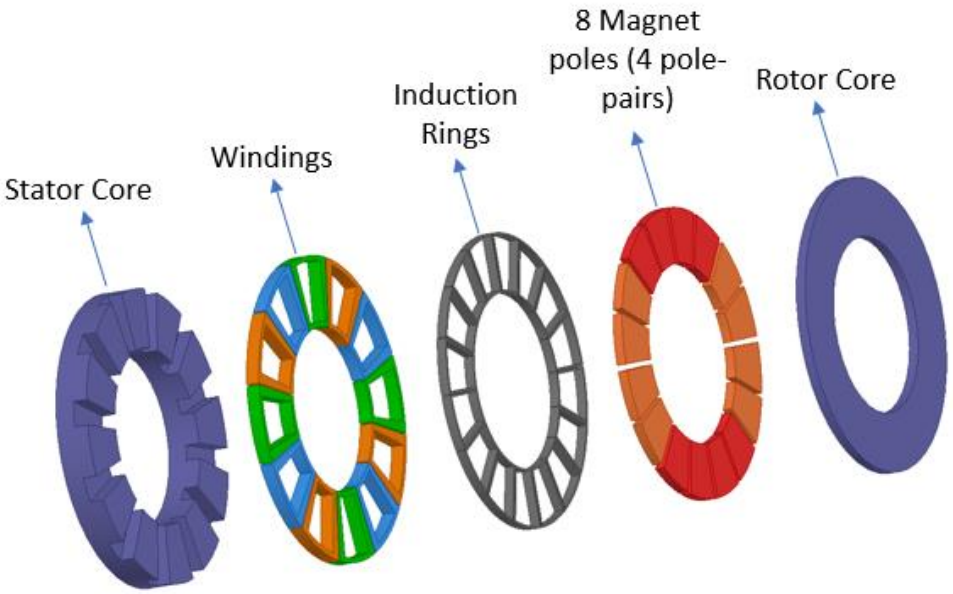

Fig 4 Exploded view of design Type-2 AFPM motor.

3.4 Design of Stator Disk

The stator of the axial motor in Figure shows the cross-section views. The stator designed by using laminated electrical steel M19_24G having outer diameter of 300mm and inner diameter of 180mm. The stator disk has axial width of 35mm out of which 15mm is for slot depth to accommodate three phase coils.

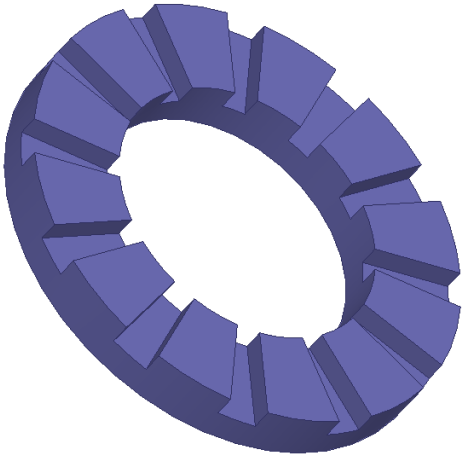

Fig 5 Stator core Geometry.

Stator disk	Data
Outer Diameter	300mm
Inner Diameter	180mm
Axial width	35mm
Slot depth	15mm

Table 4 Stator Parameters.

3.5 Design of Stator Windings

The 3 phase windings constructed using copper material having axial width of 15mm. The windings are excited through 310V line to line supply of 50Hz. The table gives the specification of parameters employed for construction and excitation.

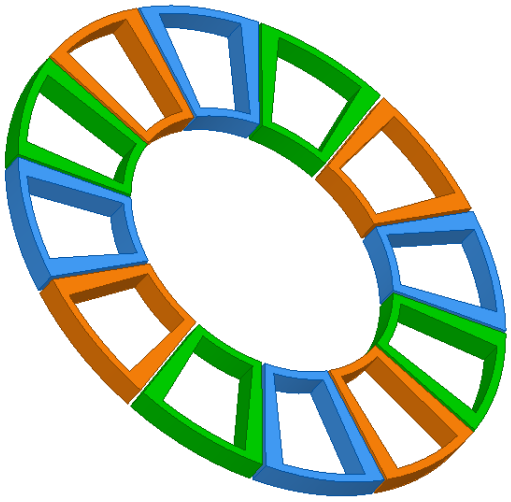

Fig 6 Stator Coil Windings.

Winding parameters	Data
Number of conductors per coil	75
Resistance	0.2ohm
Inductance	0.3mH
Phase A	240*sin(2*pi*50*time+2*pi/3) V
Phase B	240*sin(2*pi*50*time) V
Phase C	240*sin(2*pi*50*time-2*pi/3) V
Frequency	50Hz

Table 5 Stator Excitation Specifications.

3.6 Design of Rotor

The rotor disk of the motors was designed with M19_24G laminated steel having outer and inner diameter similar to that of the stator. The axial flux permanent magnet motor uses aluminum induction rings for initial startup of the motor. The magnets are placed inside the rings for the magnetic locking between stator and rotor magnetic poles. Two rotors having distinction of number of rings and magnets for comparative analysis. Figure illustrate the side view of rotors of both the motor types.

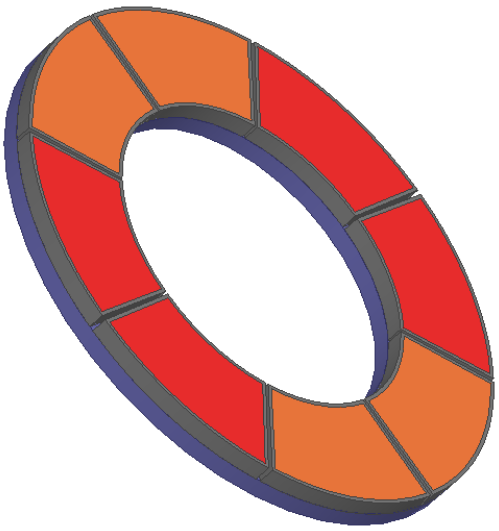

Fig 7 Rotor of AFPM Motor Type-1.

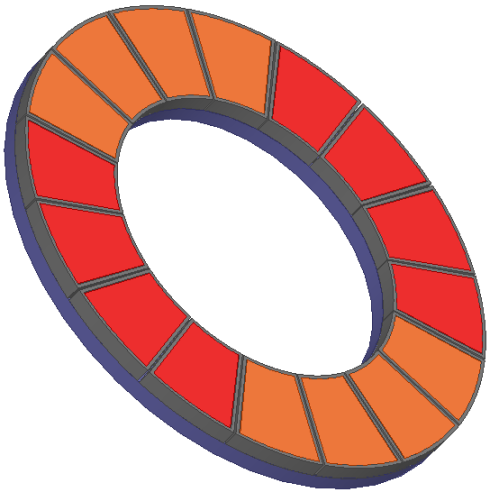

Fig 8 Rotor of AFPM Motor Type-2

Rotors parameters	Data
Outer Diameter	300mm
Inner Diameter	180mm
Width of Rotor Disk	15mm
Axial Width of Aluminium Rings	10mm
Thickness of Aluminium Rings	2mm

Table 6 Rotor Parameters

3.7 Permanent magnet

The material N36Z_20 with specifications in Table is added to the library and used in the simulations. Rare earth permanent magnets like Samarmium-Cobalt or Neodymium could be used with hardware to make motors more economical on the sake of performance to some extent. Figure 10 shows the half view of the magnets employed in two axial flux machine designs modeled for analyses. The direction of arrows shows the direction of magnetic field lines which distinguishes north pole of the magnet with south pole.

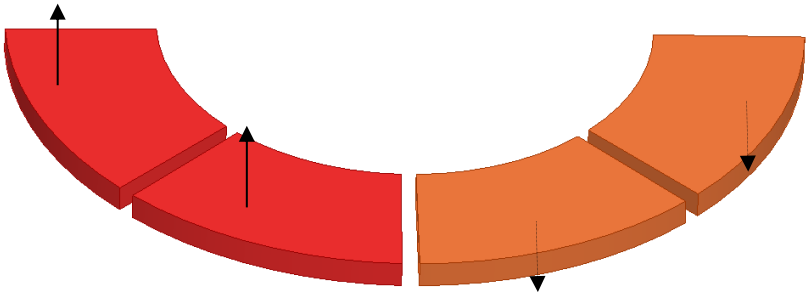

Fig 9 Magnets of AFPM Motor Type-1.

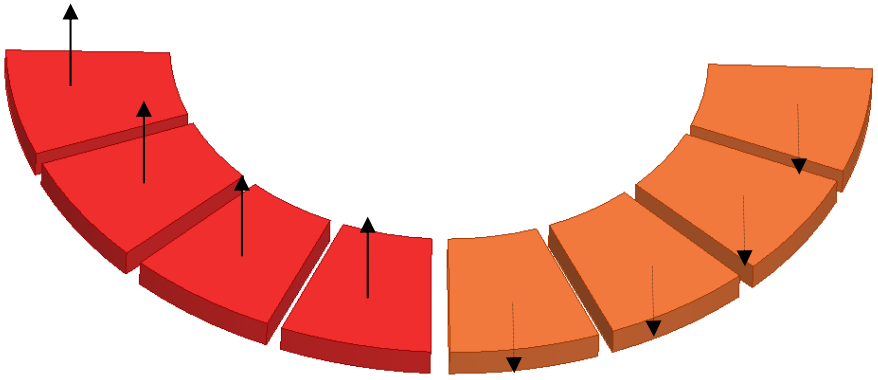

Fig 10 Magnets of AFPM Motor Type-2.

Magnet Properties	
Magnet Type	N36Z_20
Relative Permeability	1.03 B/H
Bulk Conductivity	0 siemens/m
Magnet Coercivity	-920000 A/m
Mass density	0 kg/m^3
Width of magnet	2mm

Table 7 Properties of the permanent magnet.

3.8 Rotor Induction Rings

Both the designs are analyzed with separated ring and caged ring rotor. Aluminium metal is used for construction of motor. Properties of aluminium metal is given in Table 8. The induction ring arrangement for both the design types is shown in Figure 12.

Alumimum ring properties	
Relative Permeability	1.000021 B/H
Bulk Conductivity	38000000 Ω^{-1}/m
Magnet Coercivity	-920000 A/m
Mass density	2689 kg/m^3
Width of magnet	2mm

Table 8 Aluminium ring properties

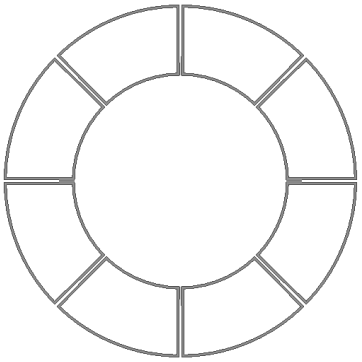

(a) Type-1 Separated Ring Inductors

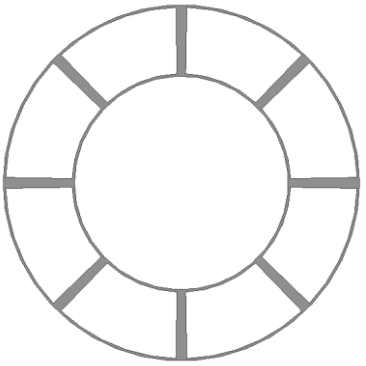

(c) Type-1 Caged Ring inductor

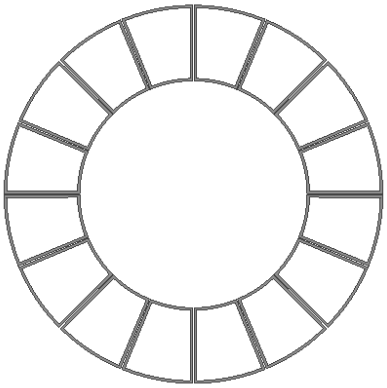

(b) Type-2 Separated Ring Inductors

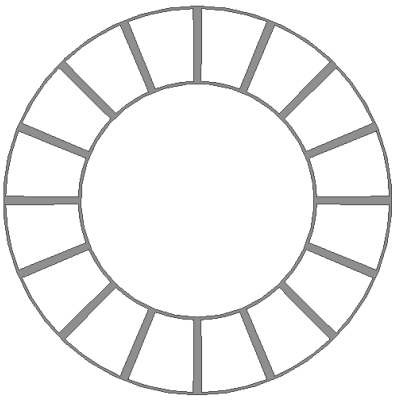

(d) Type-2 Caged Ring Inductor

Fig 11 Induction rings of rotors

Chapter 4
Simulations Results and Analysis

4.1 Method for Simulation and Analysis

The software Ansys Maxwell having approach based on Finite Element Analysis is used for the design of the three motors. The axial flux permanent magnet motors designed were simulated with and without the magnets. Magneto static and transient Analysis were performed on one-fourth of the motor using the symmetrical analysis feature (employing Master and Slave Boundary conditions) of the software. The simulations were performed with timestep of 0.5ms.

4.1.1 Meshing

Using mesh operations, meshes are defined for transient simulation. The meshes are defined in such a way that mesh density fulfil the performance requirements and aid in better analysis. Meshes for different motor parts are defined accordingly and shown in the following figures.

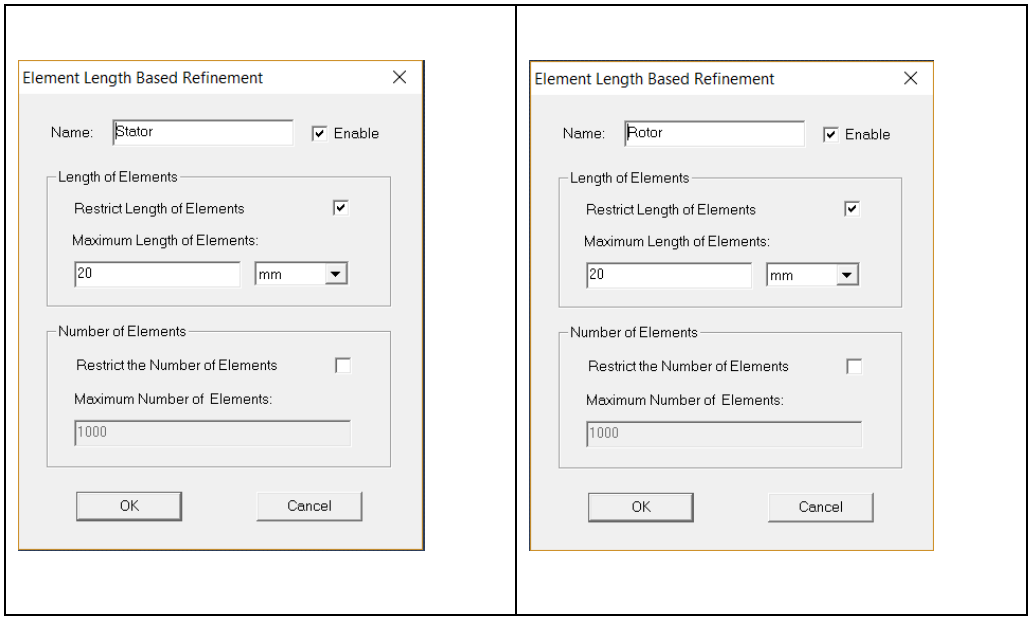

Fig.12 Mesh settings

4.1.2 Simulation

The designed motors are assigned with motion setup for simulating the motors. The parameters like inertia, damping and load torque are assigned for functioning of the motor. All the motors are assigned with inertia of $0.01\ Kgm^2$. However, damping for induction motors are set to 0 N-m-sec/rad while damping for synchronous motors are set to 0.001 N-m-sec/rad. The following figure shows settings for Motion Setup of Motors.

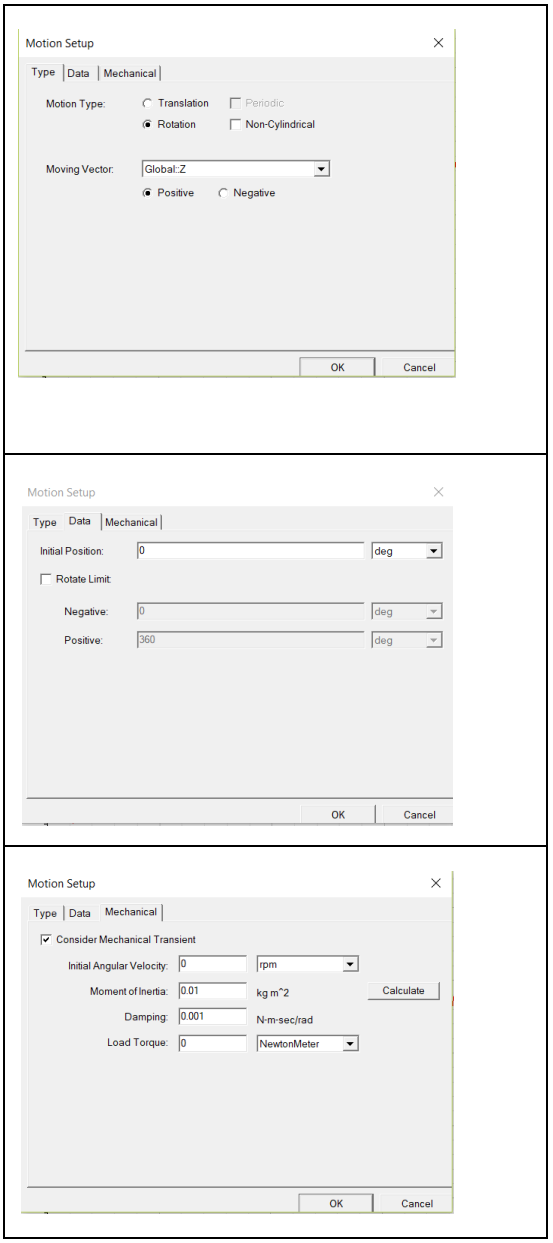

Fig 13 Motion Setup Settings

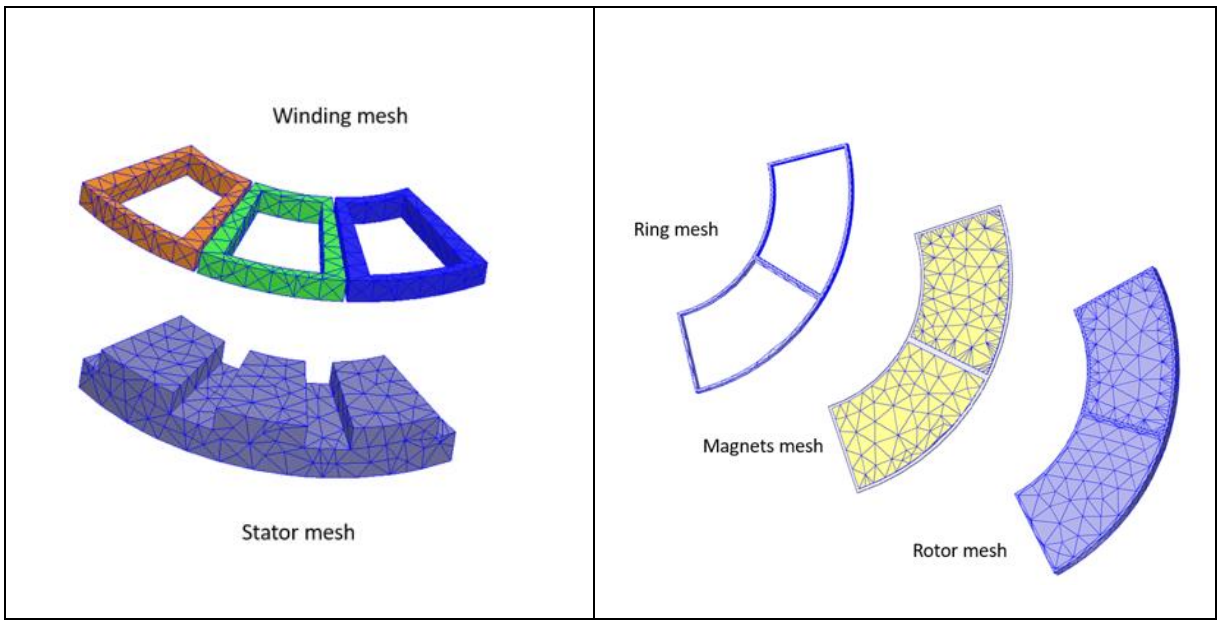

Fig 14. Meshes for parts of motor

4.1.3 Analysis

The setup for analysis is defined where parameters to run simulation are defined. All the simulations have running time from 0 to 1s with the step time to analyze after each 0.5ms. The save fields tab in setup is also assigned with same starting parameters which contributes in magnetic analysis. Figures showing analysis setup adopted for all the design operations.

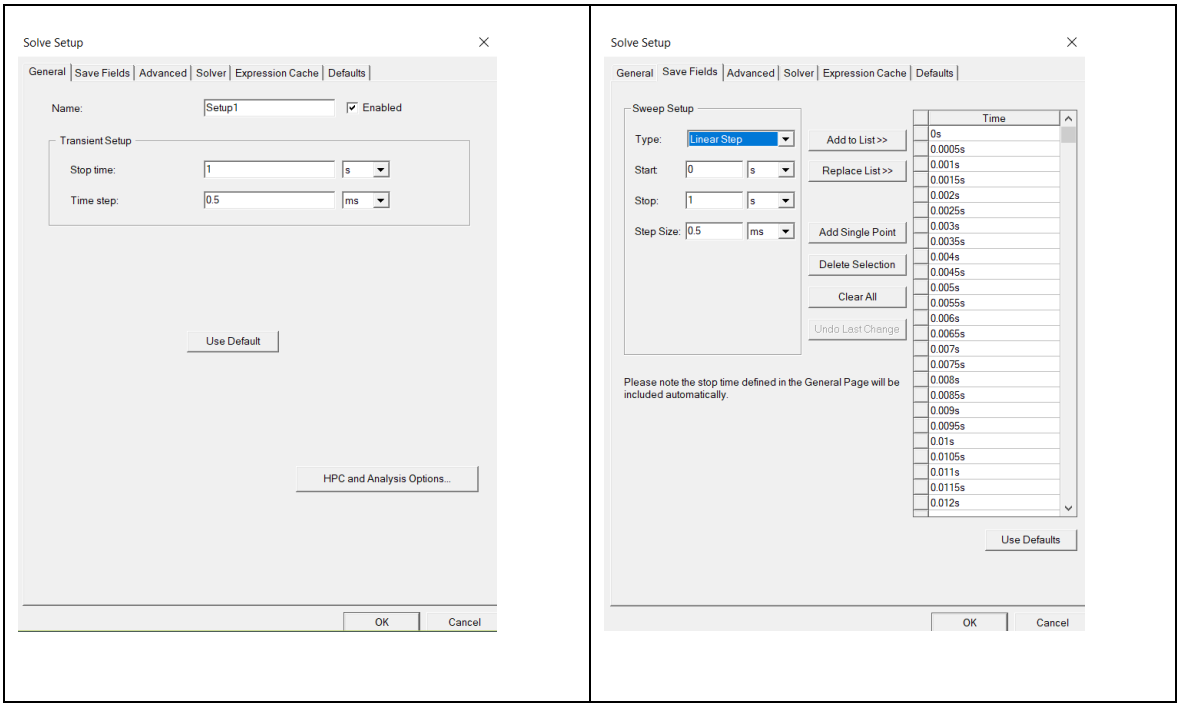

Fig 15. Analysis setup

On completion of simulation report are created for dynamic analysis. The motion setup created keep track of transient parameters such as moving speed, moving torque, winding current. Output variables is also defined to obtain performance of input/output power and efficiency.

4.2 Magnetic Analysis

Magnetic Analysis for getting magnetic field intensity and magnetic flux lines around the machine were performed. The process involves computation of magnetic field in and around the machine at specific time intervals. Magneto static analysis could be used in applications such as, motors and generators, relays, sensors and solenoids.

4.2.1 Magnetic Flux Density

The magnetic flux density for the performance evaluation of the machine is calculated in several ways. analytical (Lee, 1992; Furlani, 1994; Zhilichev, 1998; Qamaruzzaman and Dahono, 2008; Loureiro et al, 2008; Chan et al., 2009; Kano et al., 2010), quasi 3D (Azzouzi et al., 2005; Kurronen and Pyrhonen, 2007; Marignetti et al., 2010), finite element method (FEM) (Bumby et al., 2004; Rong-Jie and Kamper, 2004; Upadhyay and Rajagopal, 2006; Chan et al., 2010), and method of images (Sang-Ho et al., 2006). FEM is more accurate than analytical method is, and can be used in complicated machine constructions. Finite element analysis (FEA) has long computation time, and a different model (including re-meshing) is needed when machine geometry changes. Magnetic flux density in the motor represent intensity of magnetic field forces throughout the geometry or on their surface.

High magnetic flux density indicates high magnitude of flux linkage through the coil. The induced emf (electromotive force) due to excited stator coil is directly proportional to number of turns and flux linkage and can be given by equation.

$$Induced\ e.m.f = N\frac{d\phi}{dt}$$

Where N is number of turns and $\boldsymbol{\phi}$ is the flux in the cross section of coil which is changing with time due to rotational motion of overall flux due to three phase excitation in the geometry.

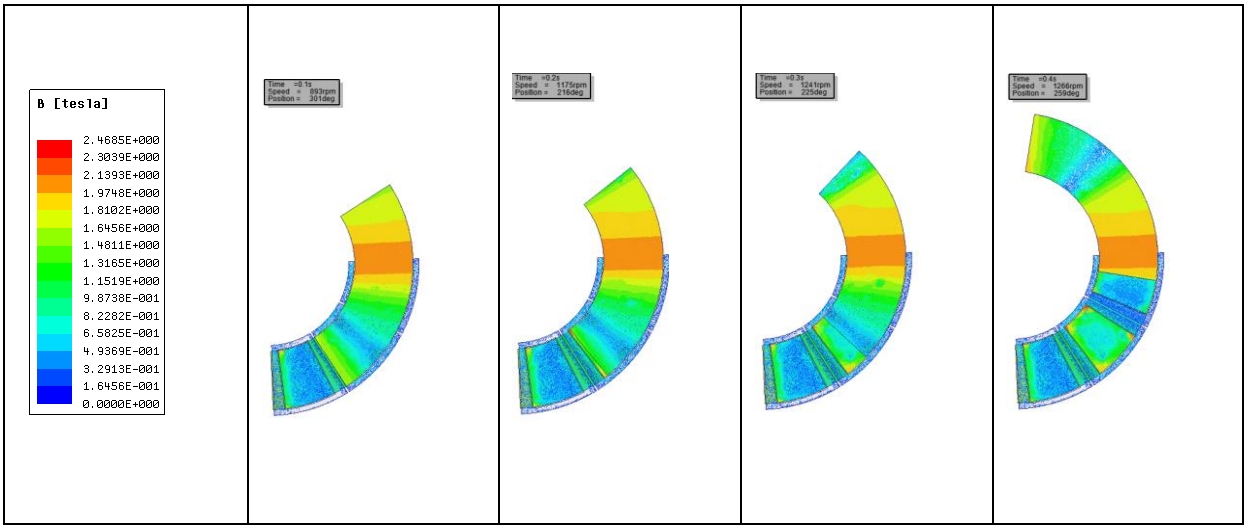

(a) Design type-1 analyzed with separate ring rotor

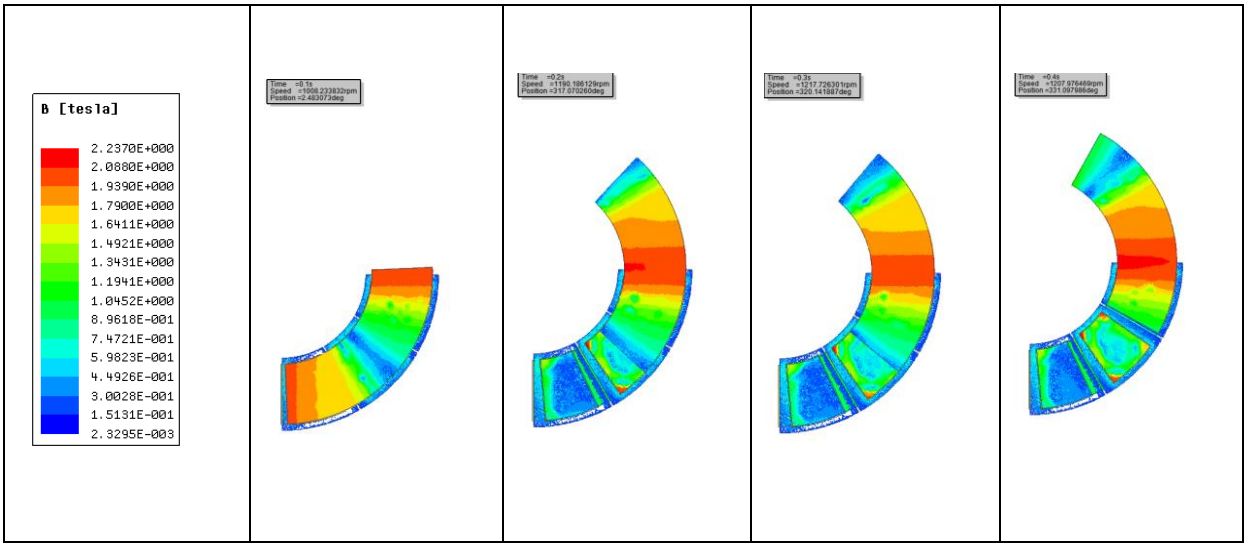

(b) Design type-1 analyzed with caged ring rotor

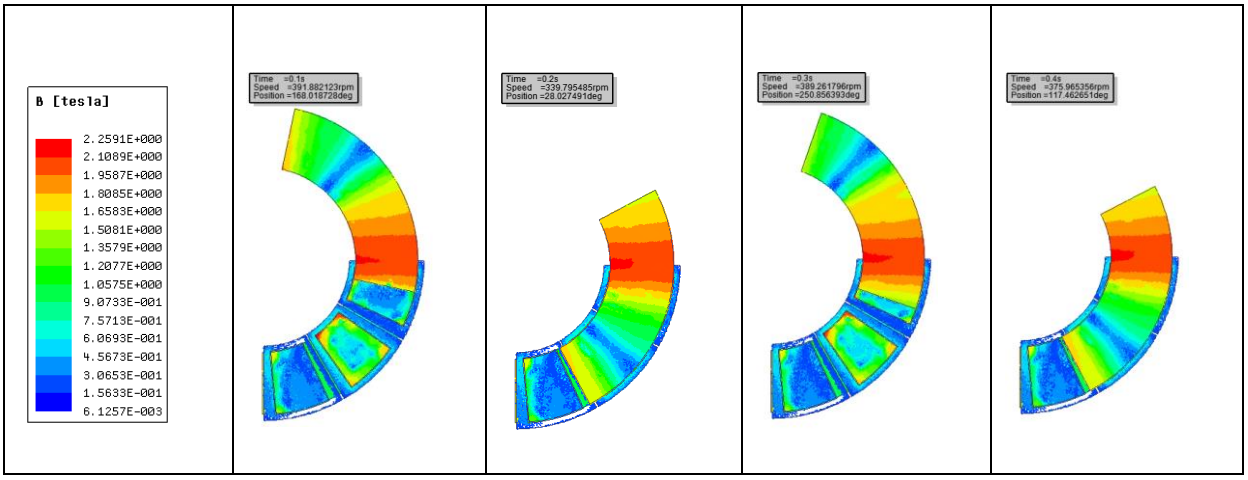

(c) Design type-2 analyzed with separate ring rotor

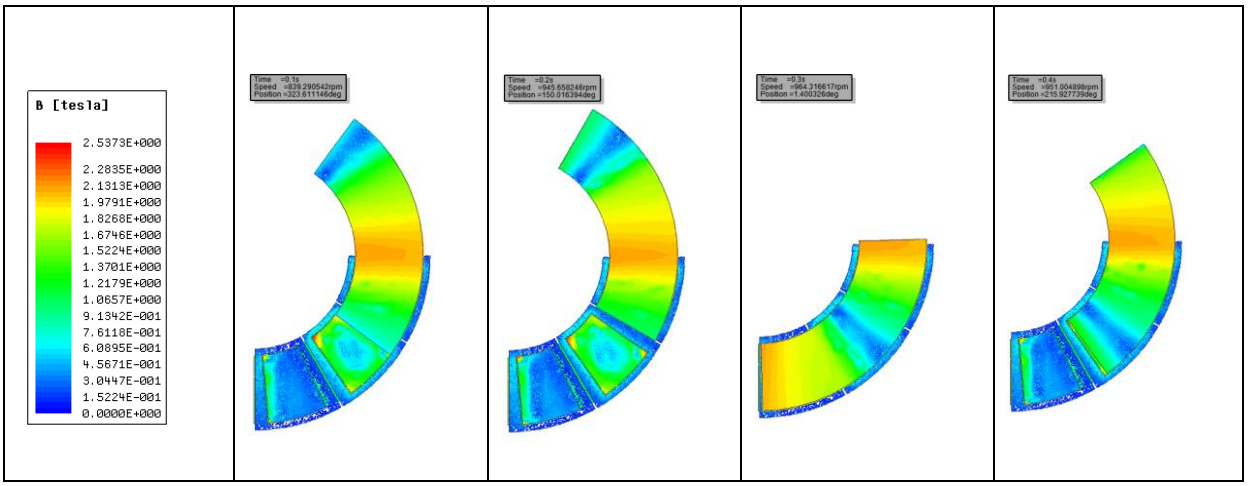

(d) Design type-2 analyzed with caged ring rotor

Fig 16 Flux density of Type-1 and Type-2 induction motors.

Fig 13 shows that the flux densities is better and higher in type-1 design when compared to design type-2. Also, when operated and analyzed with caged ring rotor rather than separate ring rotor improves the flux densities in the motor field which is due to better current distribution short circuited ring structure.

4.2.2 Air Gap Flux Density

The magnetic flux density in the airgap between the stator and rotor is also analyzed for all the four geometries at no load. From the figures airgap flux density can be seen lower in the axial regions of coils where the flux is limited by steel and shows a steep rise near the coil winding. The windings in stator is deep but still very close to stator and because it is axial flux machine the winding field is exposed to airgap without any laminated steel in the circumference where it is wounded which makes magnetic flux higher in these regions. This maximum magnitude could be reduced by employing closed slots in stator.

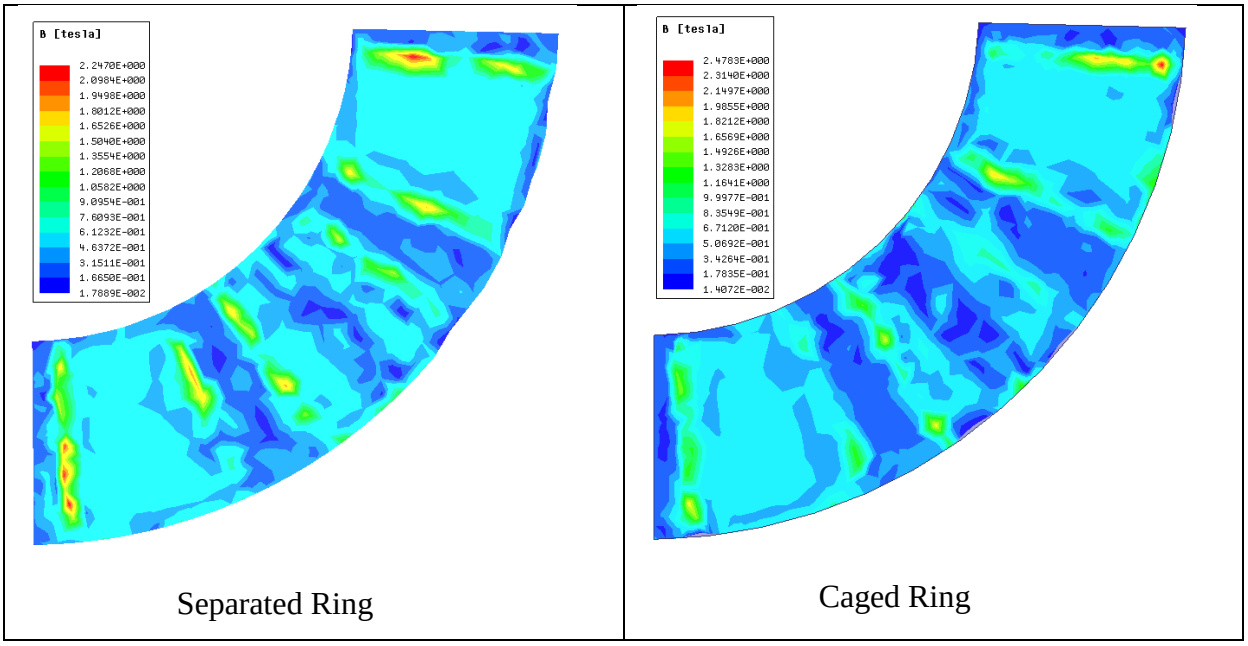

Fig 17 Air gap flux density of Type-1 AFPM motor

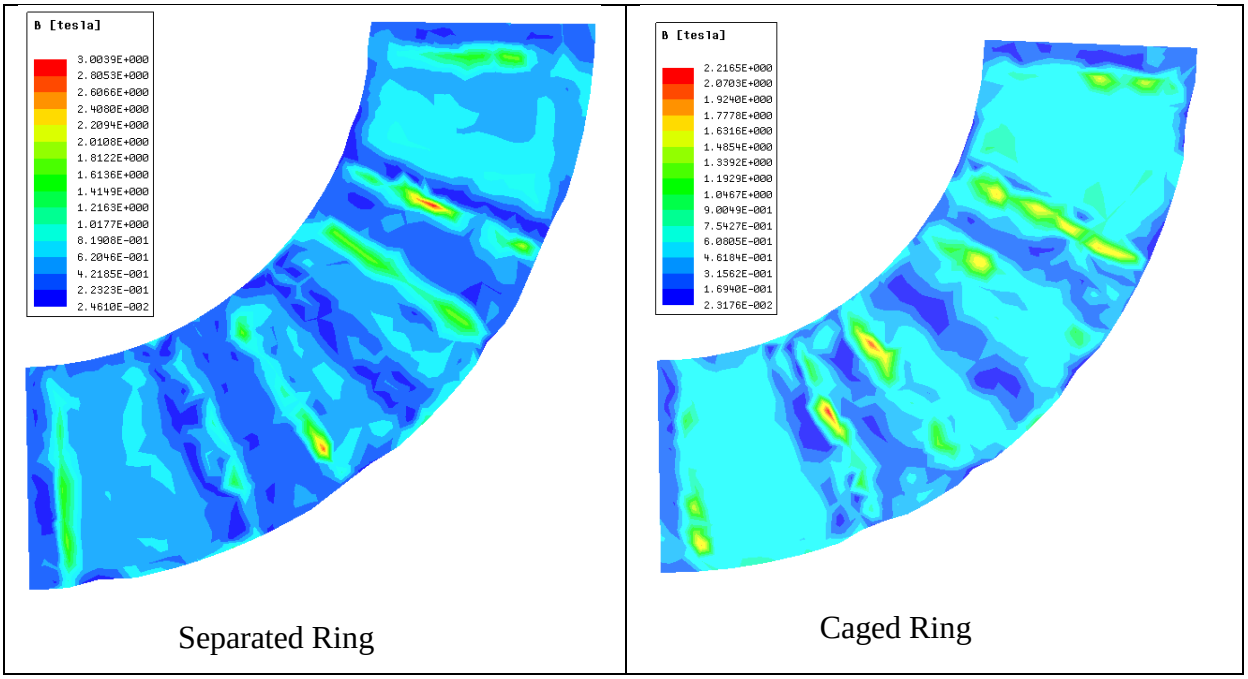

Fig 18 Air gap flux density of Type-2 AFPM motor

4.2.3 Magnetic Flux Lines

Magnetic Flux lines illustrates magnetic vector potential in the machine. Magnetic flux lines are compared for all the four motors. The rainbow color scale shows the vector potential in Wb/m. Flux lines analysis helps in understanding the locking mechanism of stator and rotor magnetic poles which could be helpful in designing motors with high performances.

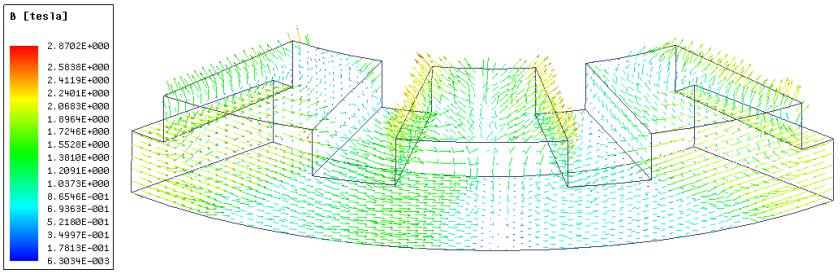

Fig 19 Stator Flux Lines in Type-1 AFPM motor.

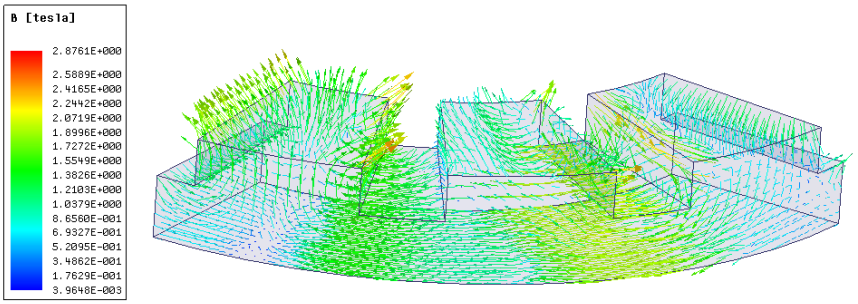

Fig 20 Stator Flux Lines in Type-2 AFPM motor.

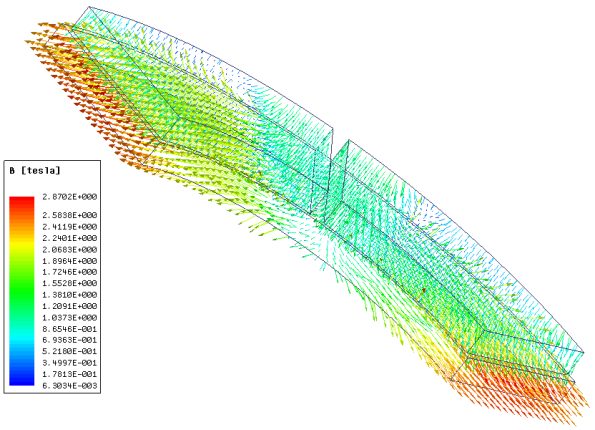

Fig 21 Rotor Flux Lines in Type-1 AFPM motor.

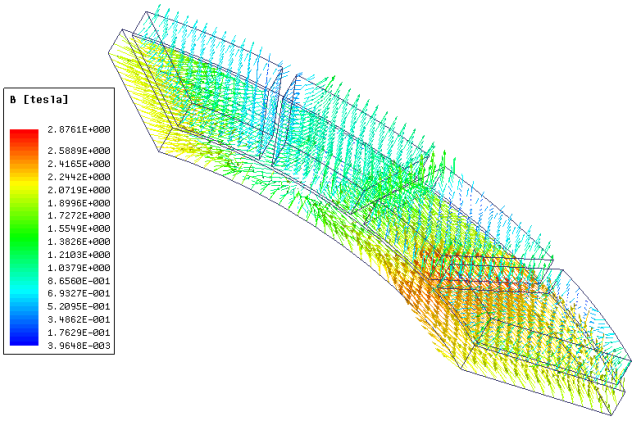

Fig 22 Rotor Flux Lines in Type-2 synchronous motor.

Magnetic flux vector representation of all four designed motors confirms the correct working of motors and helps one to understand the interaction between stator and rotor magnetic pole. The magneto static analysis of permanent magnet and induction motors designed were observed to identify behavior of travel path of flux lines throughout the motor and their interaction with each other.

For a continuous charge distribution in motion equation for Lorentz force would be

$$dF = dq(E + v \times B)$$

where dF is the force on charge dq. From this equation force density can be deduced as

$$f = \rho(E + v \times B)$$

$$f = \rho E + J \times B$$

where ρ is the charge density (charge per unit volume) and J is the current density. The total force in the volume integral over the charge distribution is

$$F = \iiint (\rho E + J \times B) dV$$

4.3 Transient analysis

The transient performance of the constructed four designs are examined for comparative analysis to understand parameters adjustment while making axial motor having optimal performance. Starting performance at no load are compared based on transient speed performance, transient torque and transient current. The performances are also analyzed at the load near to maximum bearable load for starting of the motor. All the simulations were carried out for 1 second with the time step of 0.5 milliseconds.

4.3.1 Starting and Synchronization

The starting performance of the constructed four designs are examined for comparative analysis. In this part of the chapter, the focus is on the starting of the motor and the time to reach the full rated speed is examined. For the starting analysis of the motor the plot for the Speed Vs. time is considered where input supply voltage is 240V for all the motors except Type-2 synchronous motor where supply voltage is 400V as type 2 separate ring synchronous motor was not starting at 240V. The moment of inertia of all the motors were set to $0.01 kgm^2$.The simulation was carried out for 1second and the step time was set to 0.5ms. While testing the motor for the starting performance it is tested for two different loading condition such as no-load and full load. The results for no-load and full-load are illustrated in fig 26 and fig 27 respectively.

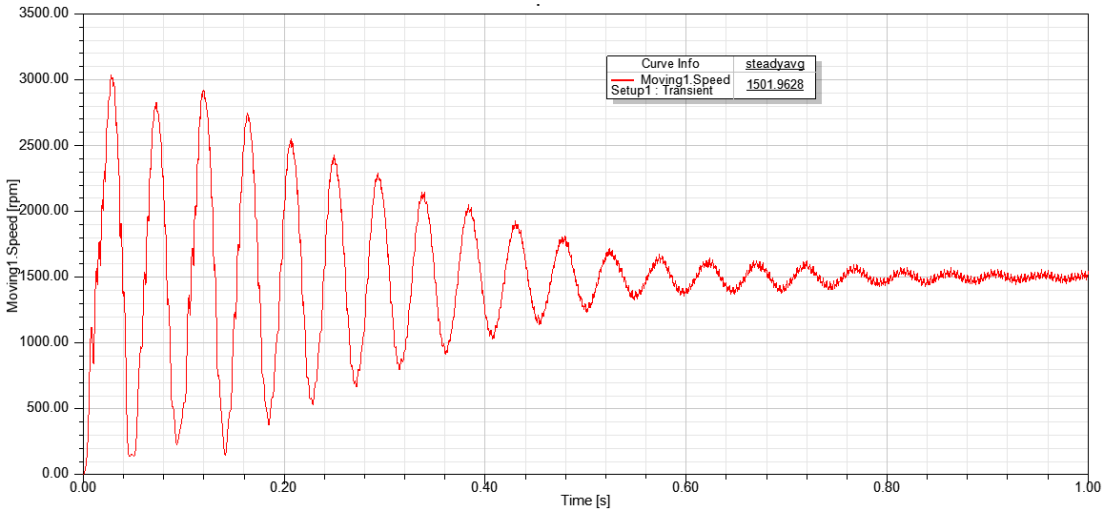

(a) Type-1 AFPM motor having separate ring rotor at No-load supplied with 240V

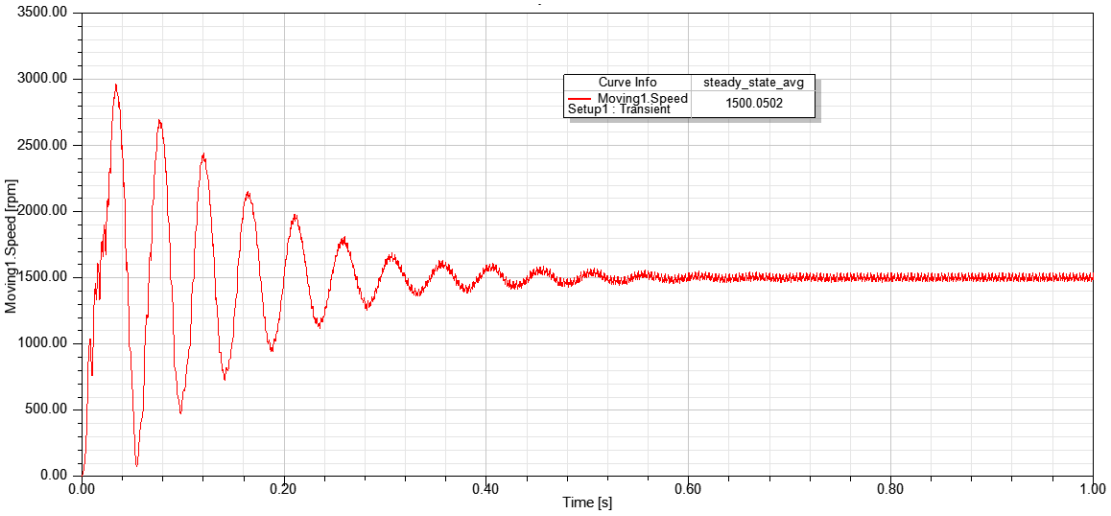

(b) Type-1 AFPM motor having caged ring rotor at No-load supplied with 240V

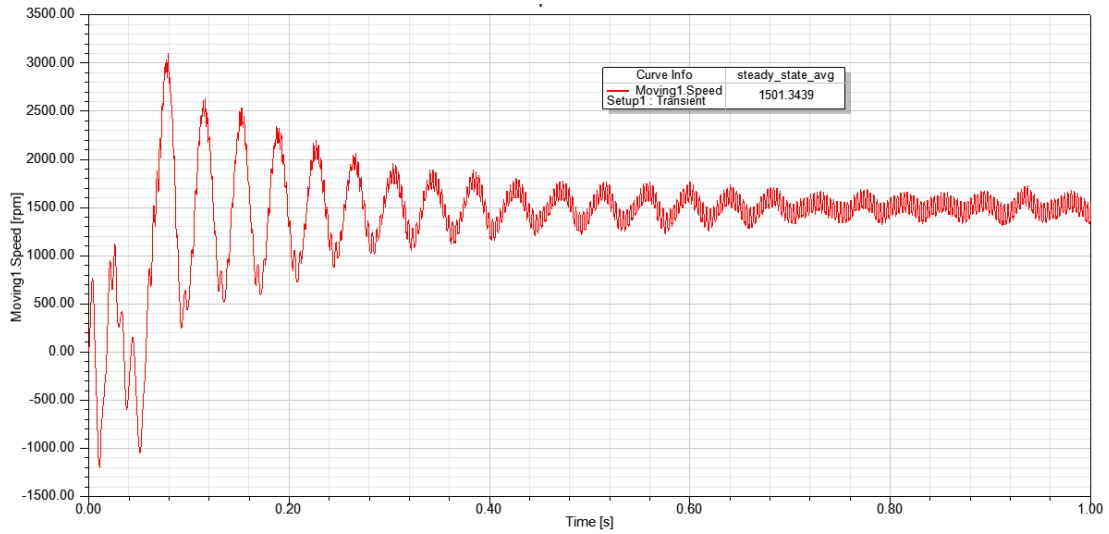

(c) Type-2 AFPM motor having separate ring rotor at No-load supplied with 400V

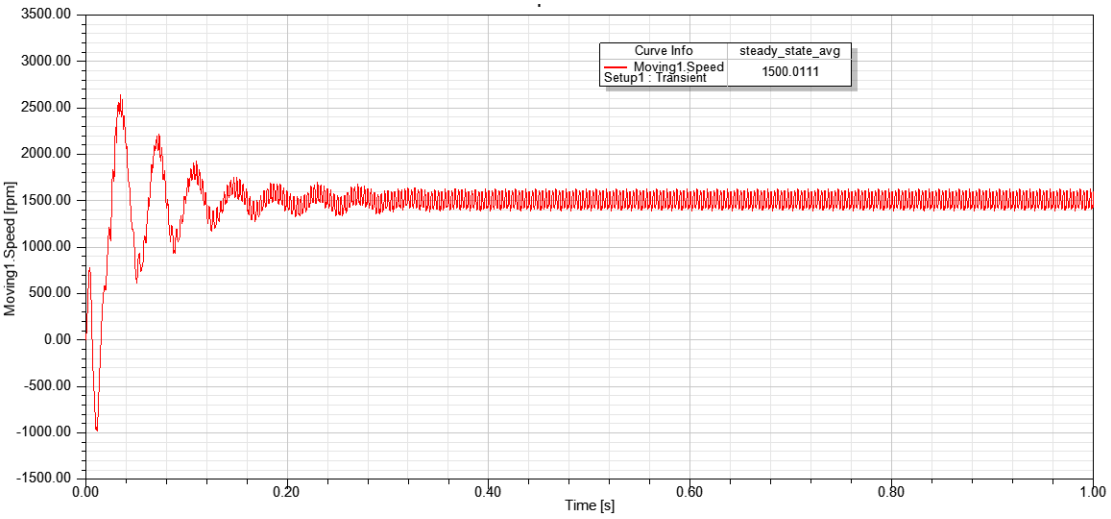

(d) Type-2 AFPM motor having caged ring rotor at No-load supplied with 400V

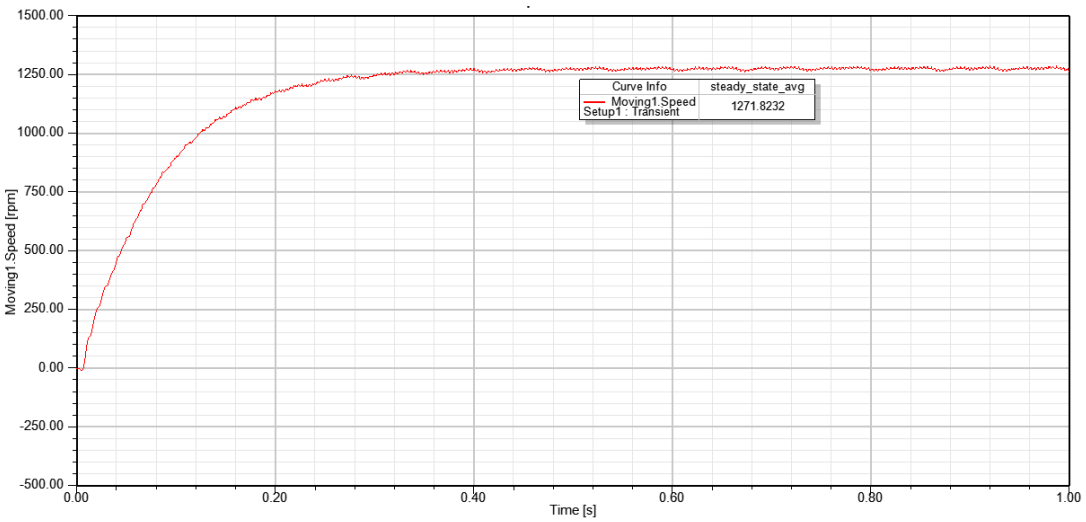

(e) Type-1 Induction motor having separate ring rotor at No-load supplied with 240V

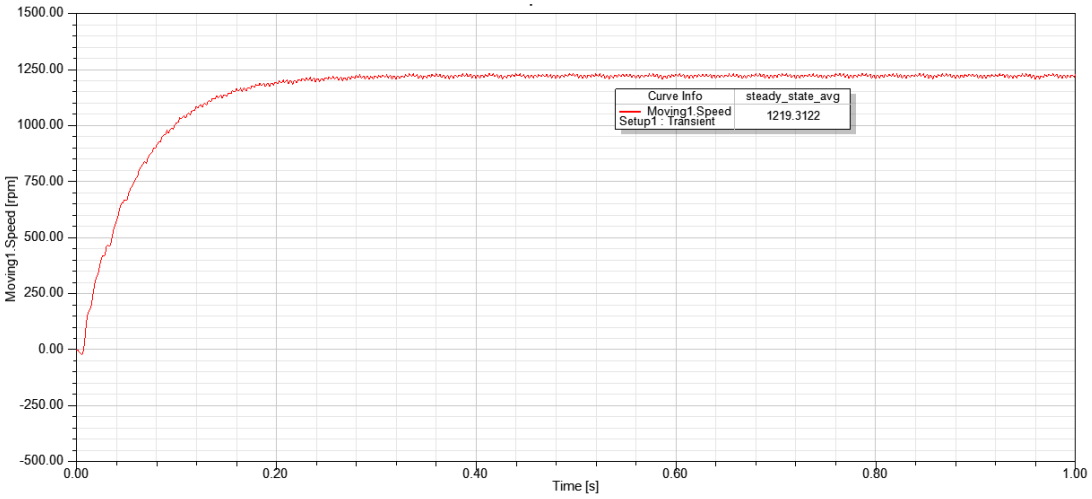

(f) Type-1 Induction motor having caged ring rotor at No-load supplied with 240V

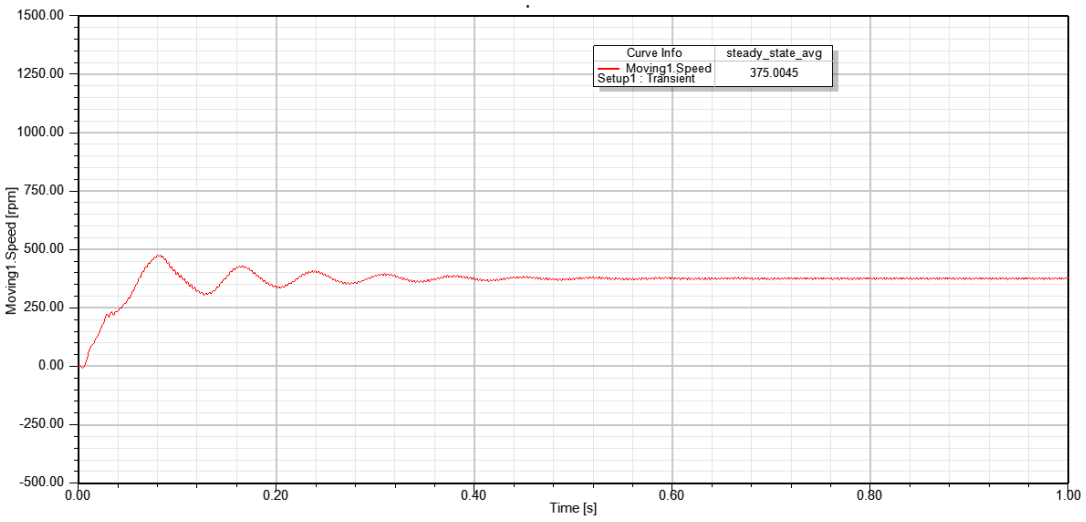

(g) Type-2 Induction motor having separated ring rotor at No-load supplied with 240V

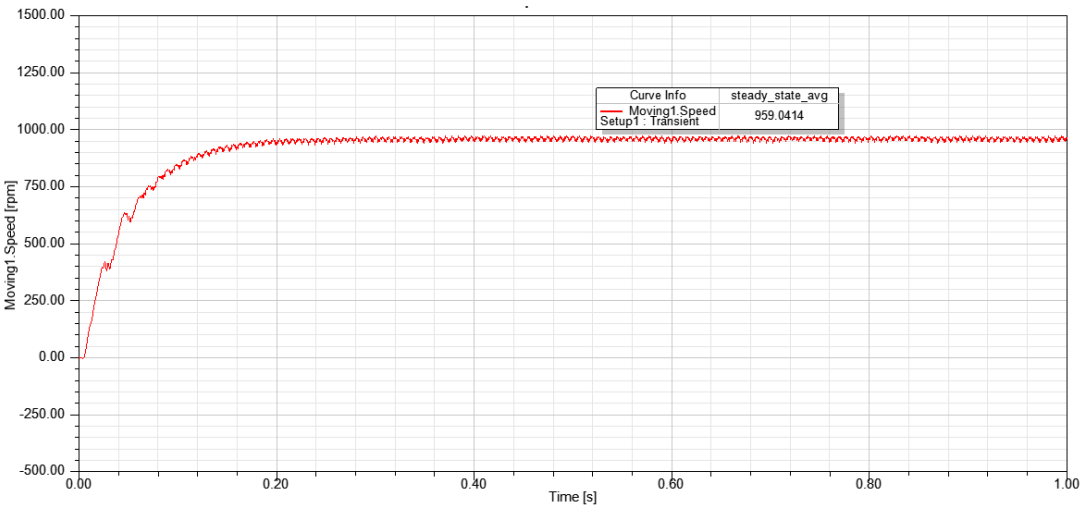

(h) Type-2 Induction motor having caged ring rotor at No-load supplied with 240V

Fig 23 Speed Vs. Time at No-load.

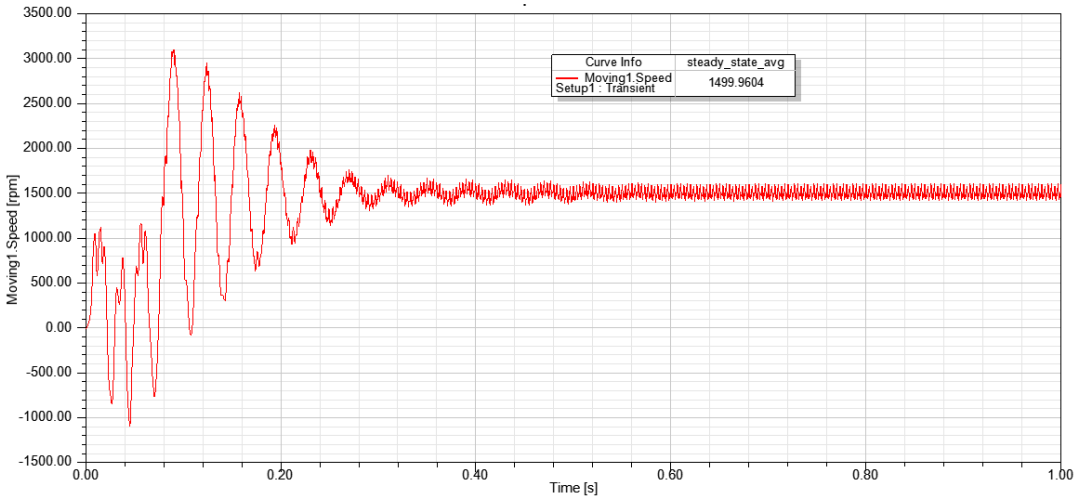

(a) Type-1 AFPM motor having separated ring rotor at 17Nm supplied with 400V

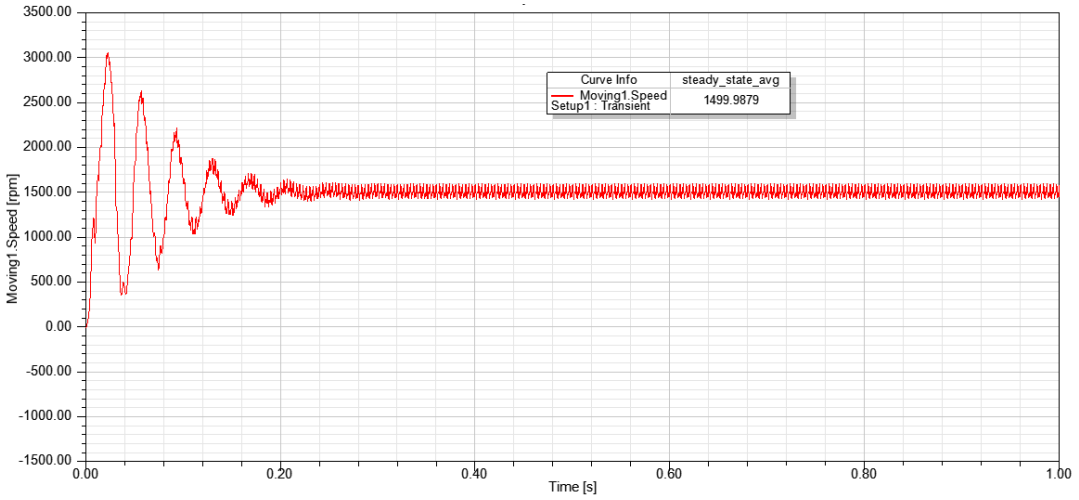

(b) Type-1 AFPM motor having caged ring rotor at 17Nm supplied with 400V

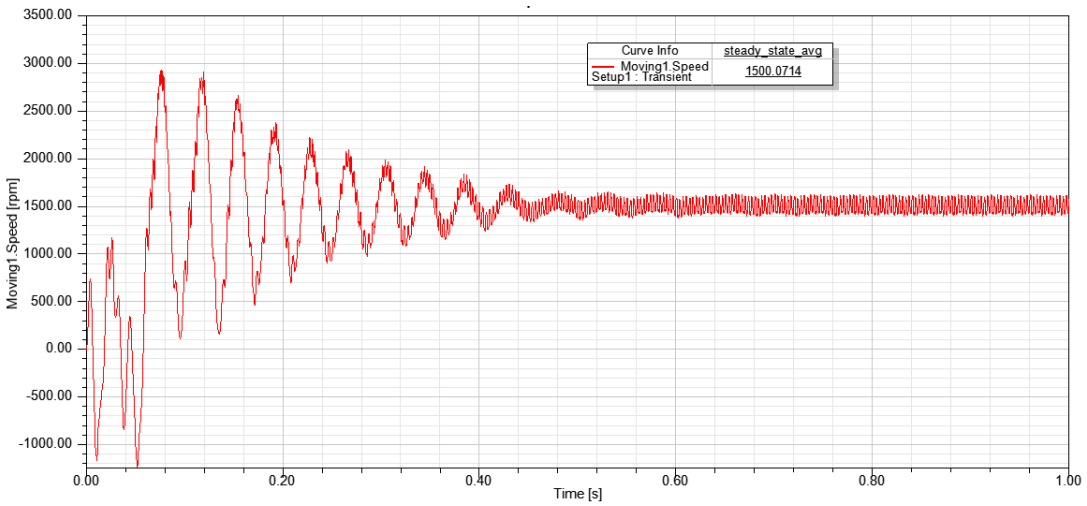

(c) Type-2 AFPM motor having separated ring rotor at 17Nm supplied with 400V

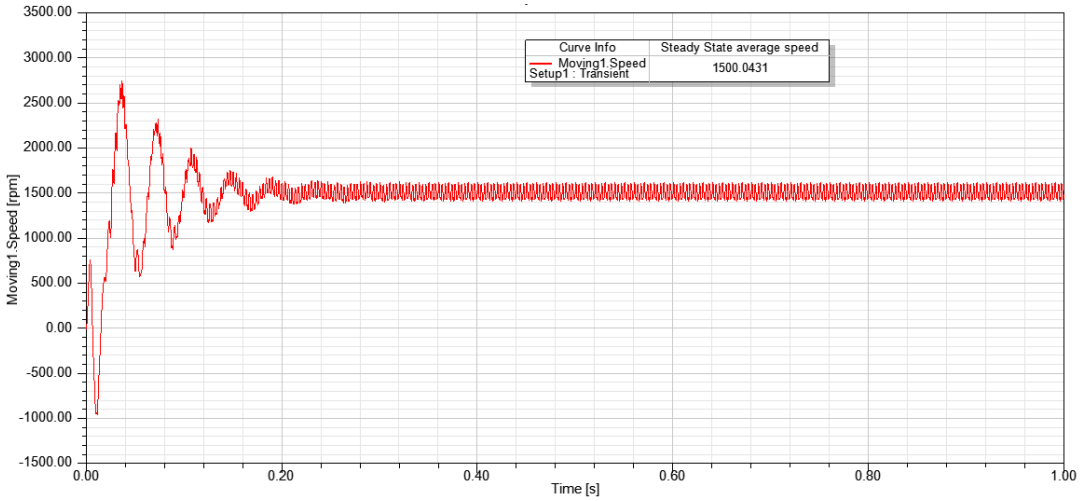

(d) Type-2 AFPM motor having caged ring rotor at 17Nm supplied with 400V

Fig 24 Speed Vs. Time at 17Nm.

Caged ring rotors were proven to be better than separated rings rotors as the transient as well as steady state response improves with better current flow in caged rotor rings. Also separated ring s rotor require more voltage to start in comparison to separated ring rotors.

When both the design types were operated without magnets as induction motors has lower steady state speed compared to that when operated as synchronous motors. Fig 24(c) and Fig 24 (d) shows that design type 1 has better starting performance than type 2 in terms of achieving steady state earlier with less fluctuations and less slip.

Design type 1 also proven to be better when both the motors were operated with magnets as synchronous motors. Design type 1 achieves synchronous speed much faster than design type 2 in fact design type 2 wasn't starting at 240 V and require higher voltage of 300V. Rising time of type 1 synchronous motor is higher than type 2 synchronous motor.

From the speed plots, it is observed that design type-1 has better performance than design type-2. The synchronous motor design and induction motor design of type-1 are better than their counterparts. The induction motor design however has less overshoot and less settling time.

The speed vs time graphs of axial flux permanent magnet motors under different load conditions in Figure illustrates the distinction between the performances of motors.

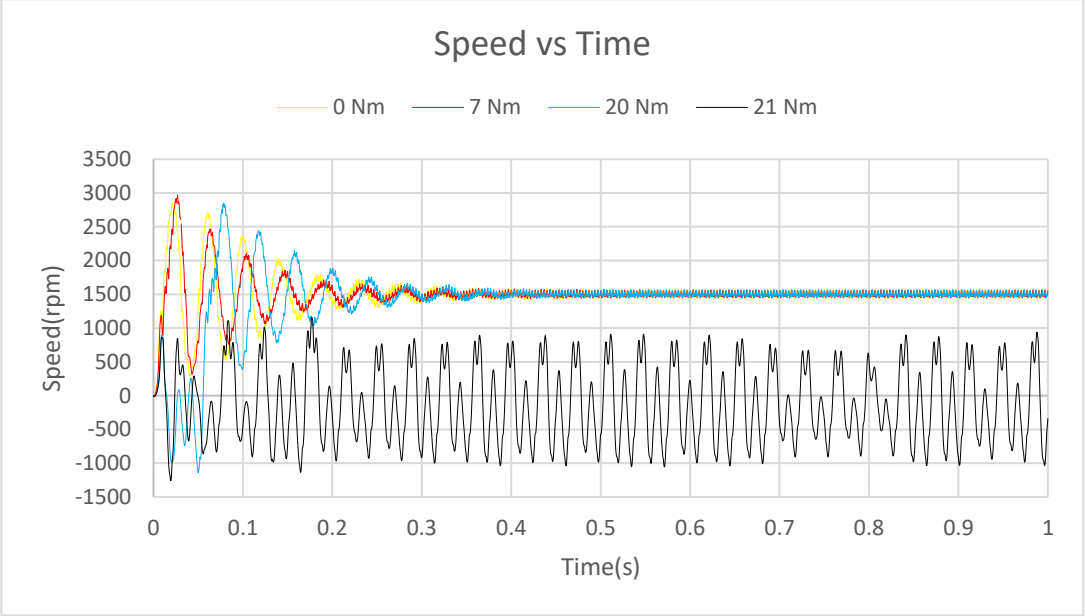

(a) Type-1 AFPM Motor having separated ring rotor supplied with 310V

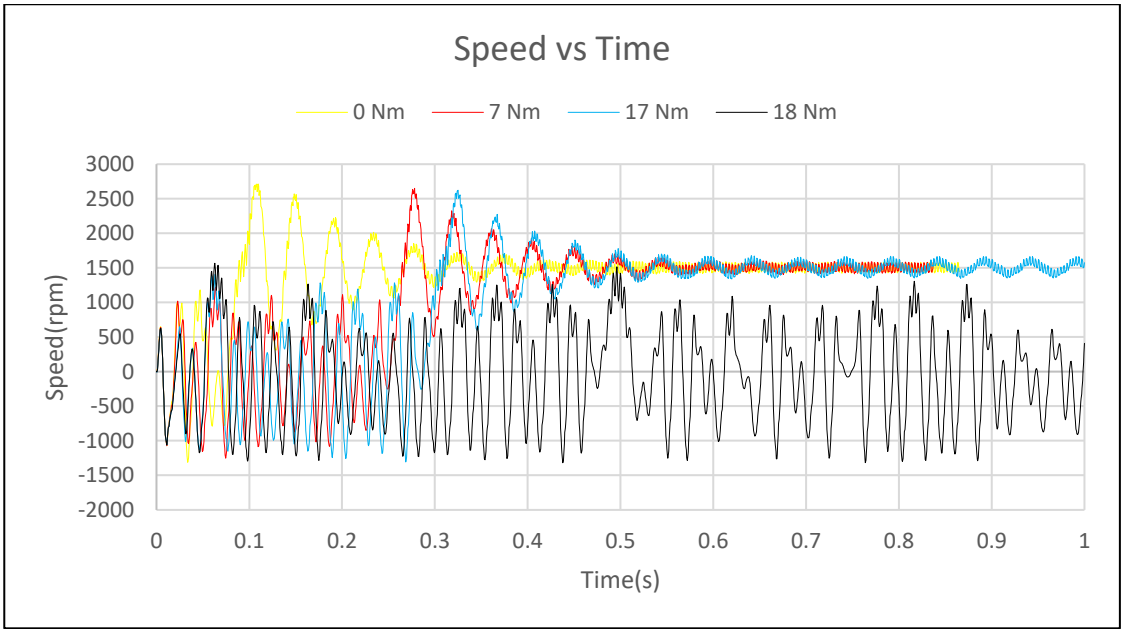

(b) Type-2 AFPM Motor having separated ring rotor supplied with 310V

Fig 25 Speed Vs Time at different load

From the Fig 25 it was founded that the design type-1 of axial flux permanent magnet motor can bear maximum load of about 20Nm as it is not starting under the load of 21Nm while the design type-2 of axial flux permanent magnet motor have less maximum load driving capability of about 17Nm and is not starting under 18Nm.

4.3.2 Transient Torque

The torque vs time graph in figure confirms that synchronous motor designs has far higher starting torque than induction motor designs. Also design type-2 of axial motors have higher starting torque and has more fluctuations in steady state in comparison with design type-1 which is due to presence of more induction rings in design type 2. So, design type-1 more stable in steady state.

Also, comparing the induction motor designs of type 1 and type 2 having same input voltage of 240V for separated and caged rotor shows that caged rotor have higher starting torque and better transient response.

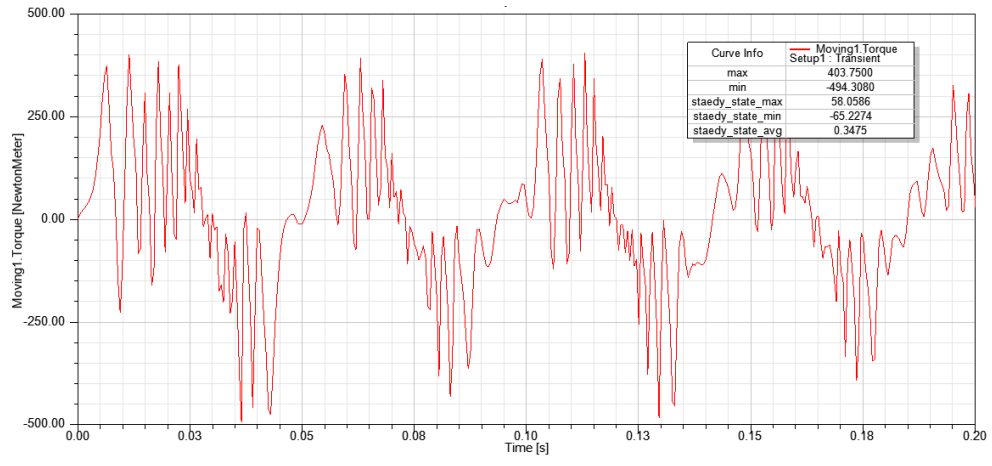

Transient State

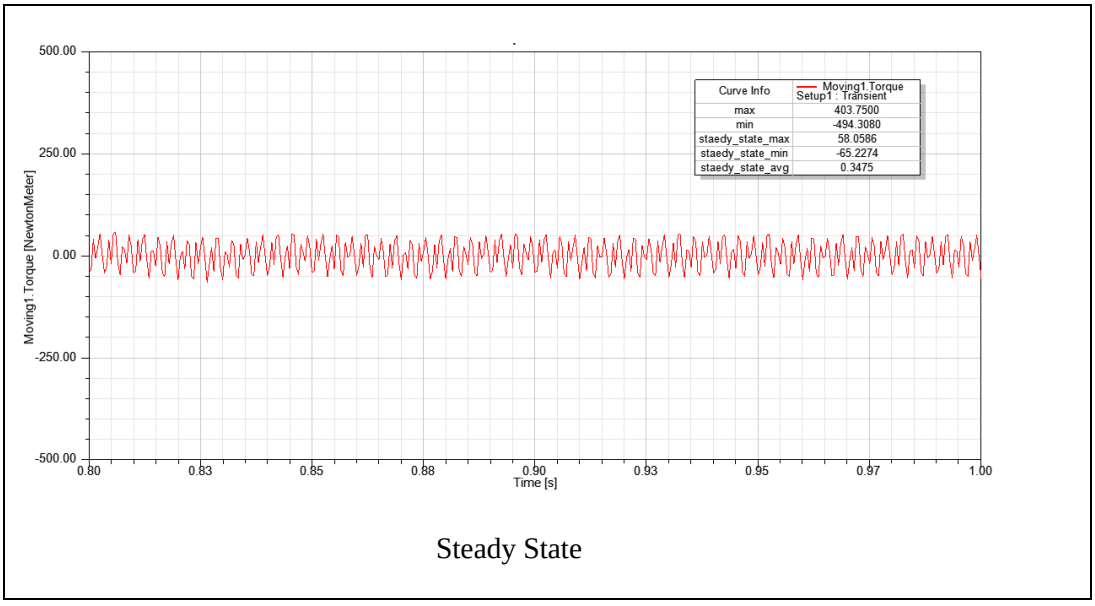

Steady State

(a) Type-1 AFPM motor having separated ring rotor at No load supplied with 240V

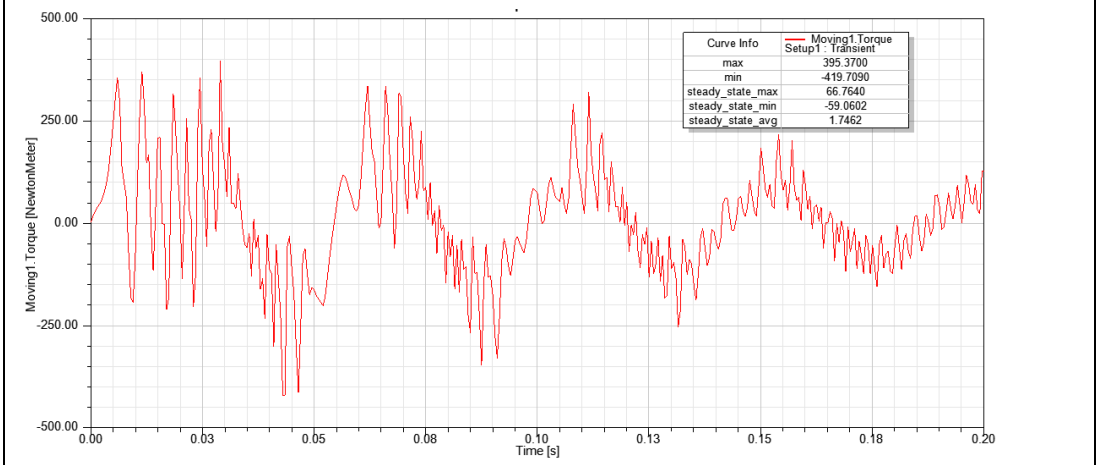

Transient State

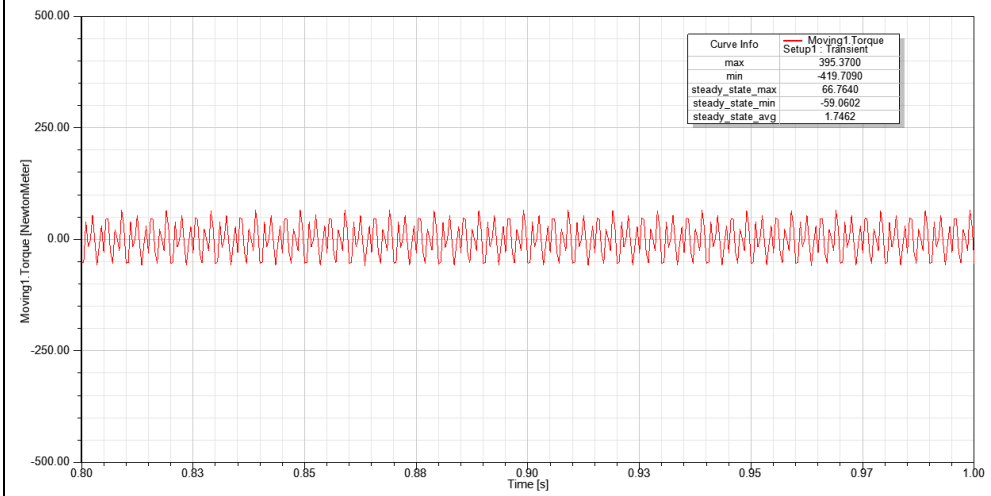

Steady State

(b) Type-1 AFPM motor having caged ring rotor at No load supplied with 240V

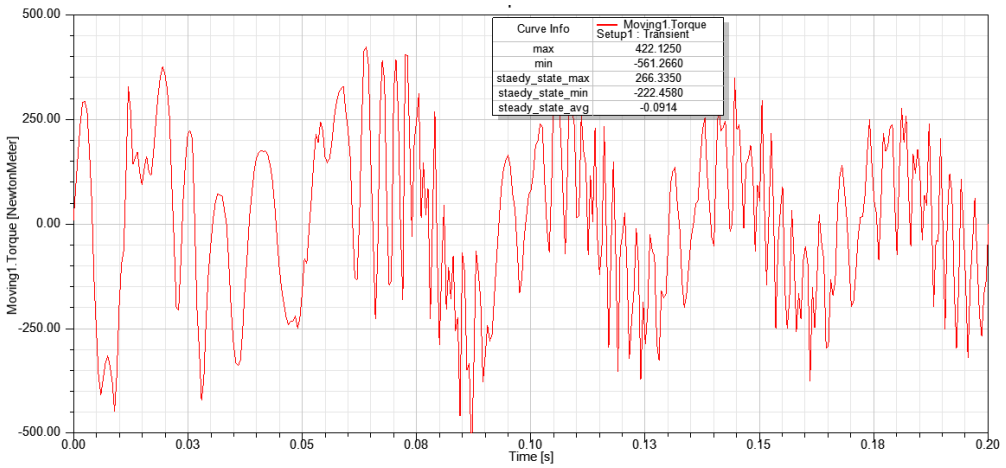

Transient State

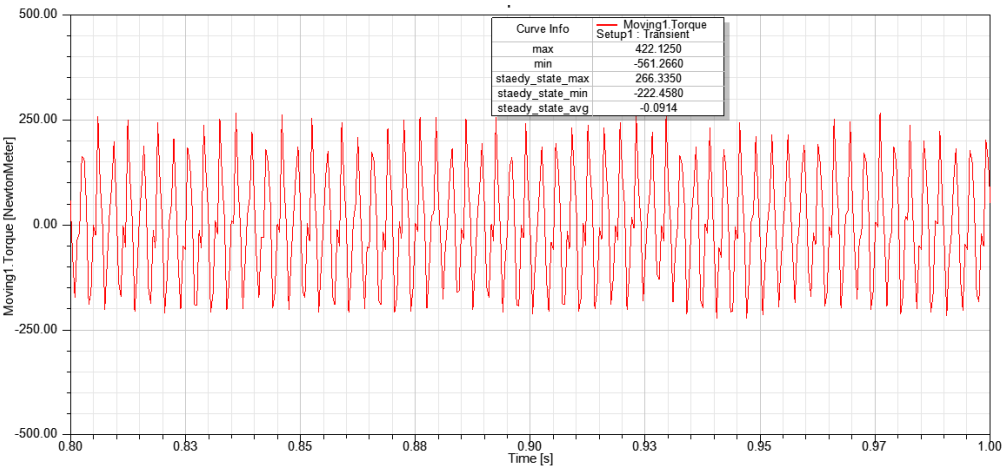

Steady State

(c) Type-2 AFPM motor having separated ring rotor at No load supplied with 400V

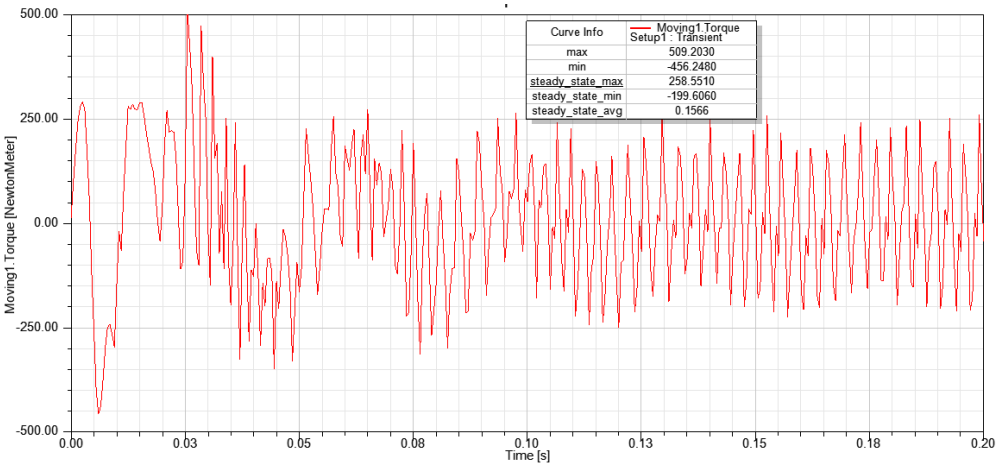

Transient State

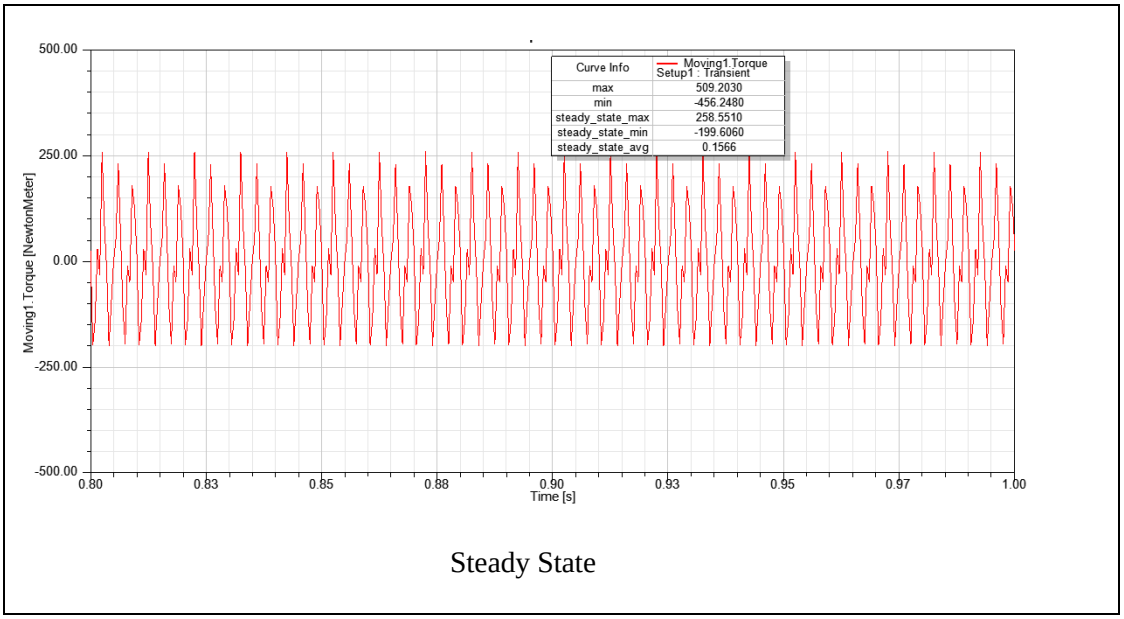

Steady State

(d) Type-2 AFPM motor having caged ring rotor at No load supplied with 400V

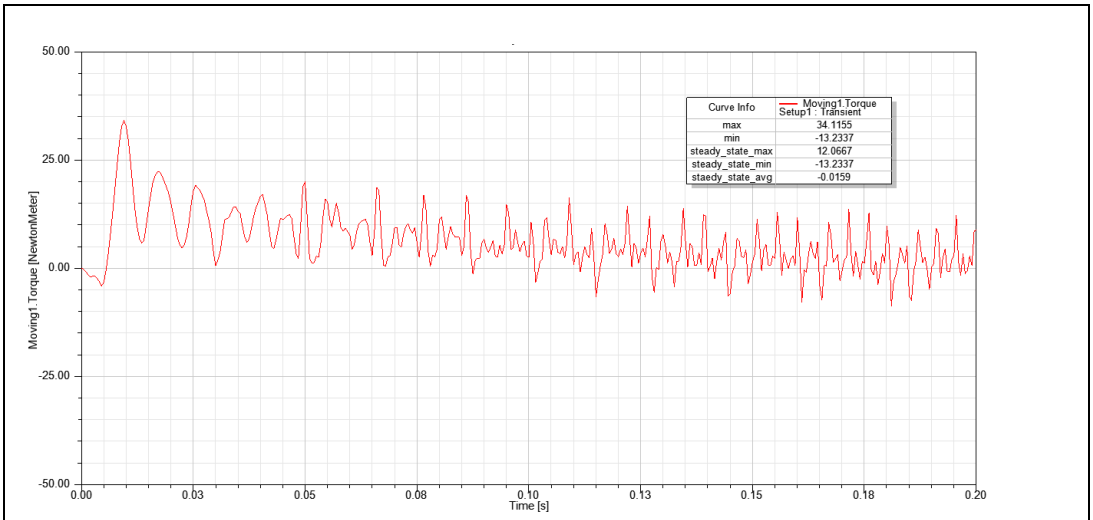

Transient State

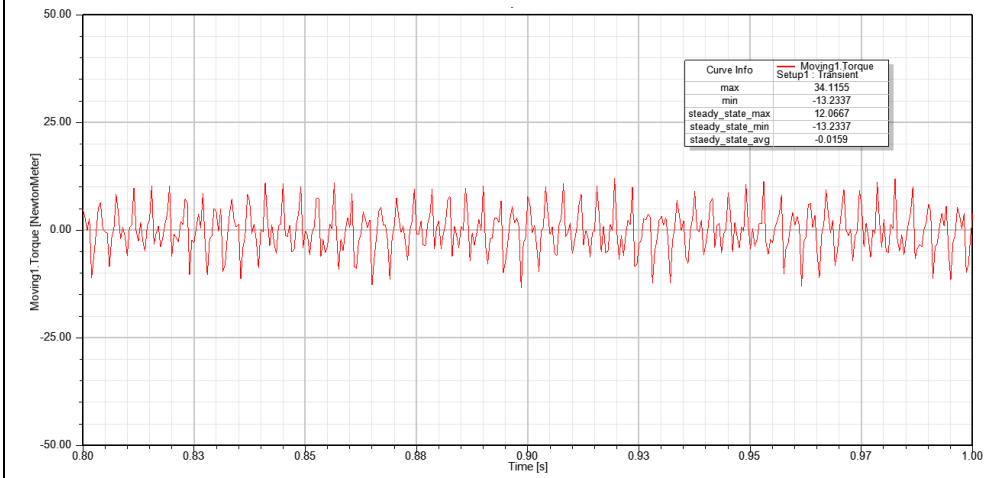

Steady State

(e) Type-1 Induction motor having separated ring rotor at No load supplied with 240V

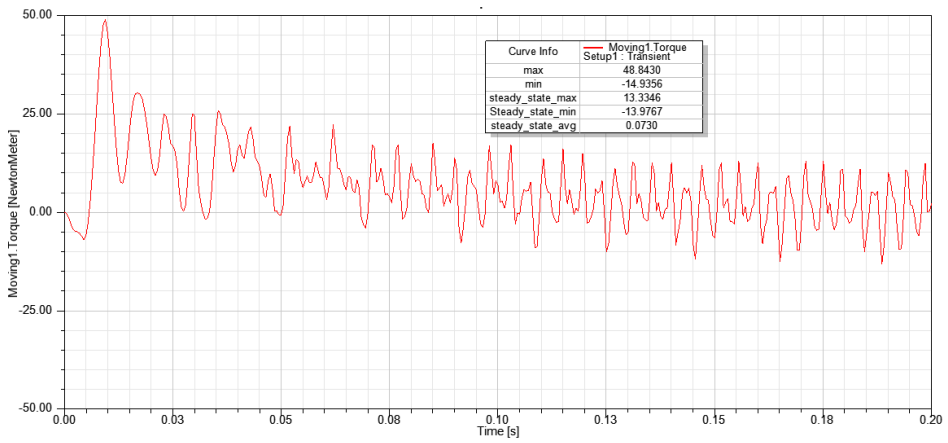

Transient State

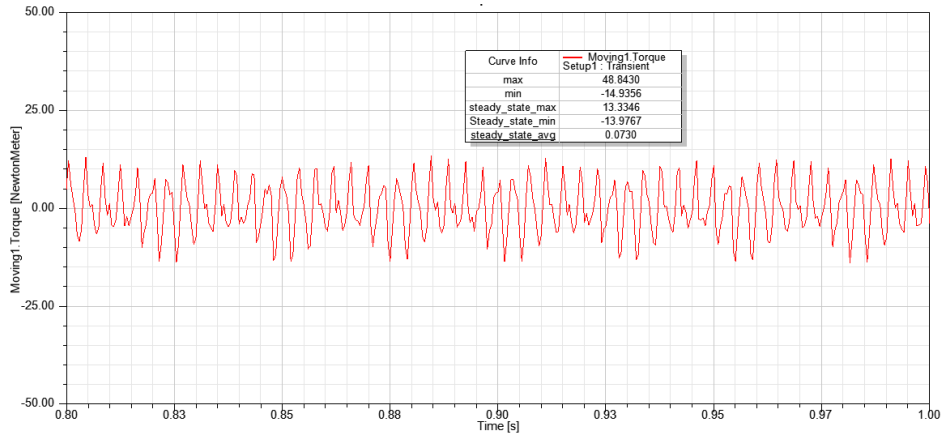

Steady State

(f) Type-1 Induction motor having caged ring rotor at No load supplied with 240V

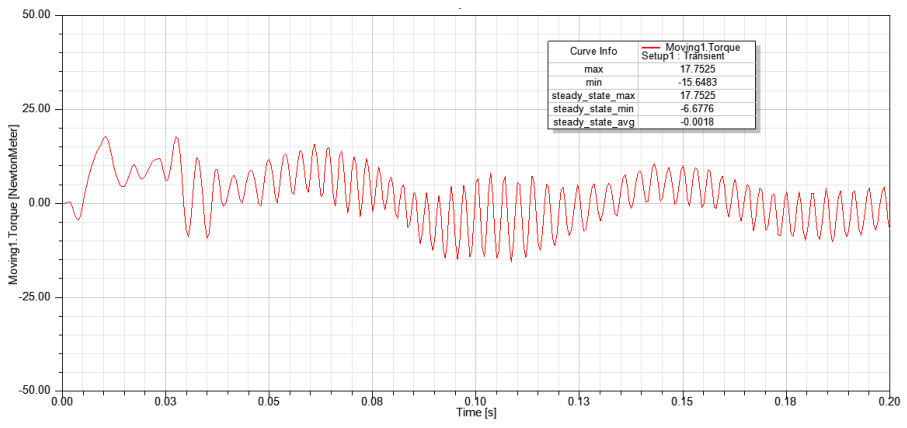

Transient State

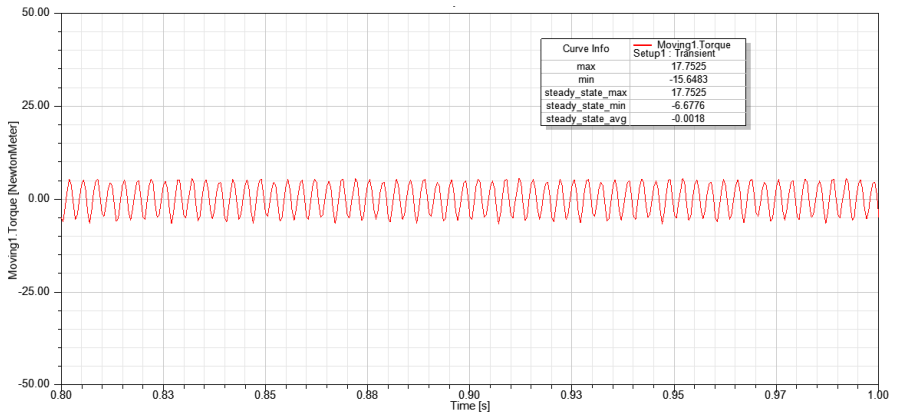

Steady State

(g) Type-2 Induction motor having separated ring rotor at No load supplied with 240V

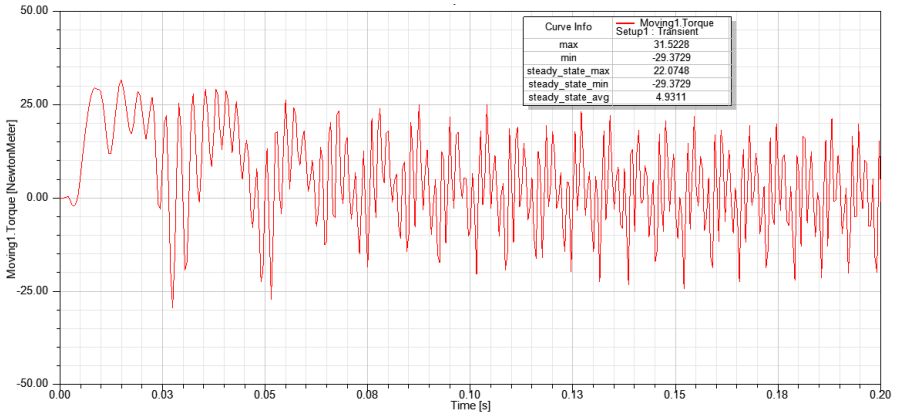

Transient State

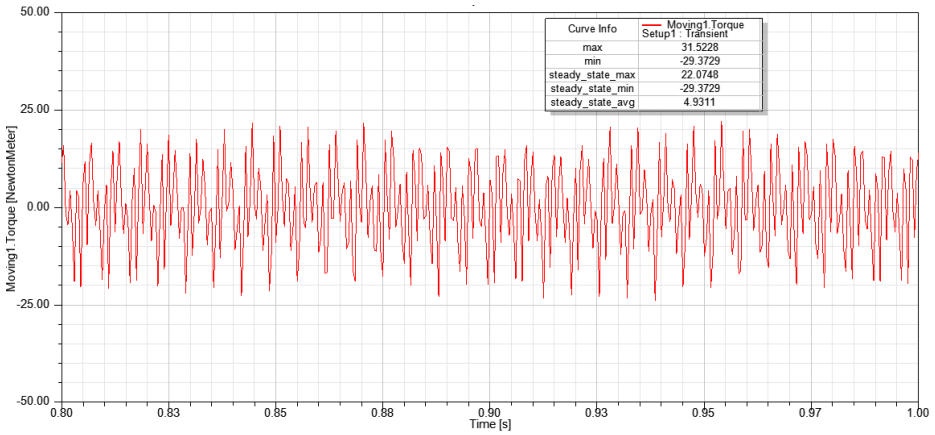

Steady State

(h) Type-2 Induction motor having caged ring rotor at No load supplied with 240V

Fig 26. Torque vs time at No load

Torque vs time at 17Nmload torque is shown for AFPM motor in Figure 27 where all of them are fed with 400V.

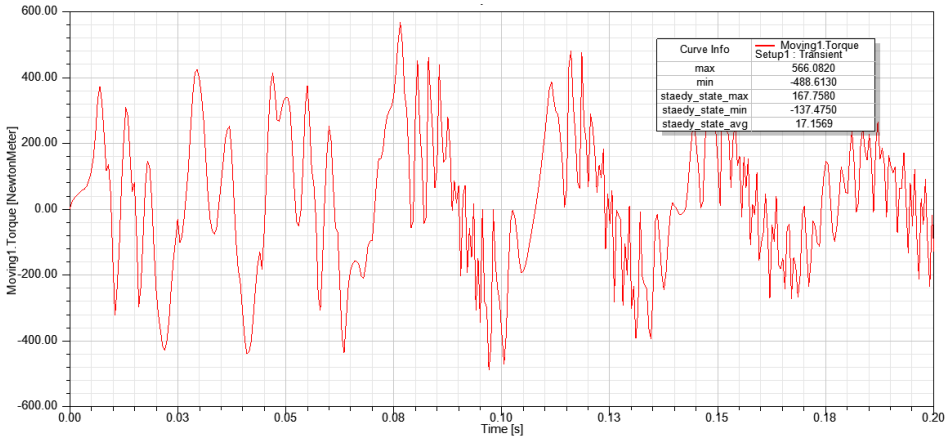

Transient State

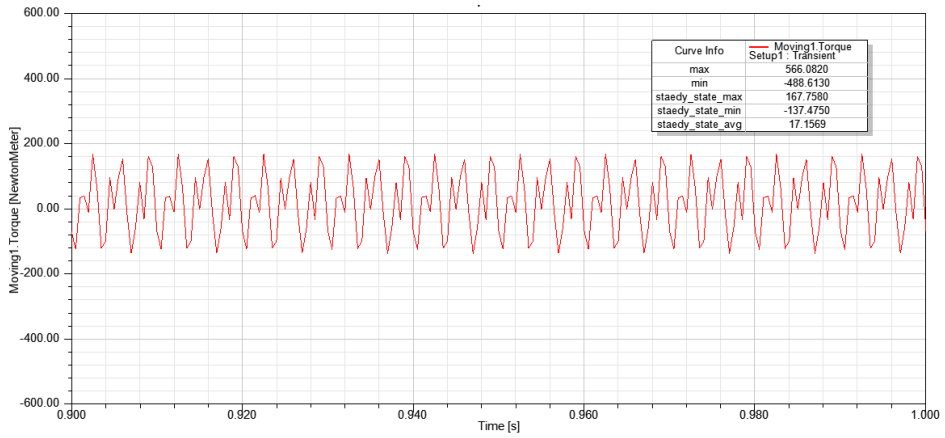

Steady State

(a) Type-1 AFPM motor having separated ring rotor at 17Nm supplied with 400V

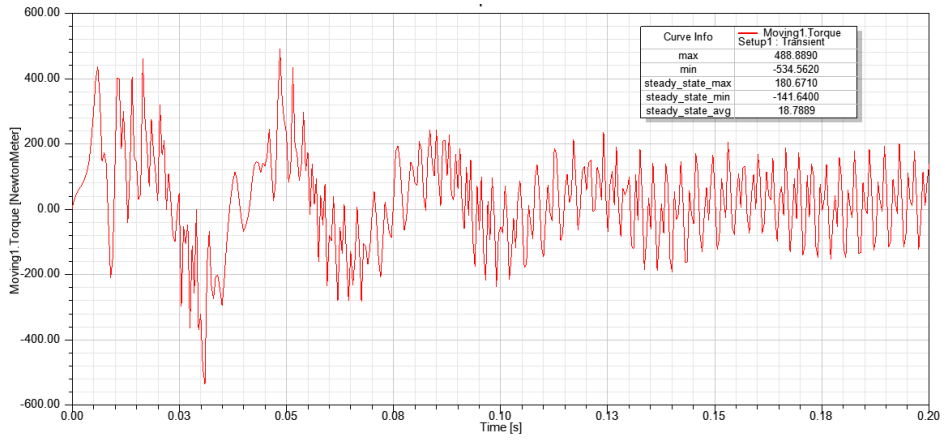

Transient State

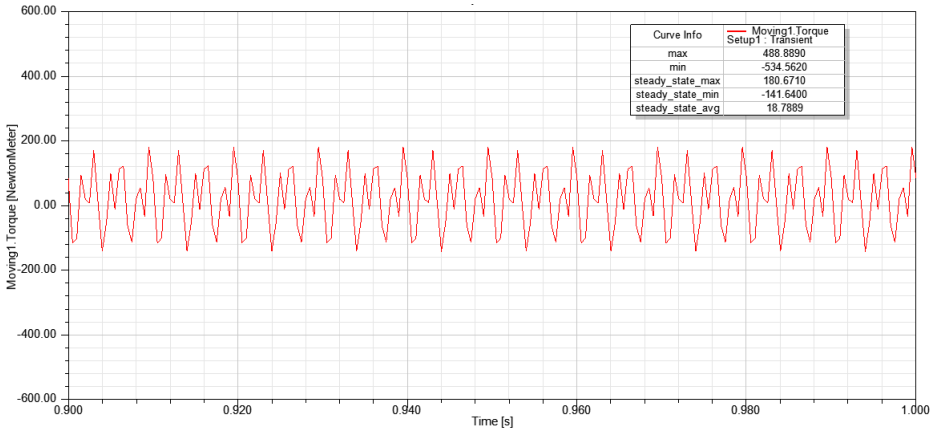

Steady State

(b) Type-1 AFPM motor having caged ring rotor at 17Nm supplied with 400V

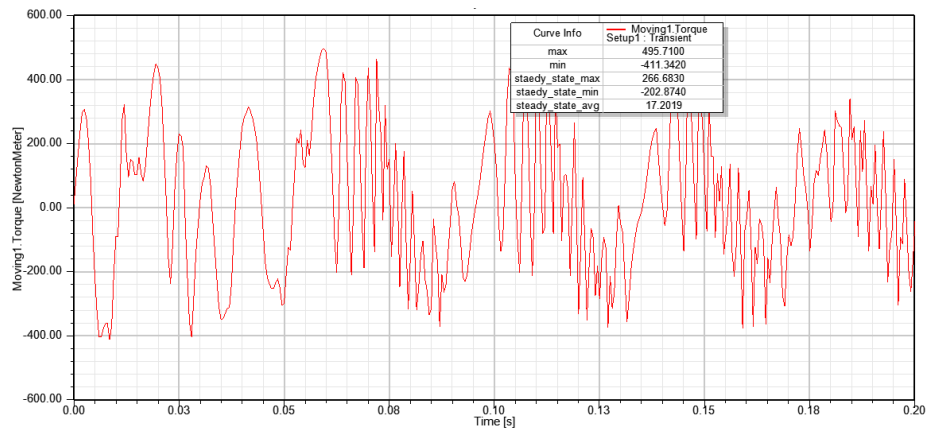

Transient State

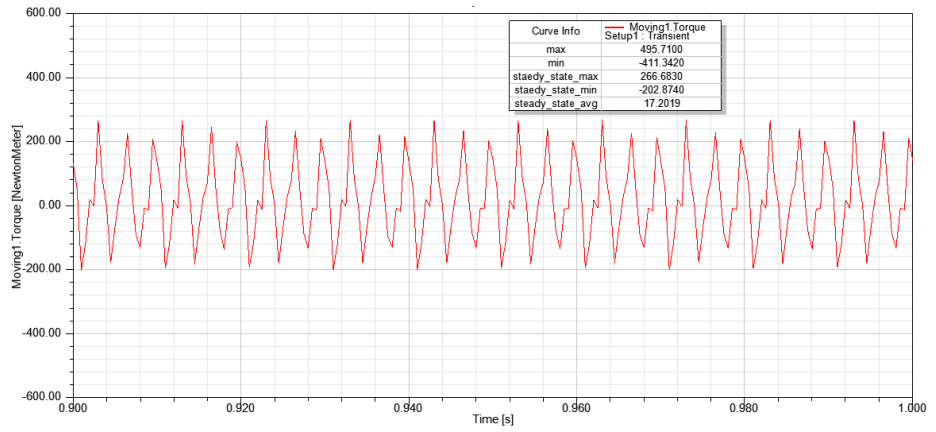

Steady State

(c) Type-2 AFPM motor having separated ring rotor at 17Nm supplied with 400V

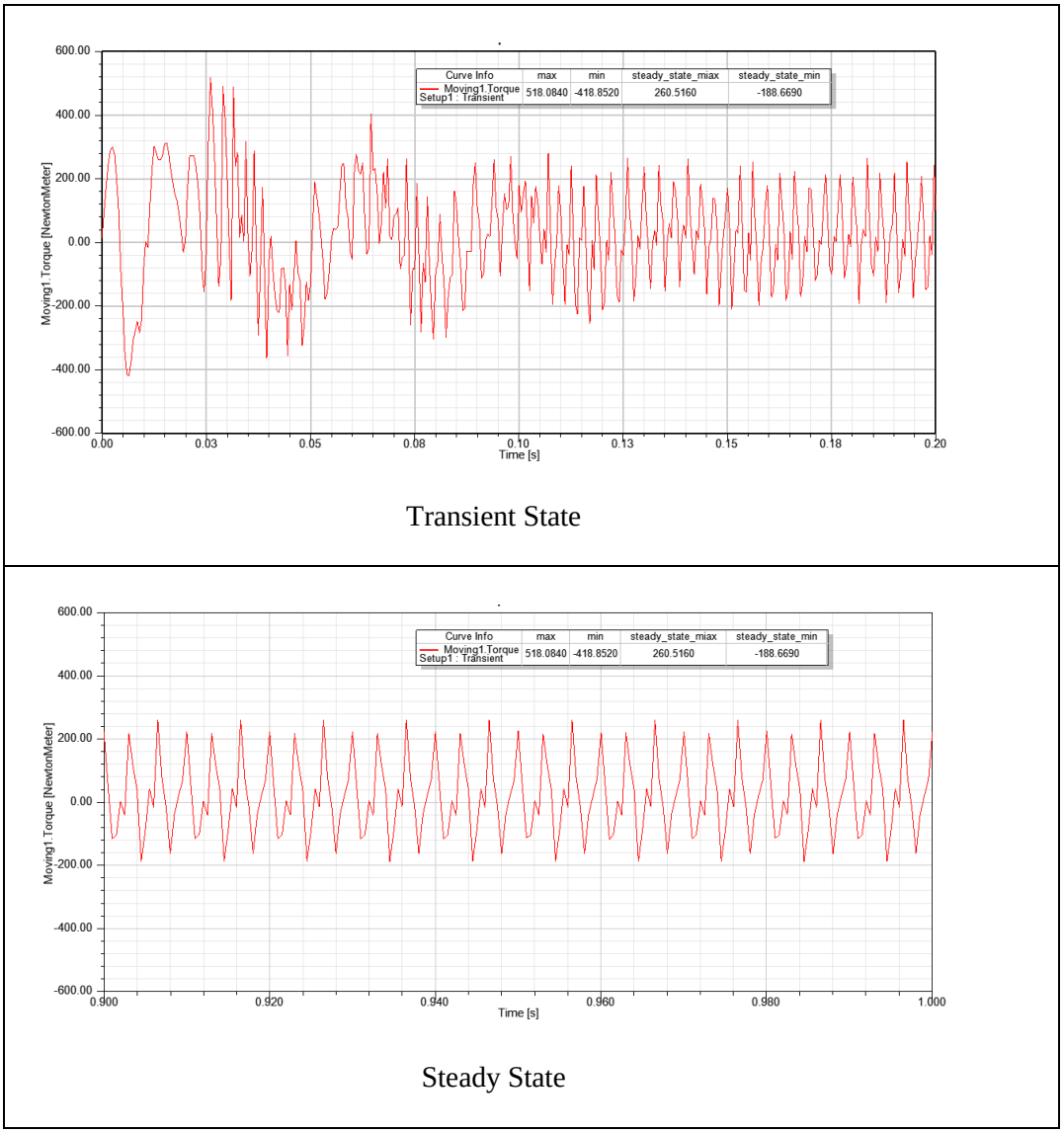

(d) Type-2 AFPM motor having caged ring rotor at 17Nm supplied with 400V

Fig 27 Torque Vs Time at 17Nm load.

The torque vs time graph at no load and 17 Nm load shows higher starting torque and explains the better steady state response of design type-1 compared to design type-2 as it has less fluctuations. The use of caged ring rotor is also reducing the fluctuations in torque to some extent as maximum moving torque value in both the direction is reducing in steady state. The fluctuations shown are however large in both the designs, but this is because of low inertia 0.01Kgm^2 taken for all the designs to reduce the simulation time and have early startup.

4.3.3 Harmonic Content in Current Waveform

The transients for winding current in all the four designs under no load condition in Fig 27 are presented. It was founded that design type-1 have good transient response as it take less time to achieve steady state. The winding currents are verified to be sinusoidal or balanced in terms of phase shift and magnitude for the appropriate working and performance of the designs.

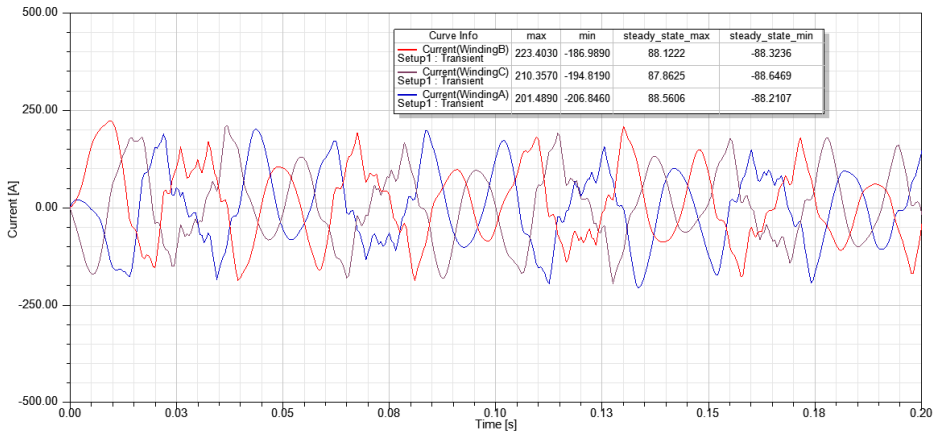

Transient State

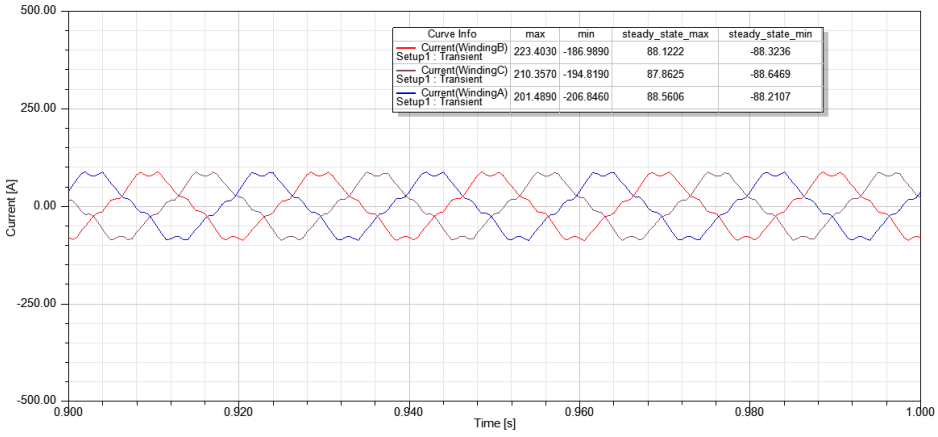

Steady State

(a) Type-1 AFPM motor having separated ring rotor at No Load supplied with 240V

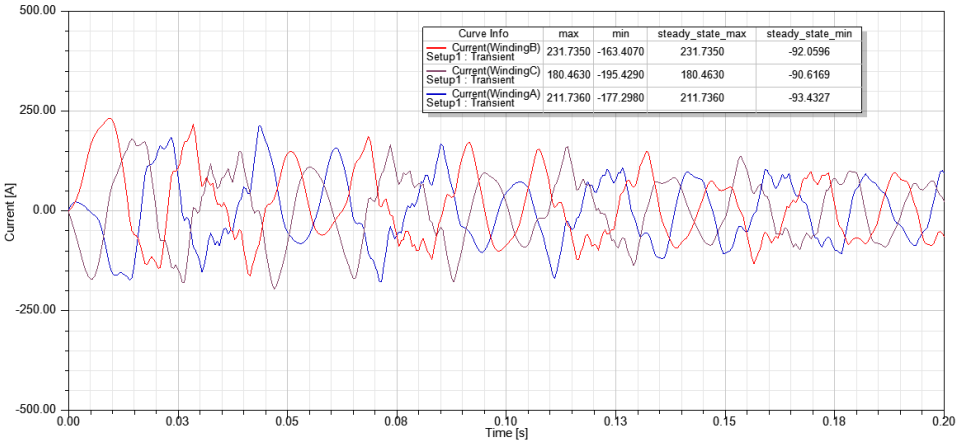

Transient State

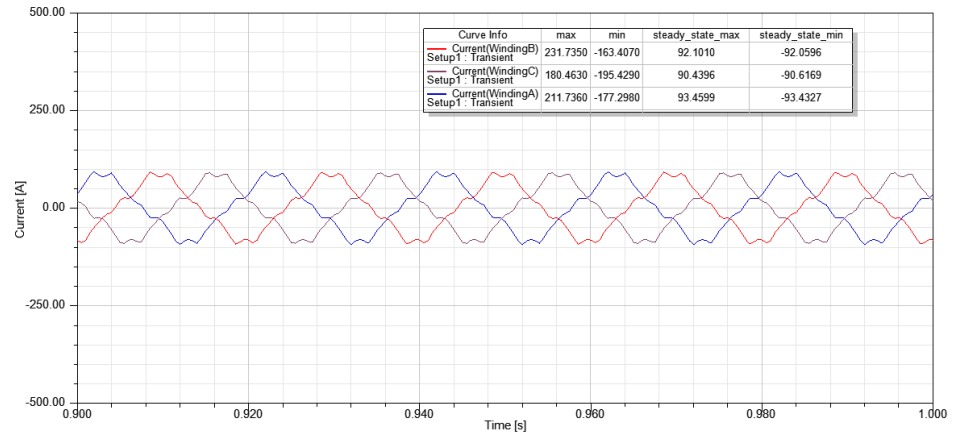

Steady State

(b) Type-1 AFPM motor having caged ring rotor at No Load supplied with 240V

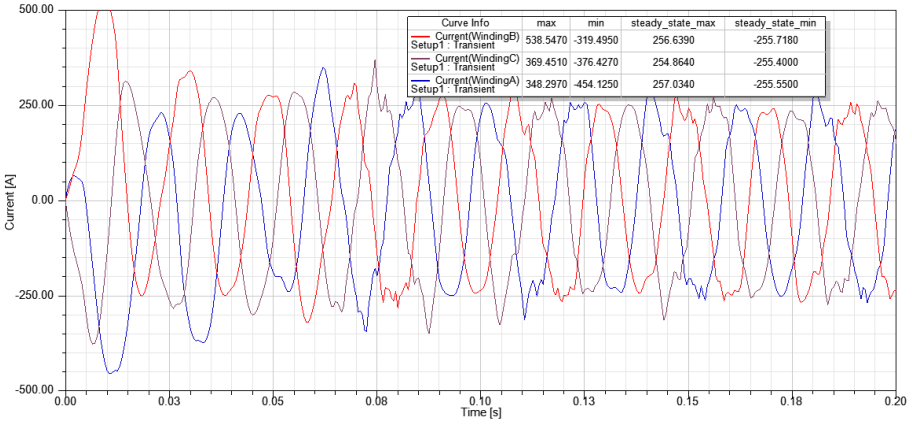

Transient State

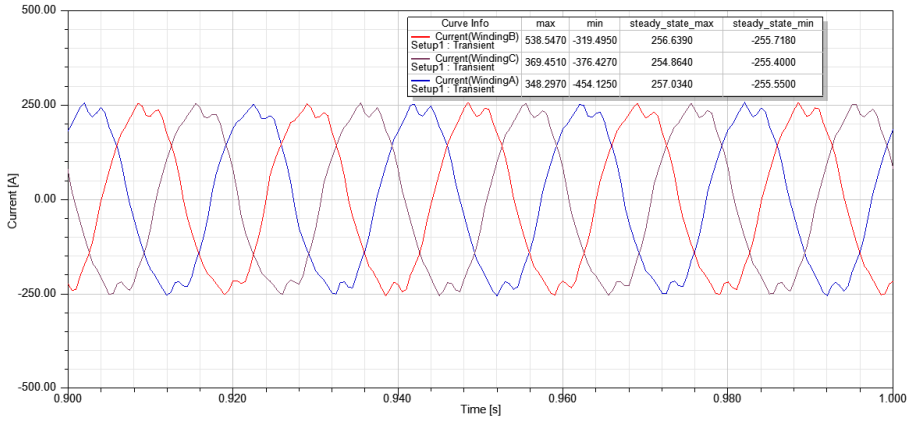

Steady State

(c) Type-2 AFPM motor having separated ring rotor at No Load supplied with 400V

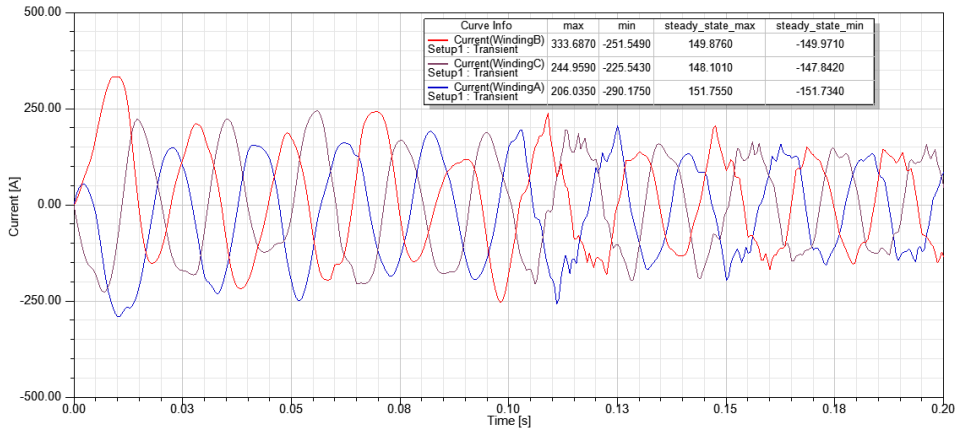

Transient State

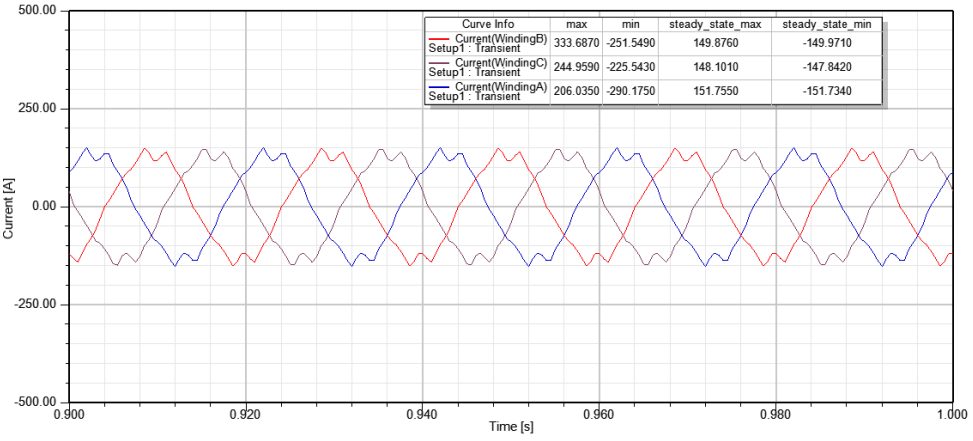

Steady State

(d) Type-2 AFPM motor having caged ring rotor at No Load supplied with 400V

Fig 28 Winding current Vs Time at No Load

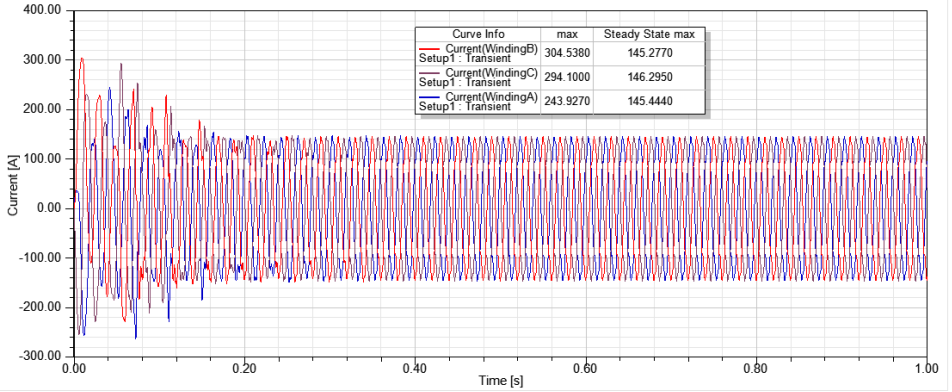

Winding Current in Type-1 AFPM motor having separated ring rotor at 20Nm

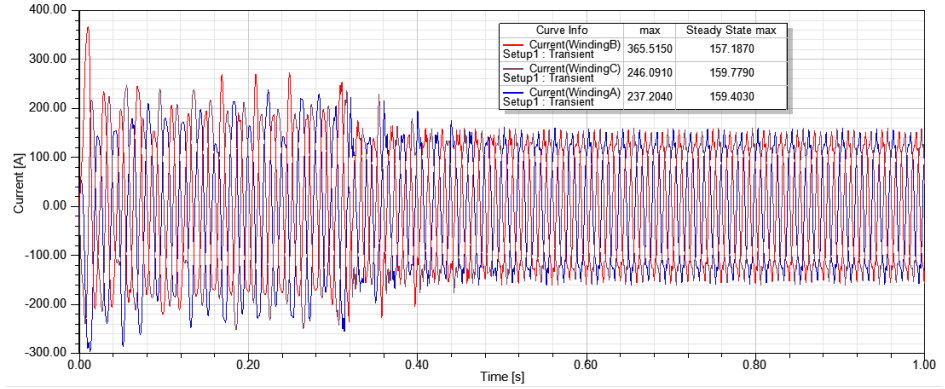

Winding Current in Type-2 AFPM motor having separated ring rotor at 17Nm

Fig 29 Winding Current at Load

From the current waveforms it is clarified that design type-1 have lower harmonic content than design type-2 during startup. Also, the harmonics improves when design are operated with caged ring rotor instead of separated ring rotor. The harmonic content is far high under load condition and comparatively design type-2 have higher starting harmonics when compared to design type-1 under load of 17Nm condition with larger transient state.

4.2.5 Current distribution in rotor rings

The current distribution plays a vital role in starting performance of motor which is comparatively different in separate ring and cage ring rotor. Therefore, current densities in induction motor designs of Type-1 and Type-2 are shown in Figures. The current density is the rotor rings throughout the simulation period are shown in the following figures at different interval of time for comparative analysis of starting performance.

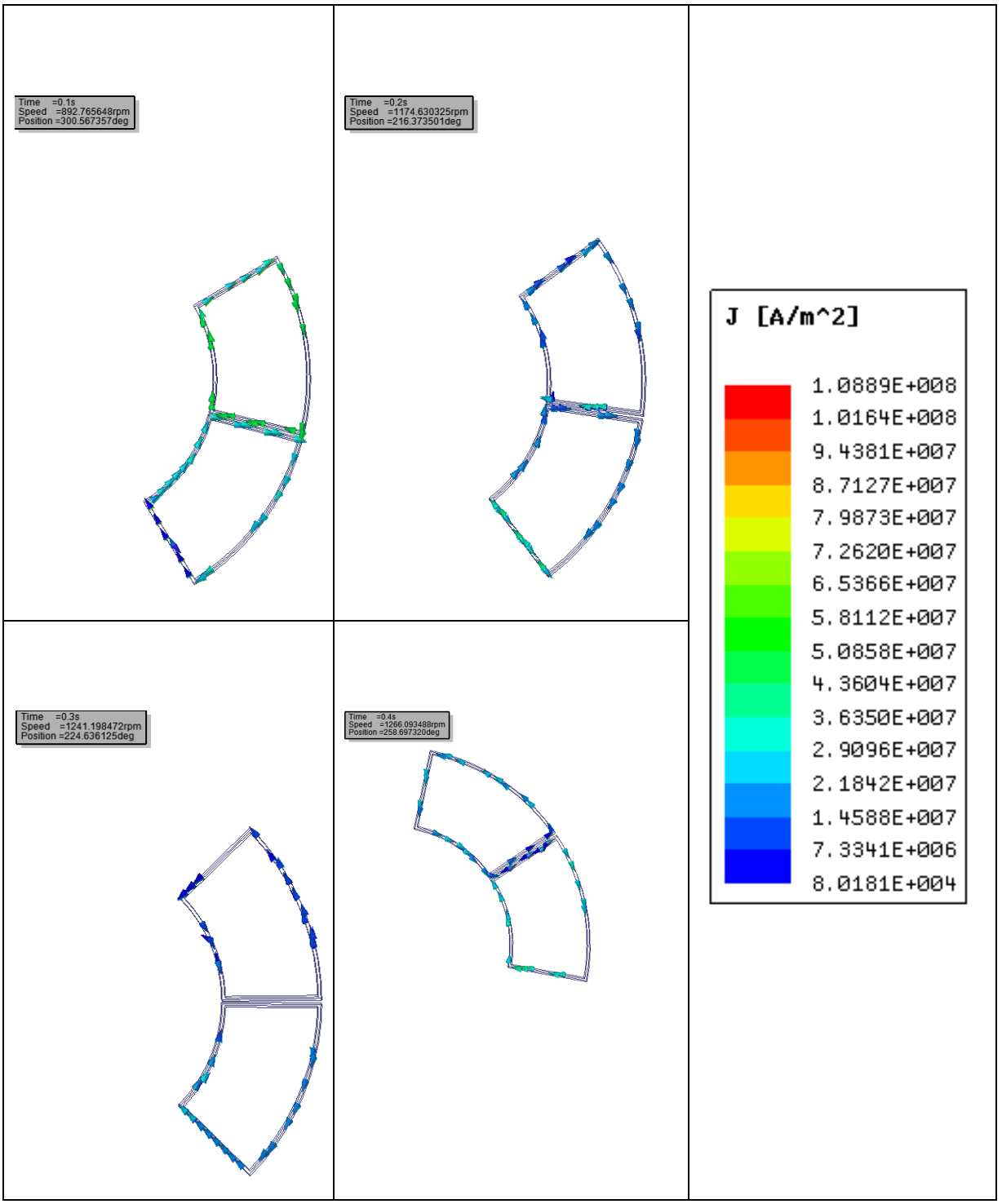

(a) Type-1 having separated ring rotor under no load

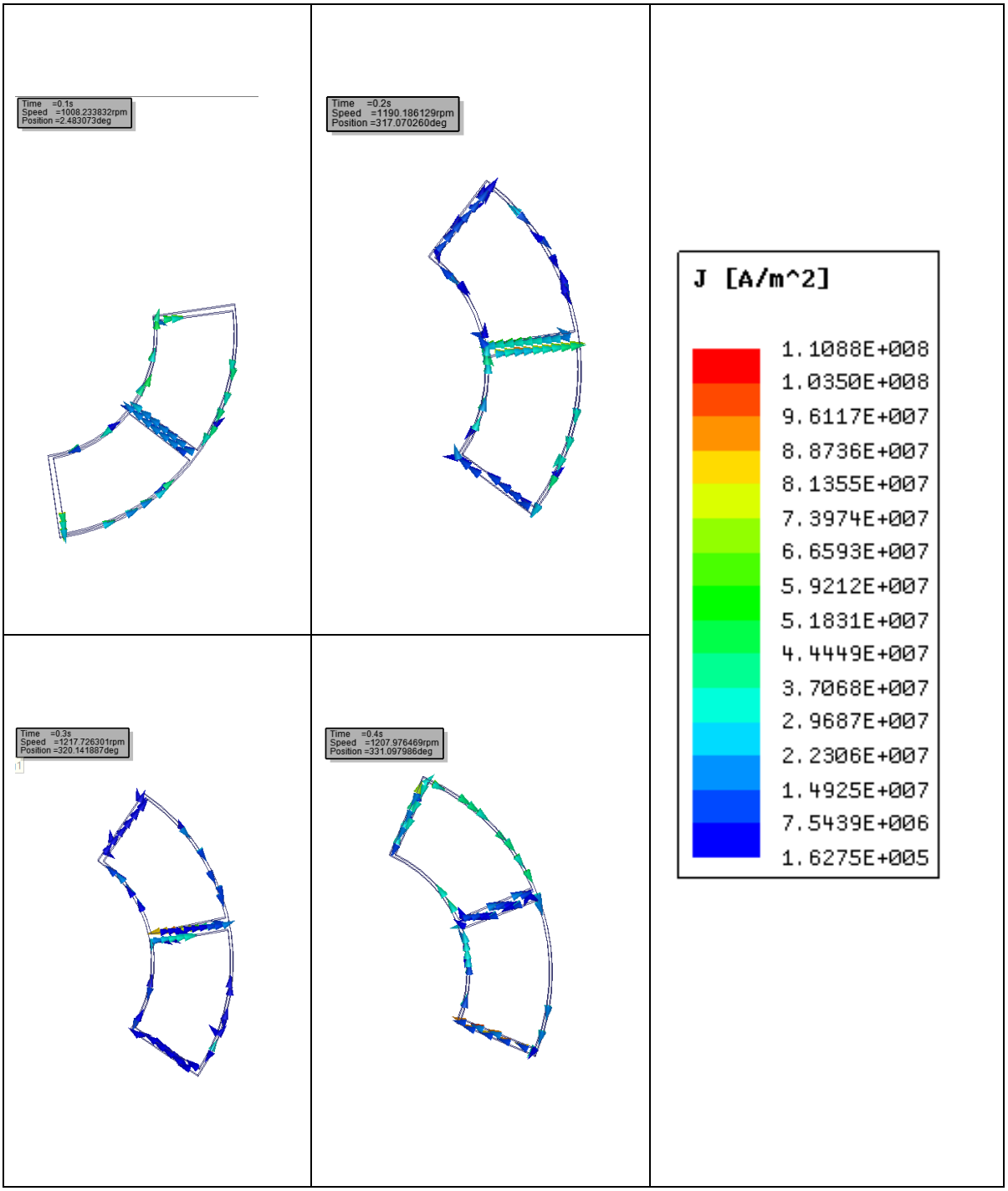

(b) Type-1 having caged ring rotor under no load

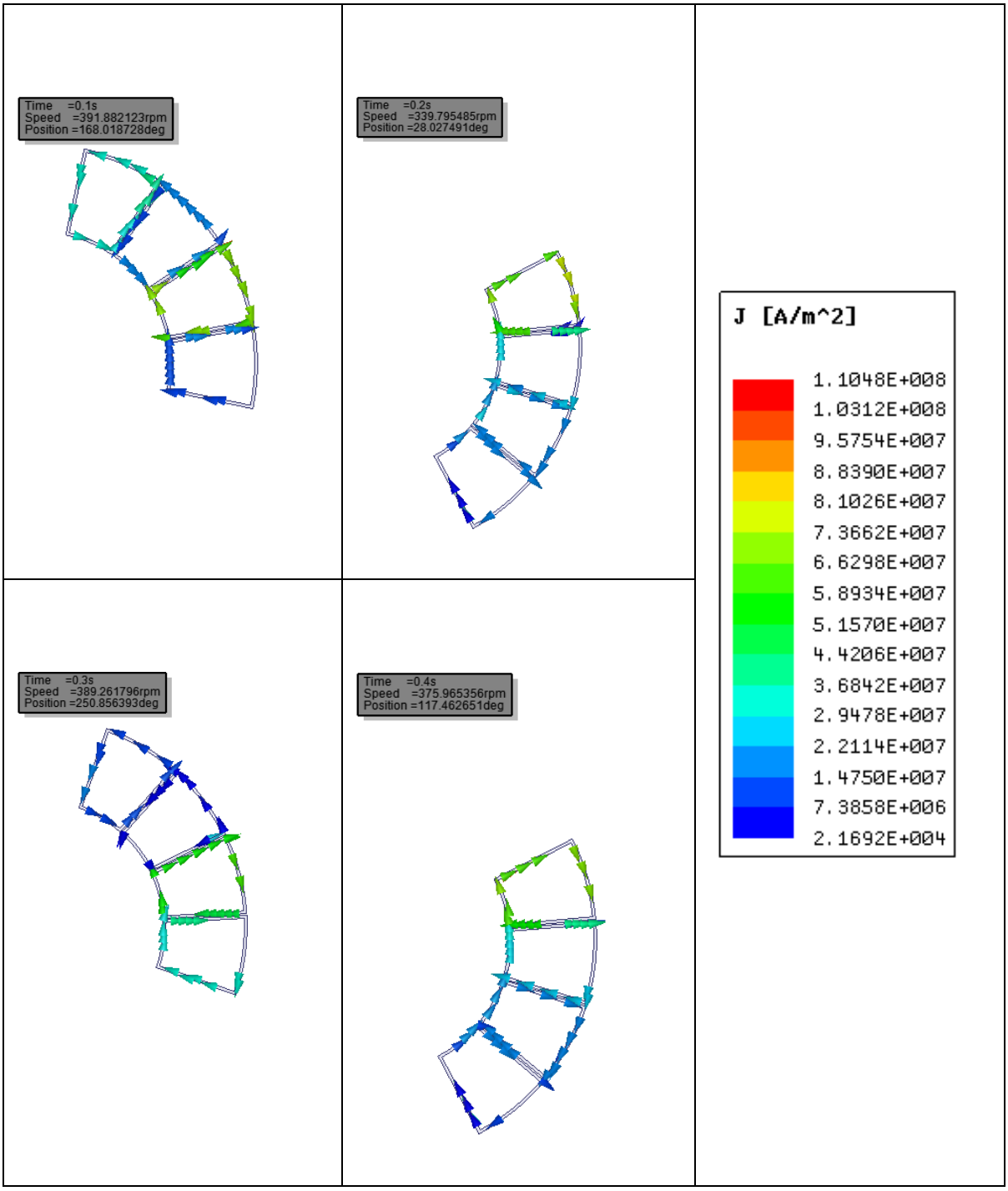

(b) Type-2 having separated ring rotor under no load

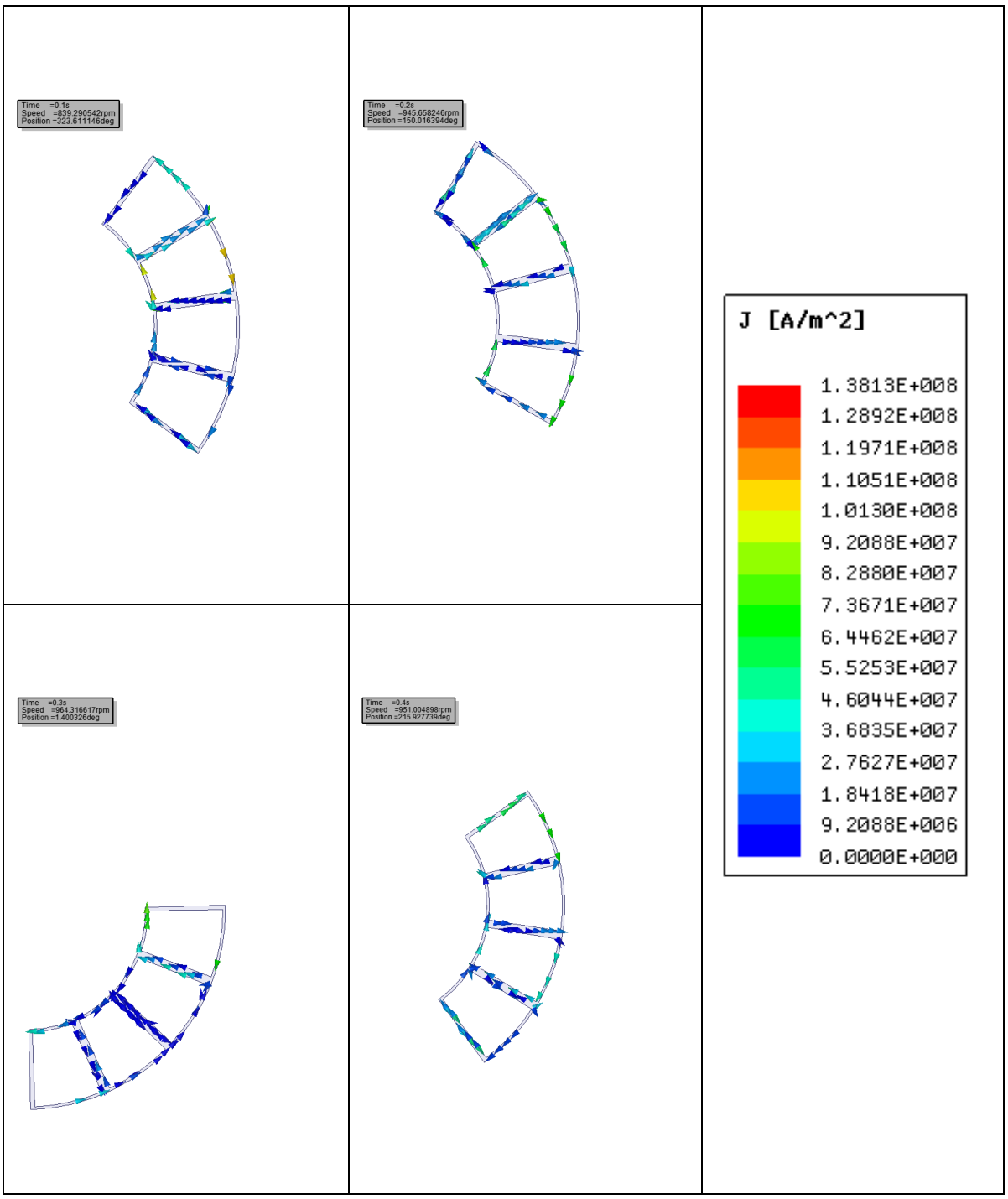

(b) Type-2 having caged ring rotor under no load

Fig. 30 Current distribution in rotor rings of Type-1 and Type-2 induction motor

It can be stated from the current density vector figures that the current distribution in cage ring rotor improves the current density magnitude and hence higher starting current in rotor ring which improvs the transient response of motor. Design Type -1 have higher current density if compared to design Type-2 which confirms the that

design Type-1 have better transient response than type-1.

4.4 Steady State Analysis

Steady State analysis is performed by analyzing the quantities such as winding currents, input and output power, steady state losses and efficiency. For steady state analysis range of time period is kept between 0.6s to 1s.

4.4.1 Induced Voltage

The induced voltage depends on the magnitude of magnetic flux and is given by the equation

$E_{\emptyset_{rms}} = 4.44\, N f \emptyset_{max}$

Where $\emptyset_{max}$ is peak to peak magnitude of flux density, N are the numbers of turns and f is the frequency. He simulations are ran for 1s but for the sake of better observable behavior graph steady state period 0.2s to 0.3 s is magnified.

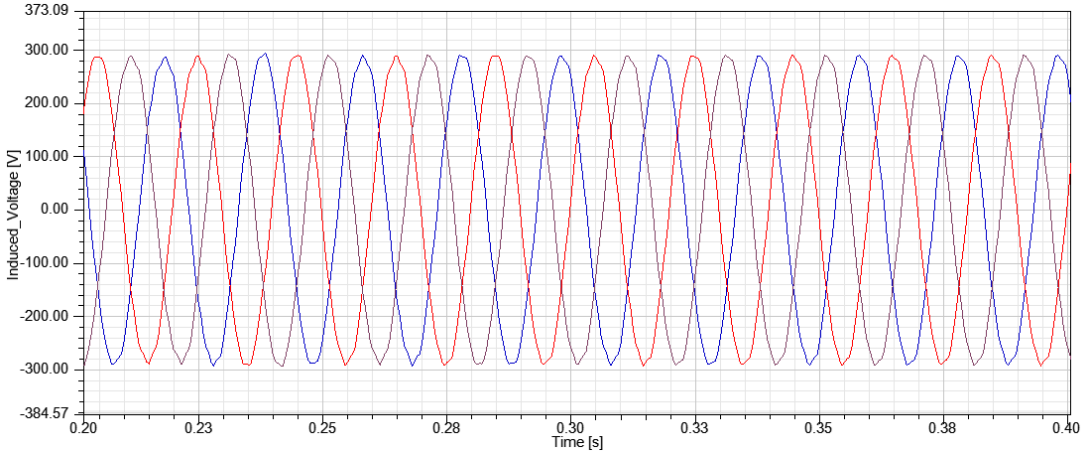

Curve Info	Max voltage at Steady State	Max_Voltage
InducedVoltage(WindingB) Setup1 : Transient	304.3860	304.3860
InducedVoltage(WindingC) Setup1 : Transient	302.6910	302.6910
InducedVoltage(WindingA) Setup1 : Transient	297.2050	297.2050

(a) Type-1 AFPM Motor

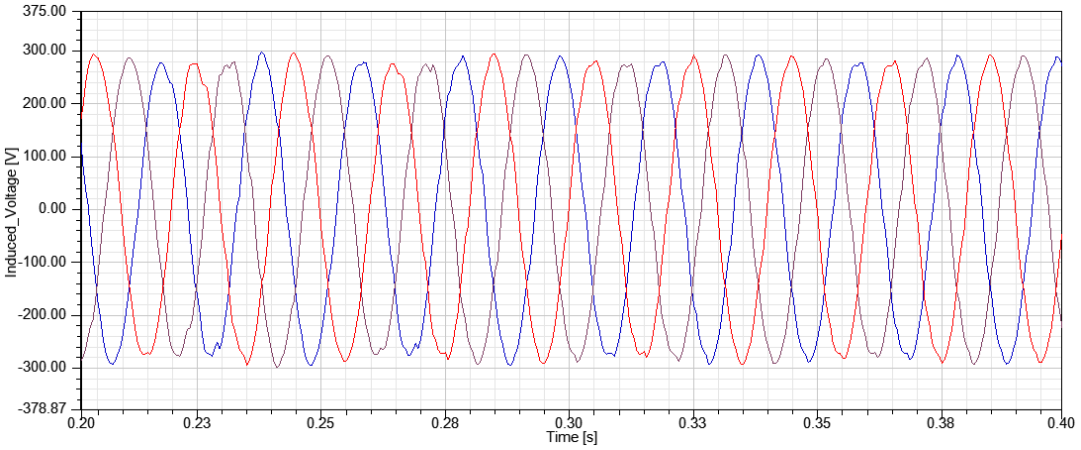

Curve Info	Max Volatage at Steady State	Max Voltage
InducedVoltage(WindingB) Setup1 : Transient	289.6040	296.5790
InducedVoltage(WindingC) Setup1 : Transient	289.9480	303.7030
InducedVoltage(WindingA) Setup1 : Transient	287.5070	299.0850

(b) Type-2 AFPM Motor

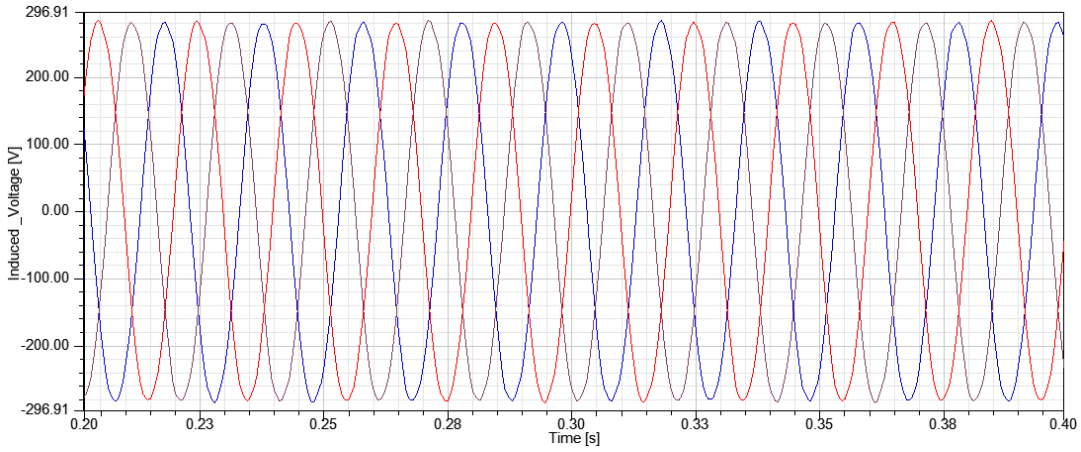

Curve Info	Maximum Voltage at Steady State	Max Voltage
InducedVoltage(WindingB) Setup1 : Transient	284.1640	284.3670
InducedVoltage(WindingC) Setup1 : Transient	284.1910	284.1910
InducedVoltage(WindingA) Setup1 : Transient	283.9200	296.4060

(c) Type-1 Induction Motor

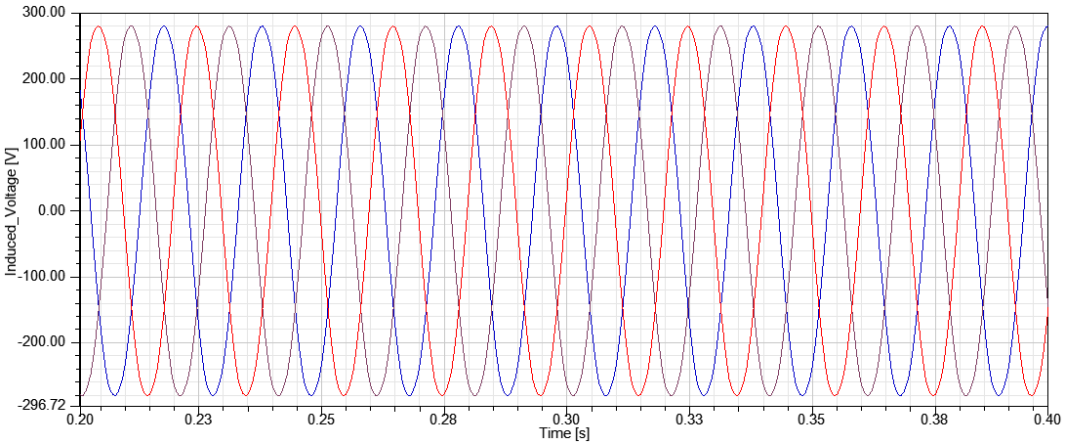

Curve Info	Max Voltage at Steady State	Max Voltage
InducedVoltage(WindingB) Setup1 : Transient	280.3430	280.7290
InducedVoltage(WindingC) Setup1 : Transient	279.4910	281.1430
InducedVoltage(WindingA) Setup1 : Transient	280.0990	297.2740

(d) Type-2 Induction Motor

Fig 31 Induced Voltage at No-Load with supply of 310V

4.4.2 Input and Output Power

The input power expressed as

$$Power_{in} = (I_A \times V_{in_A} + \times I_B \times V_{in_B} + I_C \times V_{in_C})$$

and the output power expressed as

$$Power_{out} = Moving.Torque \times Moving.Speed$$

At 2 Nm load, Input power and Output power of Type-1 AFPM designs supplied with 240V and Type-2 AFPM designs supplied with 400V AFPM are shown through Figure 32. The figures have shown that under small load caged ring rotor takes more input power to produce nearly same output power.

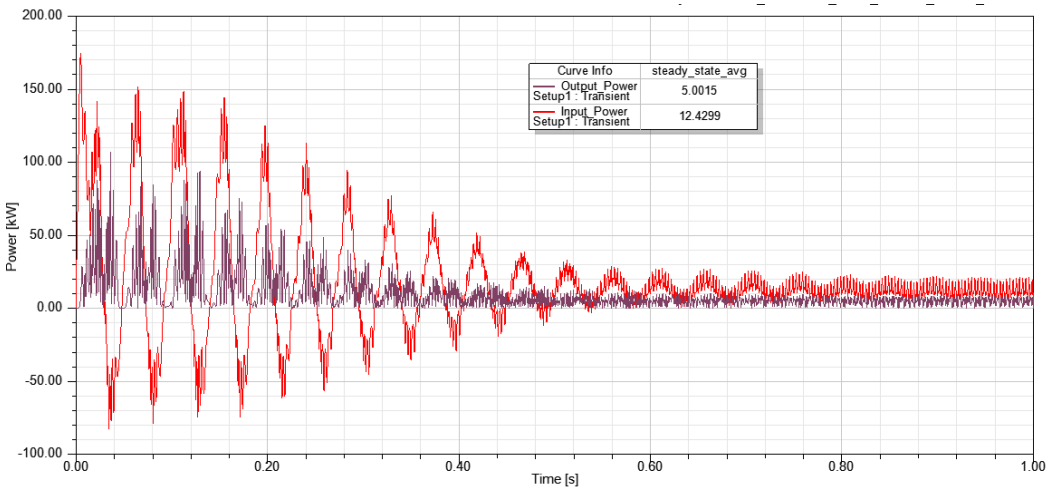

(a) Input and Output power of Type-1 AFPM Motor having separated ring supplied with 240V at 2Nm load.

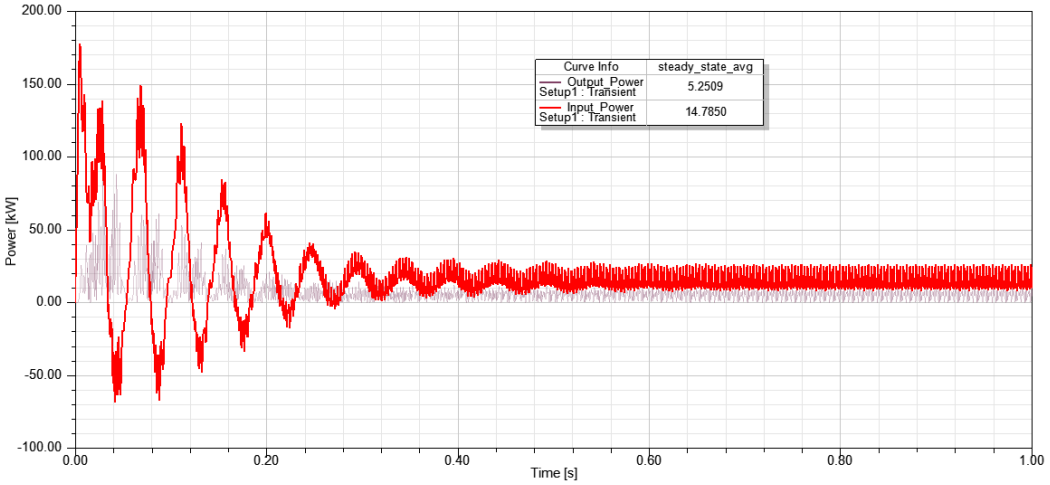

(b) Input and Output power of Type-1 AFPM Motor having caged ring supplied with 240V at 2Nm load.

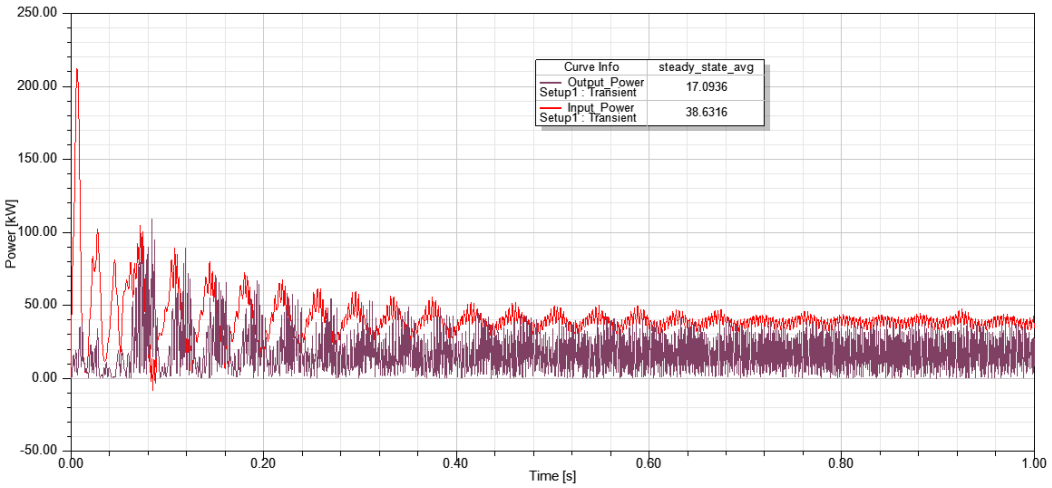

(c) Input and Output power of Type-2 AFPM Motor having separated ring supplied with 400V at 2Nm load.

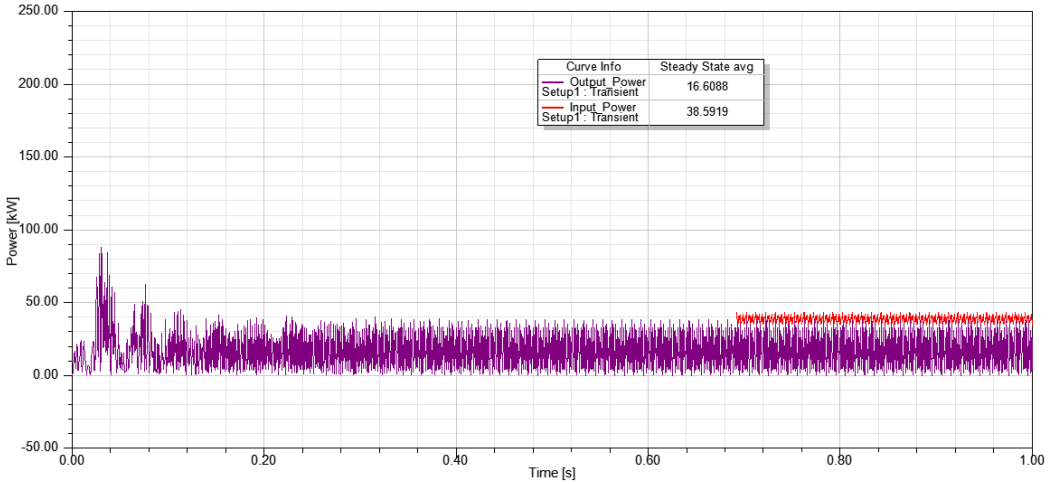

(d) Input and Output power of Type-2 AFPM Motor having caged ring supplied with 400V at 2Nm load.

Fig 32 Input and Output power of LSAFPM motor at 2Nm load

The input power and output power are obtained for induction motors under no load is illustrated below in the fig 33.

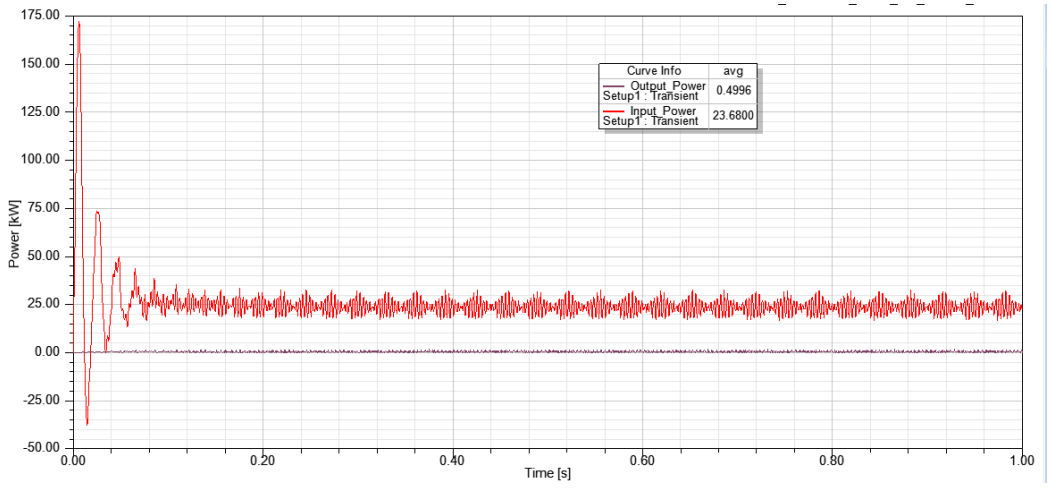

(a) Input and Output power of Type-1 Induction Motor having separated ring rotor supplied with 240V.

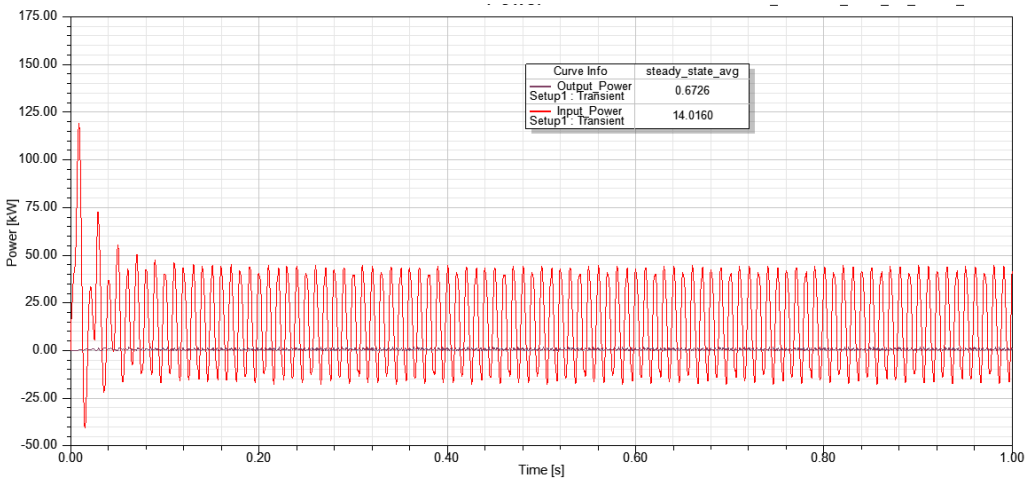

(b) Input and Output power of Type-1 Induction Motor having caged ring rotor supplied with 240V.

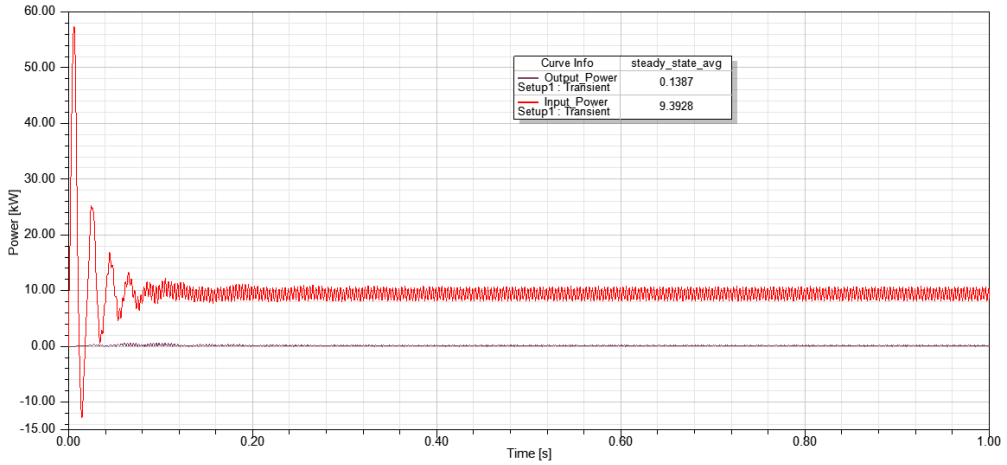

(c) Input and Output power of Type-2 Induction Motor having separated ring rotor supplied with 240V.

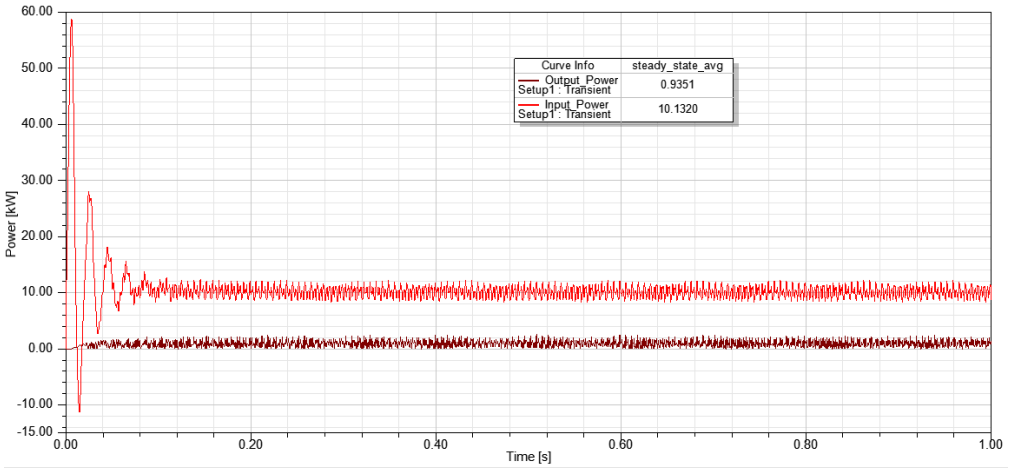

(d) Input and Output power of Type-2 Induction Motor having caged ring rotor supplied with 240V.

Fig 33 Input and Output power of Induction motors at No-load

Figure 34 shows the power levels in Type-1 and Type-2 AFPM motors under load of 17Nm.

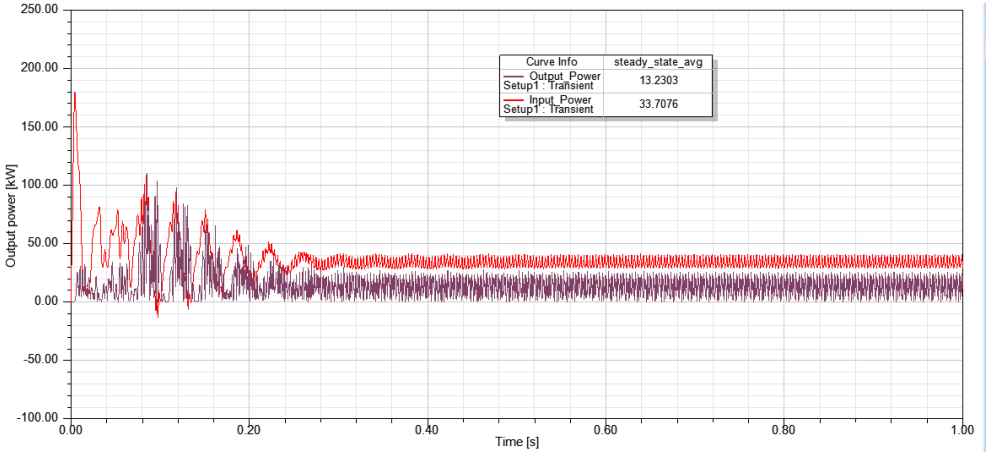

(a) Input and Output power of Type-1 AFPM Motor having separated ring rotor supplied with 400V.

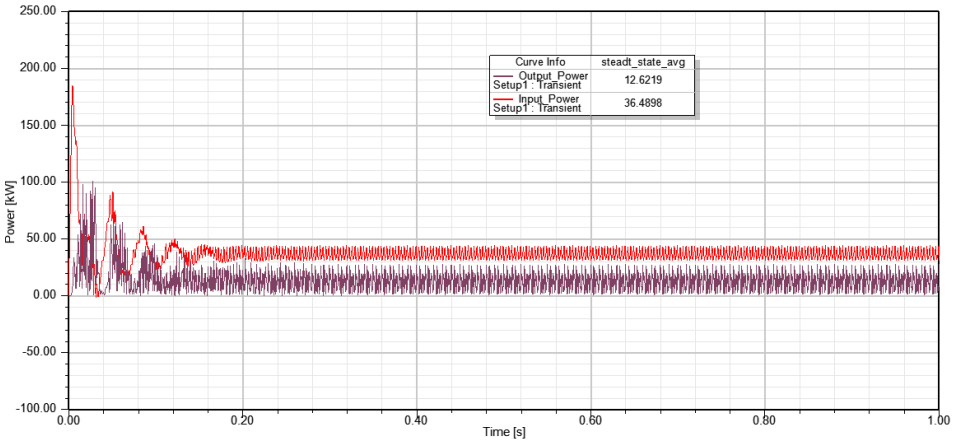

(b) Input and Output power of Type-1 AFPM Motor having caged ring rotor supplied with 400V.

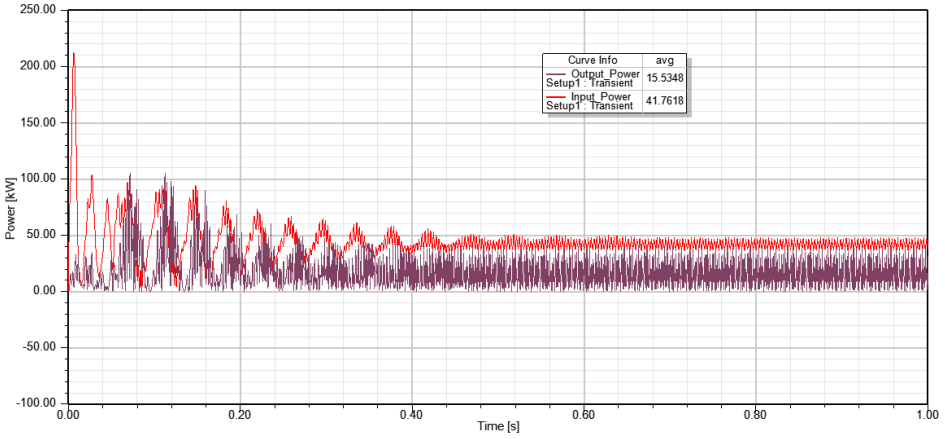

(c) Input and Output power of Type-2 AFPM Motor having separated ring rotor supplied with 400V.

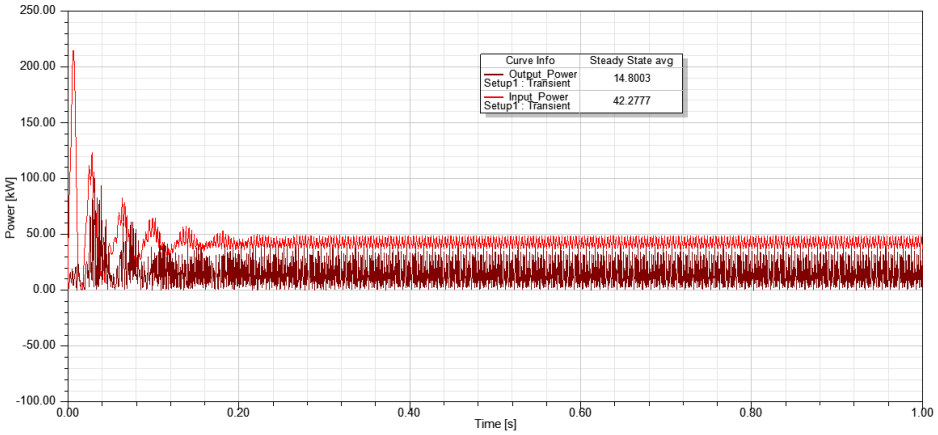

(c) Input and Output power of Type-2 AFPM Motor having caged ring rotor supplied with 400V

Fig 34 Input and Output power of Type-1 and Type-2 AFPM at 17 Nm.

It can be seen from the figures that contrary to small load conditions, cage ring rotor takes less input power than separate ring rotor to prodce nearly same output power. For the load of 17Nm cage ring rotor improves the efficiency.

4.4.3 Losses

Core loss, hysteresis loss and eddy current losses are analyzed in fig 33,34 and 35. The hysteresis losses in the machine produce because of the hysteresis effect of the material used in the machine and the eddy currents losses are produced because of the induced currents in the steel. The eddy current losses of the machine can be the reason of heating of the machine. The results for losses are illustrated in the figure 33 for the no load condition.

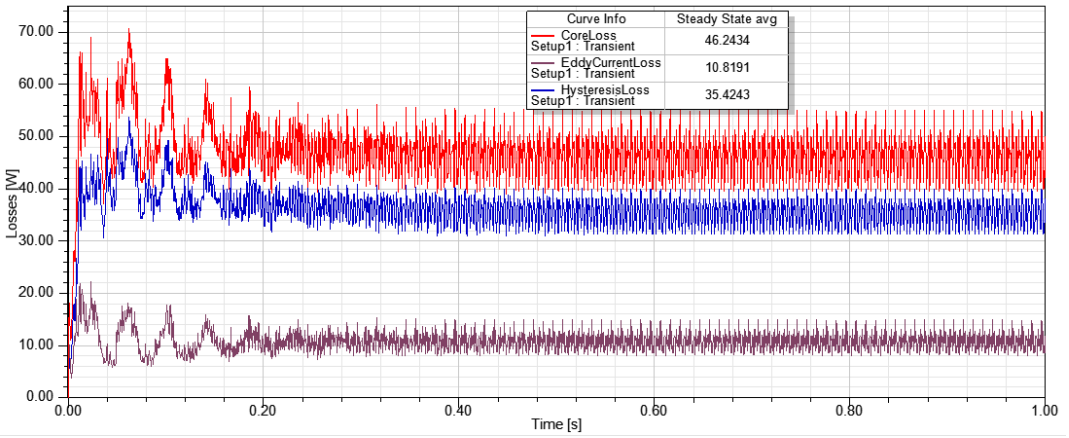

(a) Synchronous Motor Type-1.

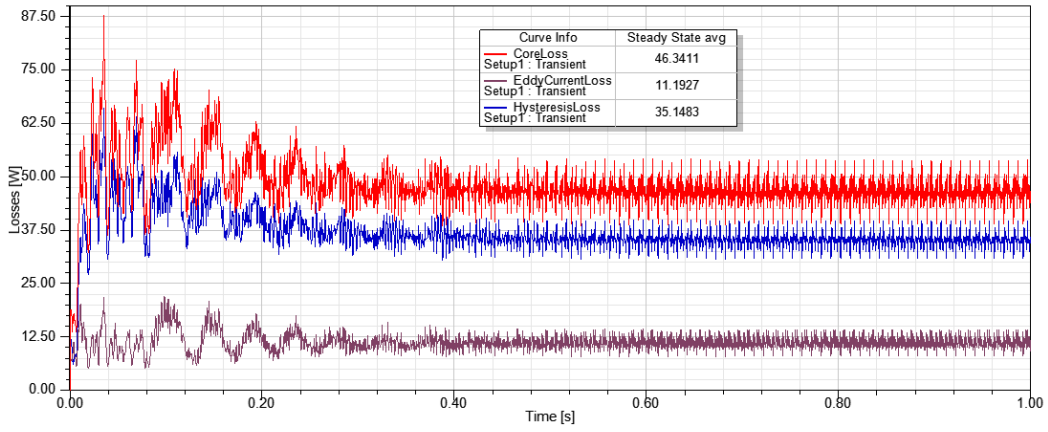

(b) Synchronous Motor Type-2.

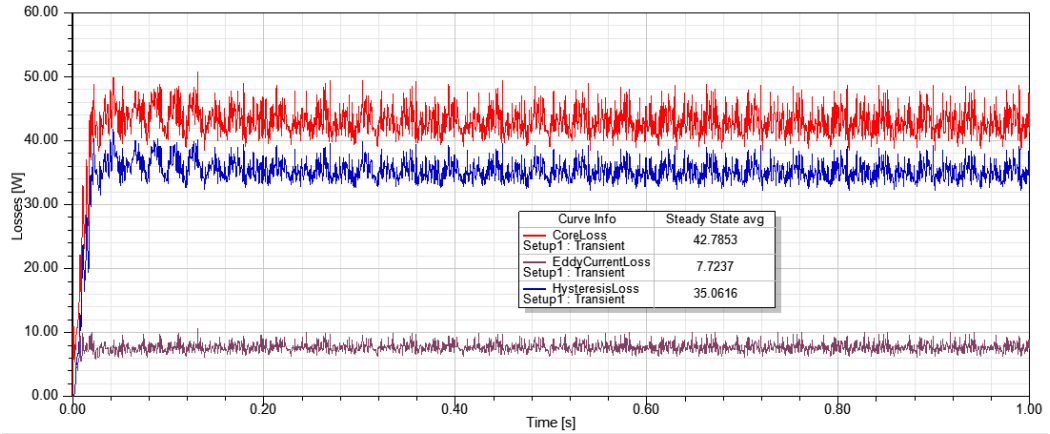

(c) Induction Motor Type-1.

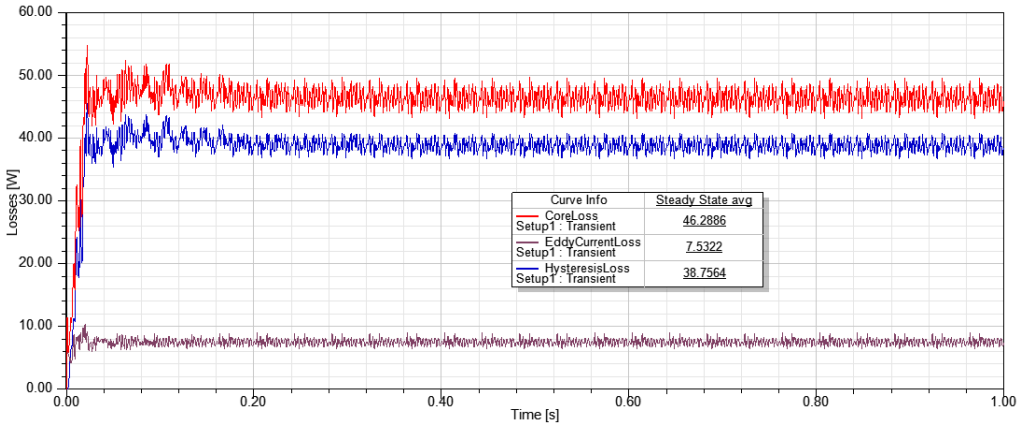

(d) Induction Motor Type-2.

Fig 35 Losses at No-load.

Also, the full load analysis is carried out for obtaining the losses of the machines at full-load condition, which is illustrated below in the fig 34 and fig 35.

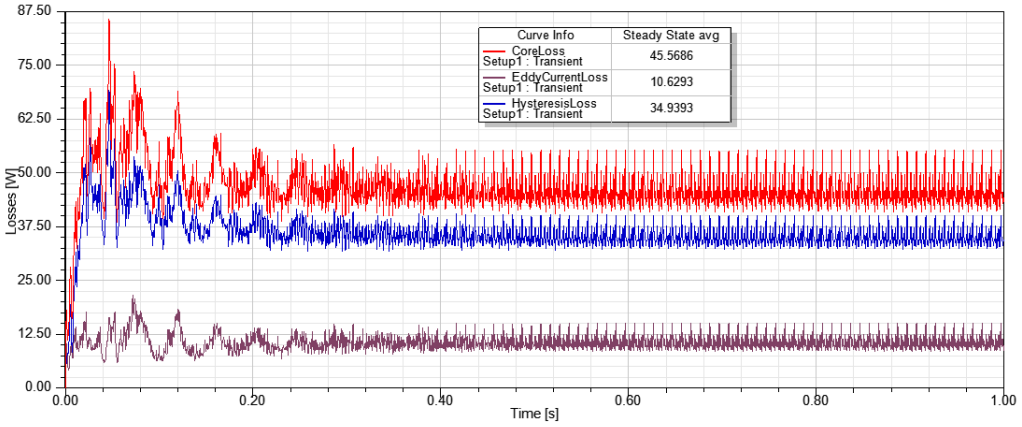

Fig 36 Losses of Synchronous Motor Type-1 at 20 Nm.

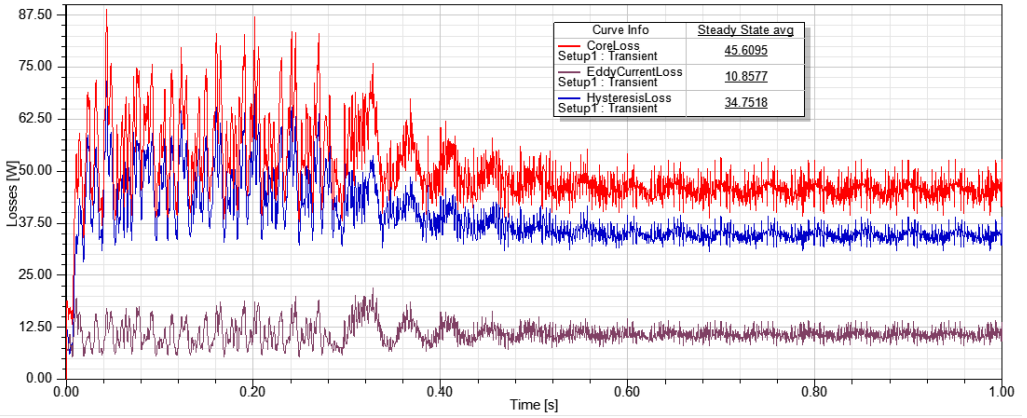

Fig 37 Losses of Synchronous Motor Type-2 at 17 Nm.

Eddy current losses are more in design type-2 because of more inductor material employed in geometry.

4.4.4 Efficiency

Efficiency of both the AFPM (Axial Flux Permanent Magnet) motor designs under 17Nm load are presented comparatively in the form of bar chart. Input and Output power are used, and the steady state average efficiencies are labeled in the bar charts. Efficiency is calculated from the expression stated

$$Efficiency = \frac{Output\ Power}{Input\ Power} \times 100$$

Figure 38 shows efficiency of type-1 and type-2 designs where all the motors are fed with 400V.

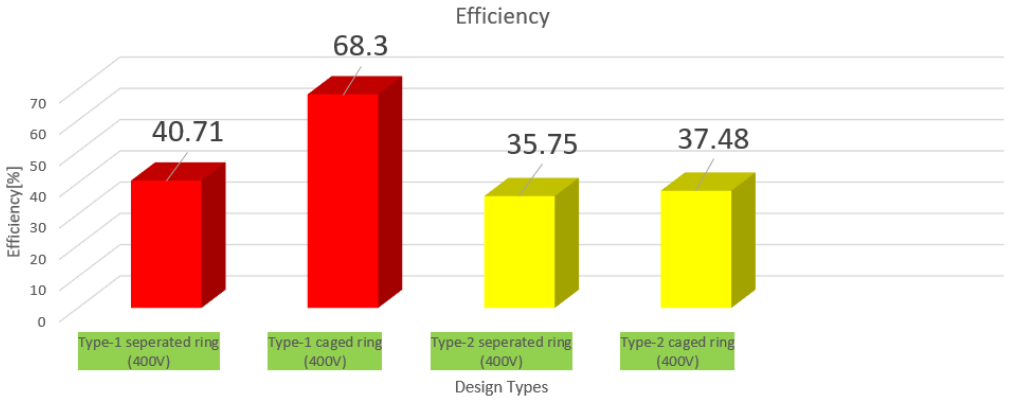

Fig 38 Efficiency plots of AFPM motors at 17Nm load supplied with 400V.

It can be deduced from both the figure that efficiency improves on employing cage ring rotor. Efficiency plot under 17Nm signifies that type-1 AFPM motor is better than type-2 AFPM motor.

Chapter 5
Conclusion and Future Work

5.1 Conclusion

The primary objective of the project was to make the two different design types of single sided axial flux permanent magnet motor along with the design of two rotor structures (separated and caged ring) for each of the design. The project successfully analyzed the approach of designing axial flux line start motor having optimal performance. Two 4pole axial-flux permanent magnet synchronous motor design having same stator configuration and approximately equal parameters for performance comparison were designed. Finite Element Method is used for analysis of the two design types having difference of number of induction rings per pole. Synchronous motor of all types are compared under same voltage of 400V under various load conditions to identify the critical load for two designs of axial-flux synchronous motor. The results have shown that design type-1 has potential of better dynamic performance than design type-2.

Starting and synchronizing of motors were closely analyzed and compared. All the motors are analyzed under supply and load conditions. The comparative analysis of separate ring rotor and cage ring rotor is also considered which showed that cage ring rotor improves the rotor improves the starting performance of the motors but should be considered accordingly whether used with low load or higher load for better efficiency.

Transient and Steady State Behavior of the designs were compared by analyzing parameters like moving speed, transient torque, harmonics in current, input and output power, power losses and efficiency. The analysis of the two design types were also performed with their magnets removed to compare the designs as induction motor.

The analysis results of single-sided solid-rotor axial-flux permanent-magnet synchronous motor states the fact that maximum bearable load for good starting decreases with number of induction rings per pole as observed in type-1 axial-flux permanent-magnet synchronous motor with two induction rings have maximum bearable load of about 20Nm while type-2 axial-flux permanent-magnet synchronous motor with four induction rings has maximum bearable load of 17Nm with input voltage of 310V.

Efficiency of the axial -flux motor design type-1 is higher for higher load torque of 17Nm while efficiency of design type-2 is higher when comparatively small load torque of 2Nm is applied to the motor designs. Efficiencies may change by changing the input voltage and other factors like inertia and damping during motion set up but project did not cover those factors and could be scope of future work.

Magnetic analysis of the designs is considered to understand the magnetic behavior inside the geometry of the designs. Magnetic flux density in the motor geometry through the simulation period is analyzed for all the motor design when operating with and without magnets. Air gap flux densities in all the synchronous motor designs are comparatively analyzed. Distribution of current in rotor induction rings is shown with current densities for all the design types.

To summarize the conclusions the following has been observed.

- Design type-1 is more prominent than design type-2 for dynamic response as it has good starting performance which is confirmed by transient report graphs such as moving speed and moving torque vs time, harmonics in winding current. Table 9 shows the comparison of starting performance of motor design under no load and 17Nm under different supply voltages.
- Employing caged ring rotor improves the transient and steady state response of the motors which is compare at no load with similar input voltage of 240V. Current distribution is also better in caged ring rotor.
- Synchronous motor design need more voltage for start-up than induction motors as deduced by the comparative performance of separate ring rotor design types where induction motor is working and easily started at voltage of 240V while synchronous motor need higher voltage of about 300 V for start-up.

Performance Measures	**AFPM Motors**								**Induction Motors**			
	Type-1				**Type-2**				**Type-1**		**Type-2**	
	Separated		***Caged***		***Separated***		***Caged***		***Type-1***	***Type-2***	***Type-1***	***Type-2***
Startup Input Voltage (V)	240	400	240	400	400	400	400	400	240	240	240	240
Load (Nm)	0	17	0	17	0	17	0	17	0	0	0	0
Steady Speed (rpm)	1500	1500	1500	1500	1500	1500	1500	1500	1271	1219	375	959

Rise Time (sec)	0.01	0.08	0.02	0.01	0.07	0.06	0.025	0.025	0.4	0.2	0.1	0.2
Settling Time (sec)	0.7	0.3	0.4	0.2	0.5	0.5	0.2	0.2	0.4	0.2	0.5	0.2
Maximum speed (rpm)	3025	3100	2950	3050	3100	2925	2650	2750	1280	1240	475	980

Table 9 Performance measures across the motor design

5.2 Future work

Prototyping

Prototypes of the all the four motors are required for the affirmation of results obtained through simulation software.

Other possibilities for the design

Although the motor is axial flux motor different magnetic field directions (radial, circumferential) inside the magnet can affect the dynamic and steady state performance depending on locking behavior between stator and rotor magnetic poles. So, different designs with different magnetic flux lines direction in magnet could be designed and analyzed in future studies. Single phase motor designs could also be possible for comparative study.

Further Analysis

The fluctuations in steady response of the designed motors need further improvement by optimizing the rotor geometry. The project compared the performances under different load conditions.

The performance of the motor could also be analyzed with different load types such as

the step load, pulse load and ramp load.

Design type-2 can give higher efficiency if supply with high voltage and different motion setup having different inertia and damping factor.

Motor performance can be further tested with using skewed induction rings. Different possible induction rings structures are included in Appendices which are preliminary designs and not used in this project and could be further optimized and tested.

References

[1] Knight, A. M. and C. I. McClay, "The design of high-efficiency line-start motors," IEEE Trans. Ind. Appl., Vol. 36, No. 36, 1555-1562, Nov./Dec. 2000.

[2] Aliabad, A. D., M. Mirsalim, and N. F. Ershad, "Line-start permanent-magnet motors: Significant improvements in starting torque, synchronization, and steady-state performance," IEEE Trans. Magn., Vol. 46, No. 12, 4066-4072, Dec. 2010.

[3] Mirimani, S. M., A. Vahedi, and F. Marignetti, "Effect of inclined static eccentricity fault in single stator-single rotor axial flux permanent magnet machines," IEEE Trans. Magn., Vol. 48, No. 1, 143-149, Jan. 2012.

[4] De la Barriere, O., S. Hlioui, H. Ben Ahmed, M. Gabsi, and M. LoBue, "3-D formal resolution of Maxwell equations for the computation of the no-load flux in an axial flux permanent-magnet synchronous machine," IEEE Trans. Magn., Vol. 48, No. 1, 128-136, Jan. 2012.

[5] De Donato, G., F. G. Capponi, and F. Caricchi, "No-load performance of axial flux permanent magnet machines mounting magnetic wedges," IEEE Trans. Ind. Electron., Vol. 59, No. 10, 3768-3779, Oct. 2012.

[6] Z. Bingyi, Z. Wei, Z. Fuyu, F. Guihong, “Design and Starting Process Analysis of Multipolar Line-Start PMSM,” Proc. ICEMS 2007, Seoul, 8-11 Oct., 2007, pp. 1629-1634.

[7] Sitapati, K., Krishnan, K., Performance Comparisons of Radial and Axial Field, Permanent Magnet, Brushless Machines, IEEE Transactions on Industry Applications, Vol. 37, No. 5, Sept./Oct. 2001.

[8] Dean J Patterson, Jessica L Colton, Brad Mularcik, Byron J Kennedy, Steven Camilleri, Rafal Rohoza,” A Comparison of Radial and Axial Flux Structures in Electrical Machines”

[9] Campbell P, Rosenberg DJ, Stanton DP (1981). The Computer Design and Optimization of Axial-Field Permanent Magnet Motors. IEEE Trans. Power Apparatus Syst. PAS-100(4): 1490-1497.

[10] Chan CC (1987). Axial-Field Electrical Machines - Design and Applications. IEEE Trans. Energy Conversion. EC-2(2): 294-300.

[11] Platt D (1989). Permanent Magnet Synchronous Motor with Axial Flux Geometry. IEEE Trans. Magnet., 25(4): 3076-3079.

[12] Parviainen, A., Niemela, M., Pyrhonen, J., Mantere, J., Performance comparison between low-speed axial-flux and radial-flux permanent magnet machines including mechanical constraints, IEEE International Conference on Electric Machines and Drives, May 2005, pages 1695-1702.

[13] A. Mahmoudi, N. A. Rahim, and W. P. Hew "Axial-Flux Pemanent Magnet Machine Modeling, Design, Simulation, and Analysis," Scientific Research and Essay (SRE), Vol. 6, No. 12, 2525-2549, June 2011.

[14] A. Mahmoudi, N. A. Rahim, and W. P. Hew, "Analytical Method for Determining Axial-Flux Permanent-Magnet Machine Sensitivity to Design Variables," Intemational Review of Electrical Engineenng (IREE), Vol. 5, No. 5, 2039-2048, September-October 2010.

[15] A. Mahmoudi, N. A. Rahim, and W. P. Hew, "Al Analylical Complementary FEA Tool for Optimizing of Arial-Flux PermanentMagnet Machines," Intemational Joumal of Applied Electromagnetics Machines (IJEAM), Vol. 37, No. 1, 19-34, September 2011.

[16] A. Mahmoudi, N. A. Rahim, and W. P. Hew "Axial-Flux PermanentMagnet Motor Design for Electnc Vehicle Direct Drive using Sizing Equation and Finite Element Analysis" Progress [n Electromagnetics Research (PIER), Vol. 122, 467 -496, 2012.

[17] A. Mahmoudi, S. Kahourzade, N. A. Rahim, and H. W. Ping, "Improvement to Performance of Solid-Rotor-Ringed Line-Start AxialFlux Permanent-Magnet Motor," Progress In Electromagnetics Research, Vol. 124, 383-404, 2012.

[18] S. Geetha and D. Platt, "Axial flux permanent magnet servo motor with sixteen poles," Industry Applications Society Annual Meeting, 1992., Conference Record of the 1992 IEEE.

[19] Chan TF, Lai LL, Shuming X (2009). Field Computation for an Axial Flux Permanent-Magnet Synchronous Generator. IEEE Trans. Energy Conversion, 24(1): 1-11.

[20] Furlani EP (1994). Computing the Field in Permanent-Magnet Axial-Field Motors. IEEE Trans. Magnetics. 30(5): 3660-3663.

[21] Lee JK (1992). Measurement of Magnetic Fields in Axial Field Motors. IEEE Trans. Mag., 28(5): 3021-3023.

[22] Kano Y, Kosaka T, Matsui N (2010). A Simple Nonlinear Magnetic Analysis for Axial-Flux Permanent-Magnet Machines. IEEE Trans. Ind. Electronics, 57(6): 2124-2133.

[23] Loureiro LTR, Filho AFF, Zabadal JRS, Homrich RP (2008). A Model of a Permanent Magnet Axial-Flux Machine Based on Lie's Symmetries. IEEE Trans. Mag., 44(11): 4321-4324.

[24] Qamaruzzaman AP, Dahono P (1997). Analytical Prediction of Inductances of Slotless Axial-Flux Permanent Magnet Synchronous Generator Using Quasi-3D Method. Int. J. Elect. Eng. Inf., 1(2): 115125.

[25] Zhilichev YN (1998). Three-Dimensional Analytic Model of Permanent Magnet Axial Flux Machine. IEEE Trans. Mag., 34(6): 3897-3901.

[26] Azzouzi J, Barakat G, Dakyo B (2005). Quasi-3-D Analytical modeling of the magnetic Field of an Axial Flux Permanent-Magnet Synchronous Machine. IEEE Trans. Energy Conversion Actions. 20(4): 746-752.

[27] Kurronen P, Pyrhonen J (2007). Analytic Calculation of Axial-Flux Permanent-Magnet Motor Torque. IET J., 1(1): 59-63.

[28] Marignetti F, Colli VD, Carbone S (2010). Comparison of Axial Flux PM Synchronous Machines With Different Rotor Back Cores. IEEE Trans. Mag., 46(2): 598-601.

[29] Bumby JR, Martin R, Mueller MA, Spooner E, Brown NL, Chalmers BJ (2004). Electromagnetic Design of Axial-Flux Permanent Magnet Machines. IET J., 151(2): 151-160.

[30] Chan TF, Weimin W, Lai LL (2010). Performance of an Axial-Flux Permanent Magnet Synchronous Generator from 3-D Finite-Element Analysis. IEEE Trans. Energy Conversion, 25(3): 669-676.

[31] Rong-Jie W, Kamper MJ (2004). Calculation of Eddy Current Loss in Axial Field

Permanent-Magnet Machine with Coreless Stator. IEEE Trans. Energy Conversion, 19(3): 532-538.

[32] Upadhyay PR, Rajagopal KR (2006). FE Analysis and Computer-Aided Design of a Sandwiched Axial-Flux Permanent Magnet Brushless DC Motor. IEEE Trans. Mag., 42(10): 3401-3403.

[33] Sang-Ho L, Su-Beom P, Soon OK, Ji-Young L, Jung-Jong L, Jung-Pyo H (2006). Characteristic Analysis of the Slotless Axial-Flux Type Brushless DC Motors Using Image Method. IEEE Trans. Mag., 42(4): 1327-1330.

[34] Almeida, AT de, Ferreira, F and Duarte, A (2014), 'Technical and Economical Considerations on Super High-efficiency three-phase motors,' IEEE Trans. Ind. Appl., vol. 50, no.2, pp. 1274-1285

[35] Seda Küla , Osman Bilgina , Mümtaz Mutluerb (2015), 'Application of Finite Element Method to Determine the Performances of the Line Start Permanent Magnet Synchronous Motor,' Procedia - Social and Behavioral Sciences 195 (2015) 2586 – 2591

Appendices

Appendix A: Stator Excitation Setting.

Appendix B: Mesh plots.

Appendix A: Stator Excitation Setting

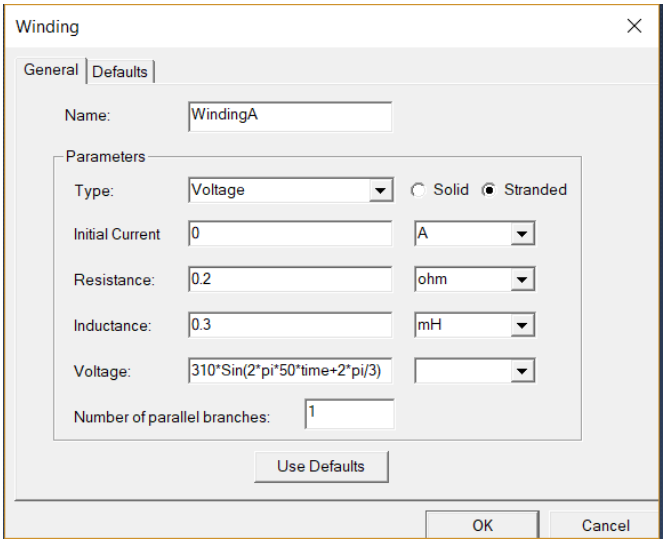

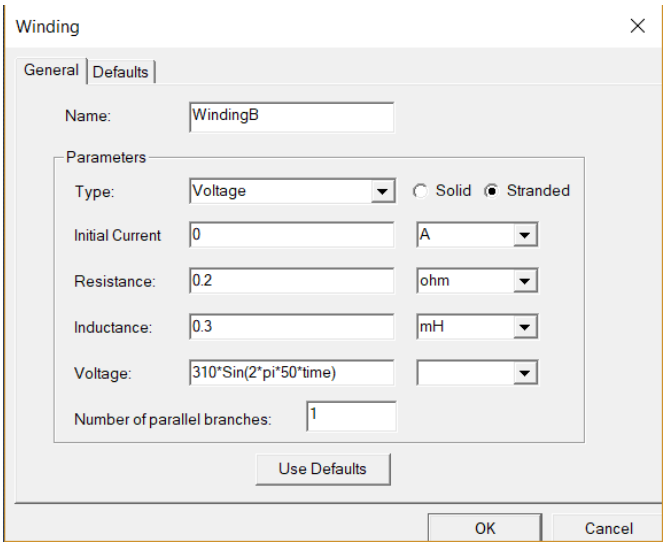

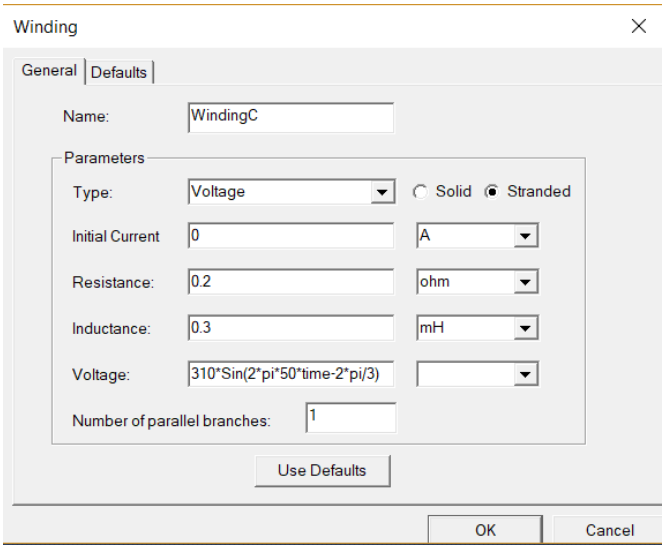

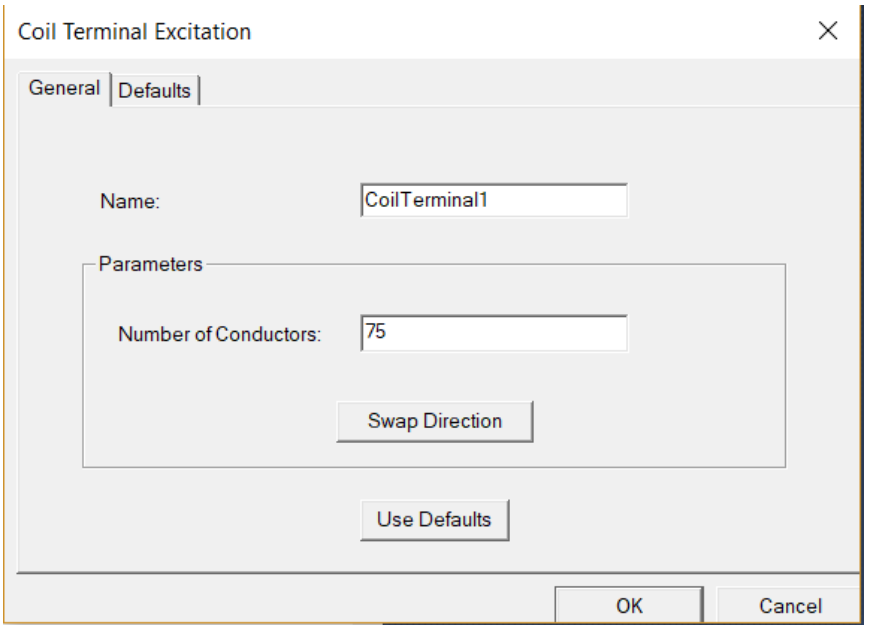
Coil Terminal Excitation
General
Defaults
Name:
CoilTerminal1
Parameters
Number of Conductors:
75
Swap Direction
Use Defaults
OK
Cancel

Appendix B: Mesh plots

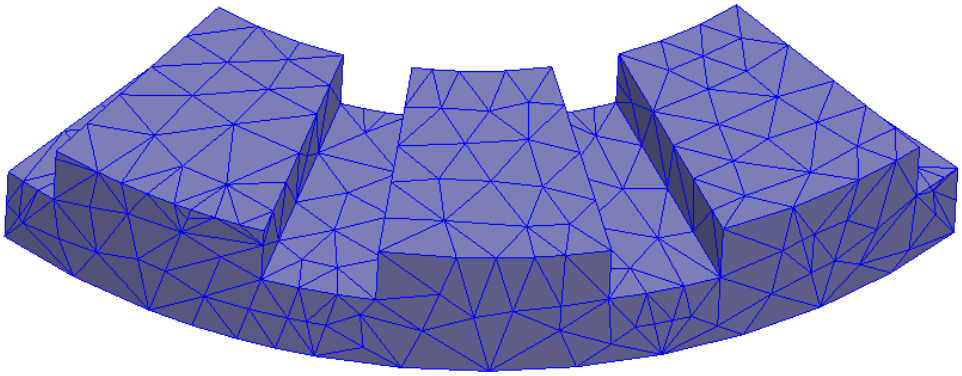

Stator Mesh

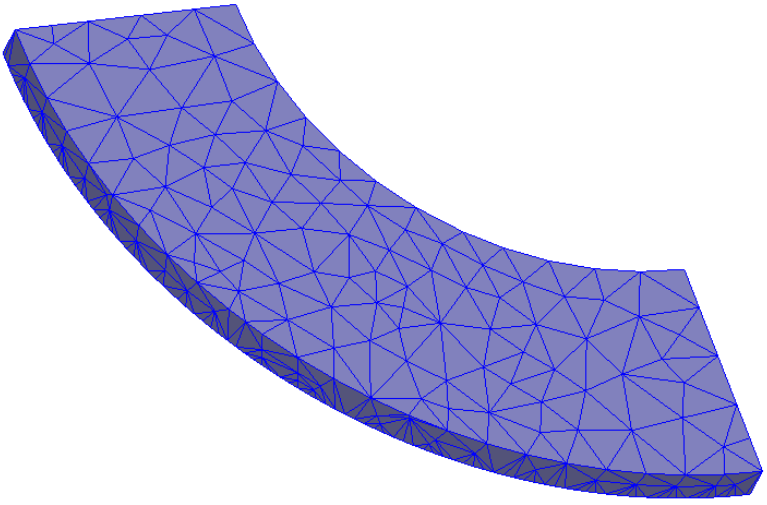

Rotor Disk Mesh

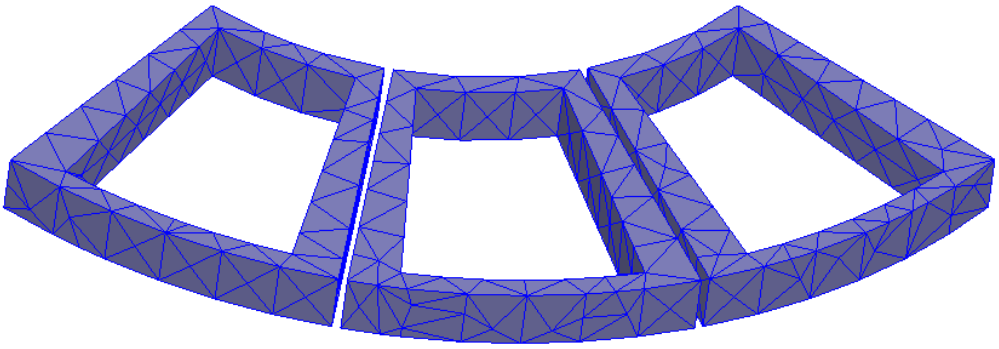

Coil Mesh

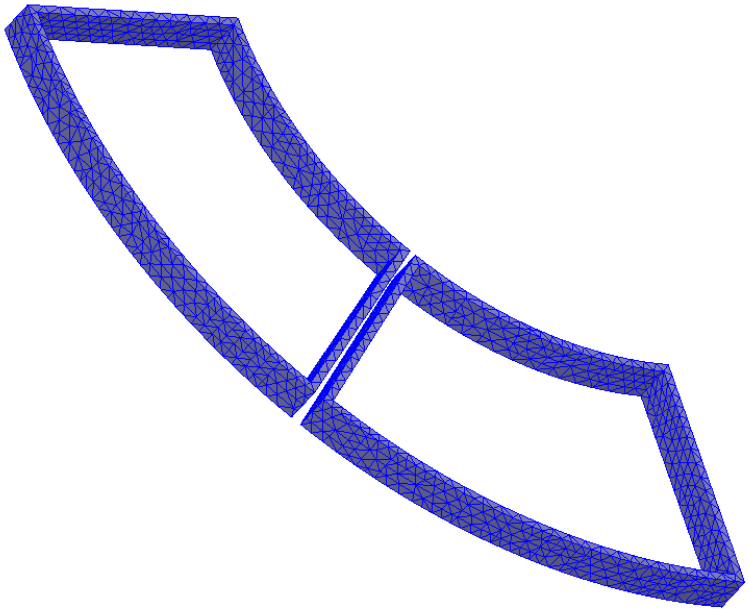

Induction Rings Mesh for Type-1 design

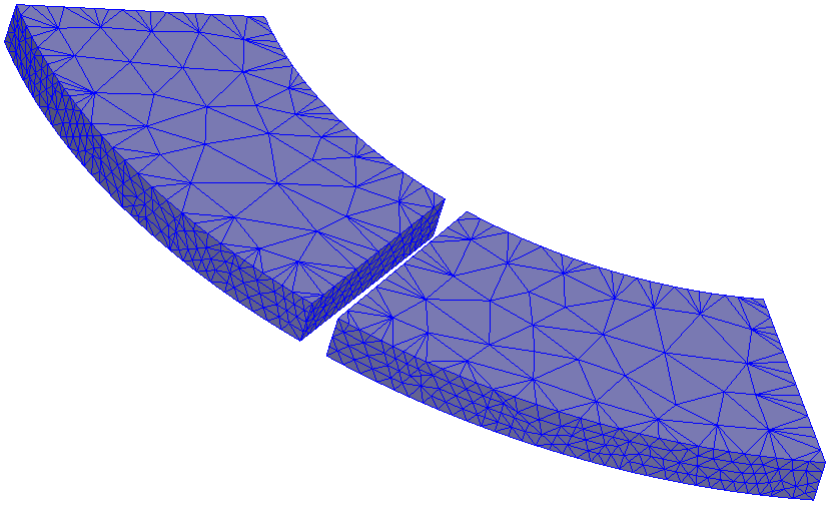

Magnet mesh for Type-1 design

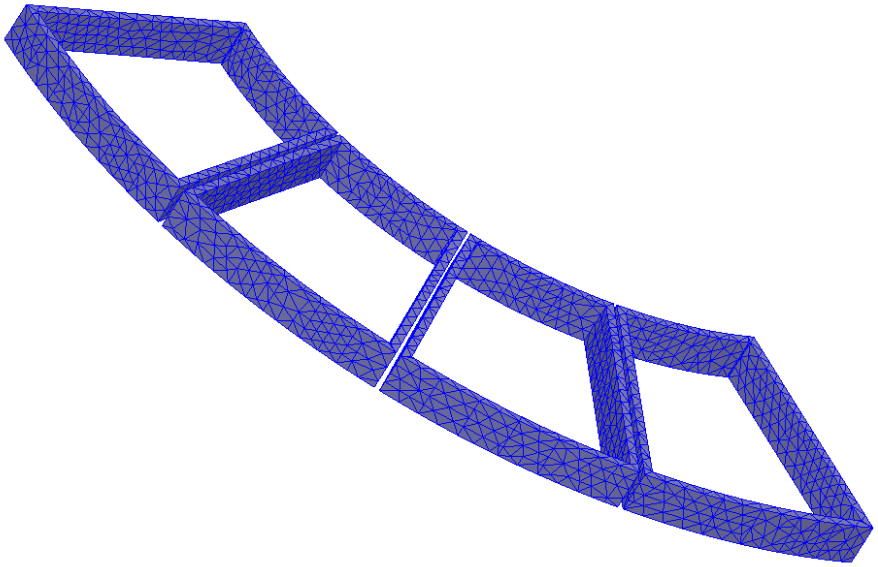

Induction Rings Mesh for Type-2 design

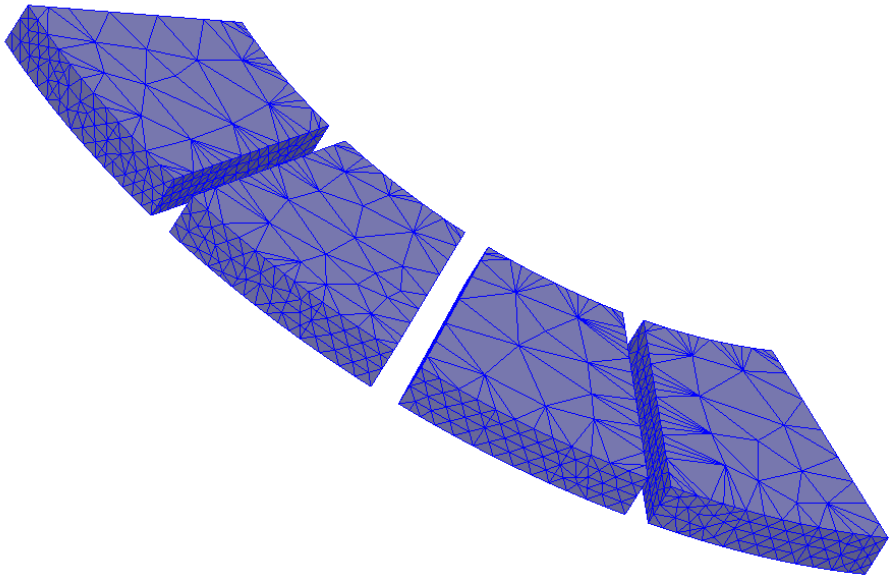

Magnet mesh for Type-2 design

Appendix C: Exploded view of quarter of geometry used in simulation

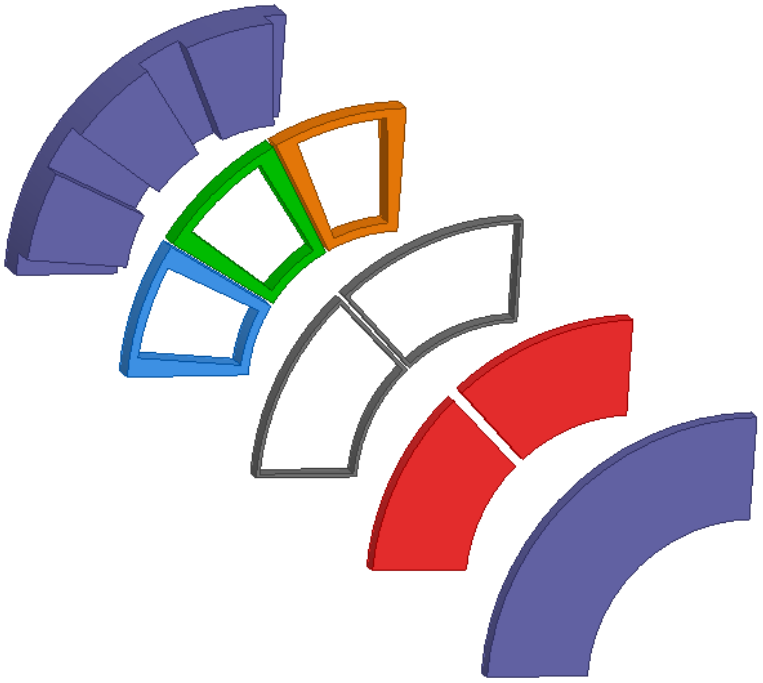

Exploded view of quarter of type-1 axial-flux permanent motor with separated ring

Appendix D: Other geometry designs made, and simulation performed during the project

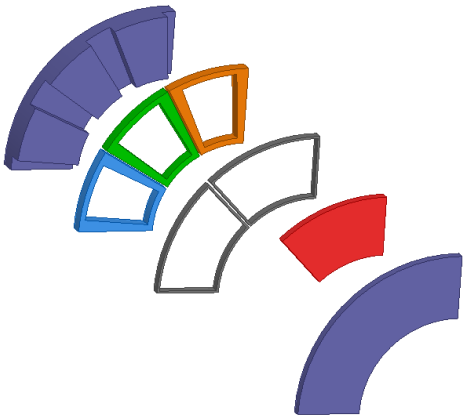

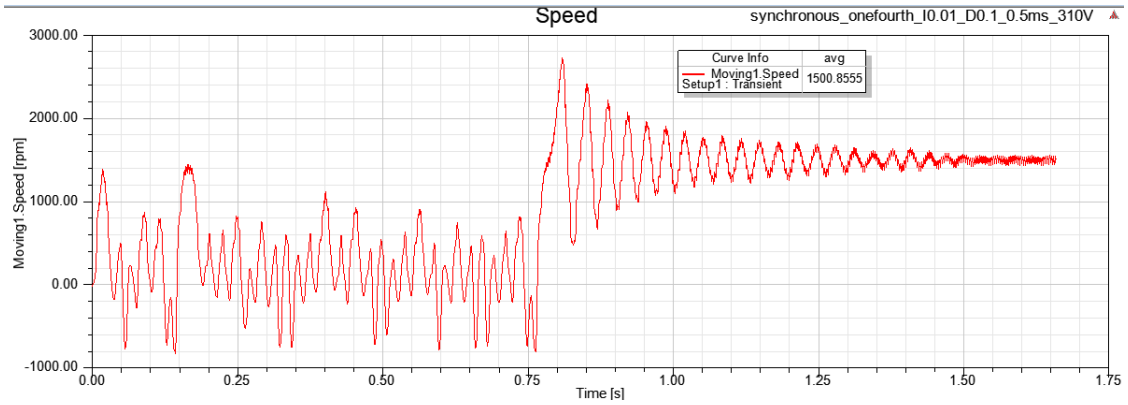

Starting performance of type-1 Axial-flux permanent-magnet motor having separated ring with single magnet in quarter

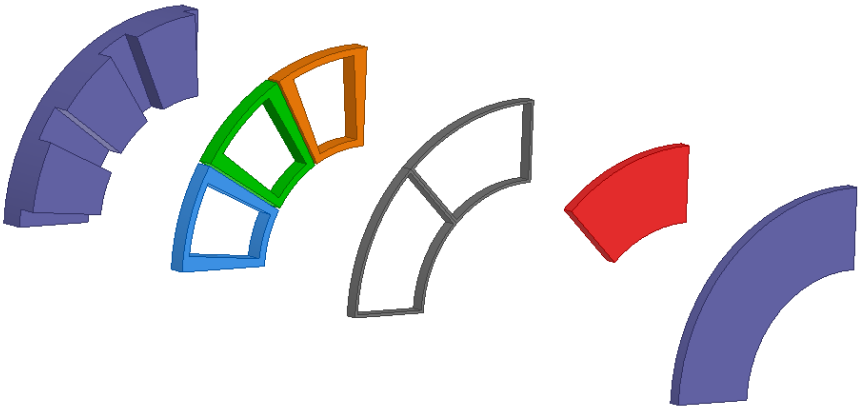

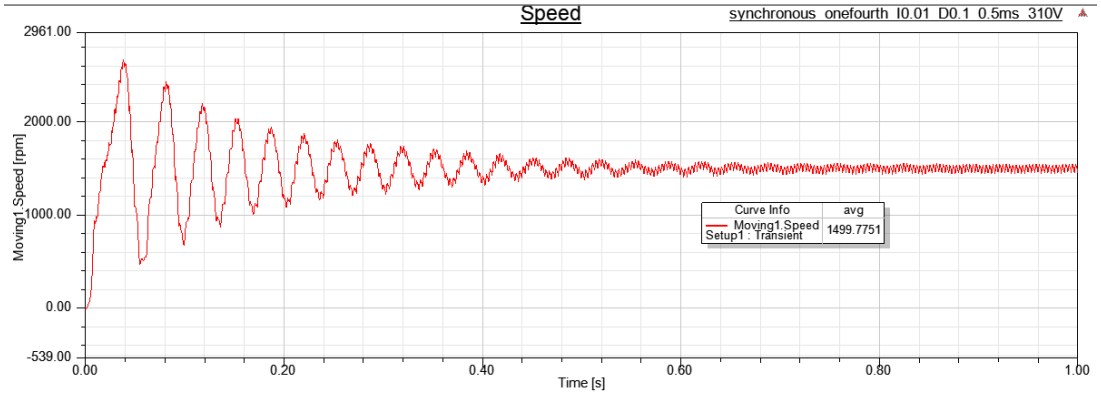

Starting performance of type-1 Axial-flux permanent-magnet motor having caged ring with single magnet in quarter

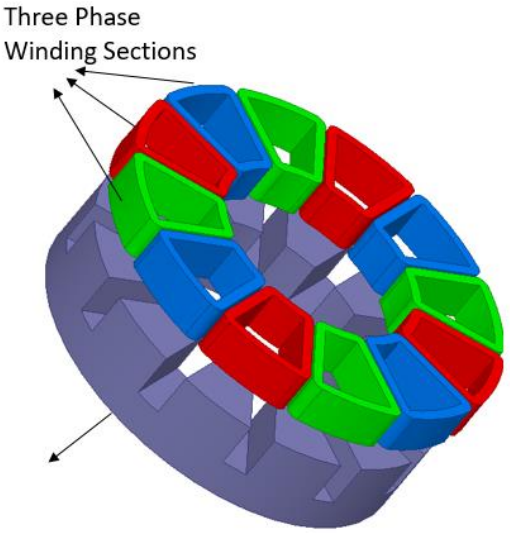

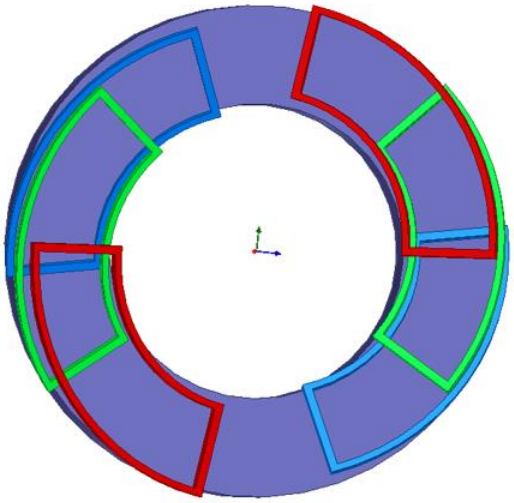

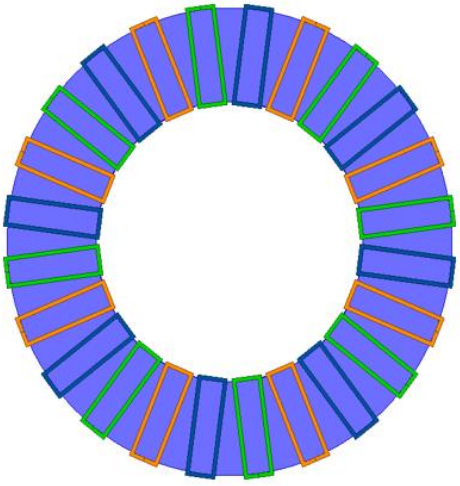

PRELIMINARY STATOR DESIGNS FOR AXIAL FLUX MOTOR

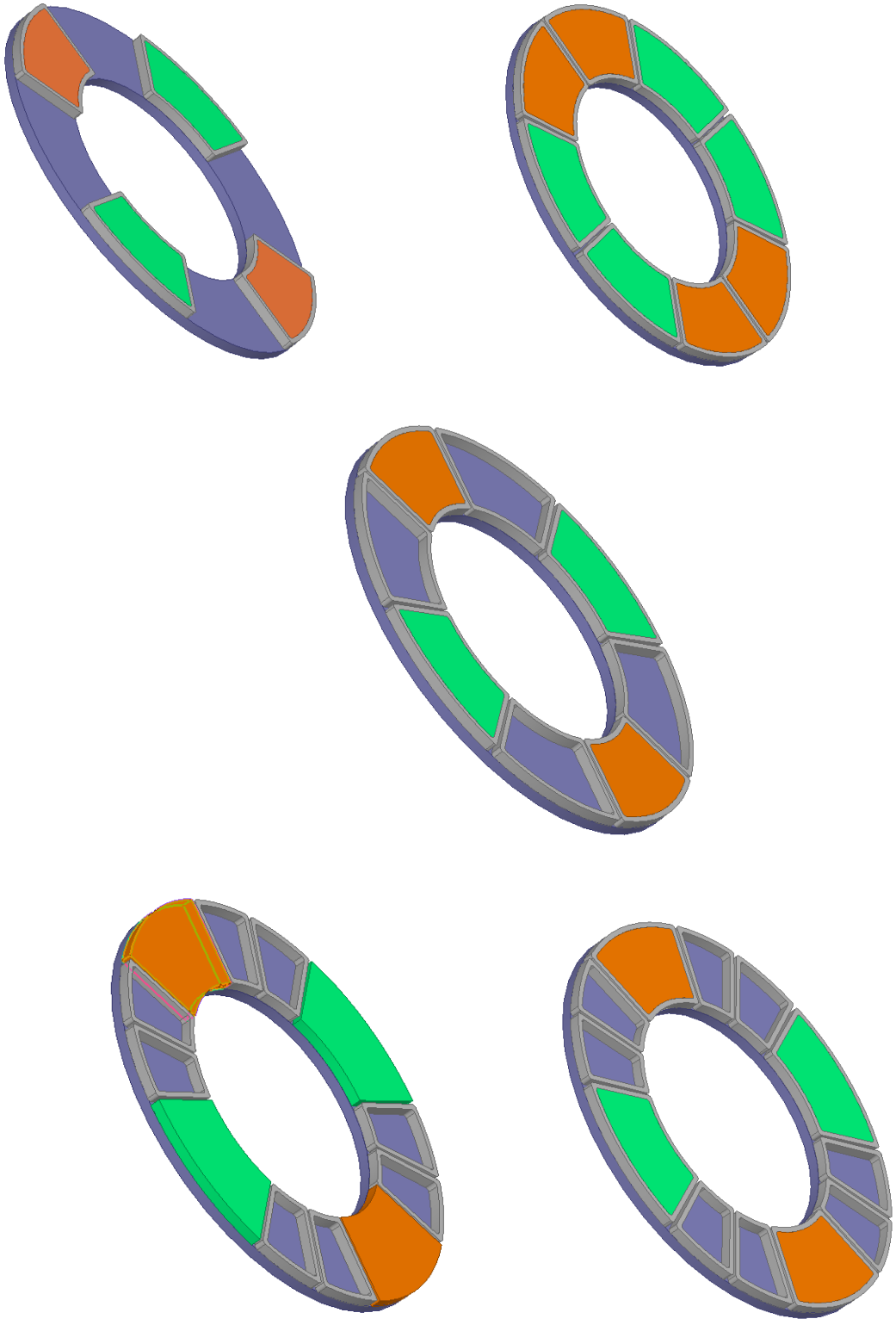

PRELIMINARY ROTOR DESIGNS FOR AXIAL FLUX MOTOR